

Response to Reviewers Comments:

Blowing snow detection from ground-based ceilometers: application to East Antarctica

Alexandra Gossart¹, Niels Souverijns¹, Irina V. Gorodetskaya^{2,1}, Stef Lhermitte^{3,1}, Jan T.M. Lenaerts^{4,1,5}, Jan H. Schween⁶, Alexander Mangold⁷, Quentin Laffineur⁷, and Nicole P.M. van Lipzig¹

¹Department of Earth and Environmental Sciences, KU Leuven, Leuven, Belgium

²Centre for Environmental and Marine Sciences, Department of Physics, University of Aveiro, Aveiro, Portugal

³Department of Geosciences and Remote Sensing, Delft University of Technology, Delft, the Netherlands

⁴Institute for Marine and Atmospheric research Utrecht, Utrecht University, Utrecht, The Netherlands

⁵Departement of Atmospheric and Oceanic Sciences, University of Colorado, Boulder CO, USA

⁶Institute of Geophysics and Meteorology, Koeln University, Koeln, Germany

⁷Royal Meteorological Institute of Belgium, Brussels, Belgium

For clarifying our answers to the referees' comments, the following scheme is used: comments of the referees are denoted in **bold**, our answers are denoted in black and quotes from the revised text are in *italic*. Please note that reference to figures in the answer refer to the original manuscript, or to the improved figure displayed in the Response document. Figures referenced in the italic text are relative to the new manuscript.

5

Contents :

- Reviewer 1 answers to comments p 2
- Reviewer 2 answers to comments p 23
- Reviewer 3 answers to comments p 32

10

- Marked up Manuscript
- Marked up Supplements

REVIEWER 1

General comments: The paper is generally well written, although a more rigorous attention is required in some parts when describing and discussing the blowing snow processes. The results are interesting and original and can be of great potential but a substantial revision is needed before the paper becomes acceptable for publication. More specifically, I

5 **have some reservations on the profile classification procedure in its current form. The distinction between precipitation and mixed blowing snow – precipitation events (Fig. 5) is not convincing. Information is lacking on how precipitation data are used to identify the occurrence of precipitation, as well as on the availability of data over the measurement period at PE. The (monthly and annual) frequency of occurrence is not studied at PE despite 7 years of measurements. Other potentially valuable information may be produced such as the inter-annual variability in blowing snow frequency**

10 **(at both locations) or the relative proportion of mixed and pure blowing snow events (at least at PE). If you can use your profile classification to discriminate between blowing snow and mixed blowing snow events at Neumayer, this would be also of great interest. More generally, some parts need clarification and/or rearrangement, and the switching between different notions or locations make the manuscript sometimes difficult to read. Section 4.2 is not very useful. The conclusion, as well as the abstract, could contain more of the main (potential) results (annual and monthly frequencies,**

15 **inter-annual variability, relative proportions of mixed blowing snow events, mean blowing snow layer heights). Indicate also in the abstract the respective locations (Neumayer/PE) and the time period to which your results correspond to. I recommend that all co-authors carry out thorough reading of the paper before resubmission.**

Thank you for your thorough and advised comments. First of all, the methodology has been revised and the profiles classification is now used to detect the presence of clouds and/or precipitations from the ceilometer attenuated backscatter signal

20 shape only. This enables to conduct the analysis of dry blowing snow versus blowing snow mixed with snowfall at both stations. Additionally, cases where blowing snow is mixed with heavy snowfall are also identified and occur 67 % of the cases at Neumayer III and 43 % of the cases at PE station, while 25 - 27 % of the events take place under cloudy or precipitating events. Cloudless blowing snow is rare (8%) at Neumayer III station, and reaches 30 % at PE. Figure 5 has also been adapted

25 by choosing more adequate examples. Concerning the results and the detailed comments, please find individual answers below. Regarding the availability of the data, a graph is added to the Supplements (Fig. S2). Frequencies at PE are also present in the Supplements (Fig. S1). However, since only one year of full measurements is available, the Antarctic winter cannot be studied. For instance, the high frequency in July 2015 and lower frequencies for the May, June, and August months are not robust enough. Regarding the inter-annual blowing snow frequency, it is not displayed in the Annual cycle at PE, but is present

30 in Fig. 7 in the original manuscript as the error bar and is in the range of $\pm 5\%$. Section 4.2 has been removed. Abstract and conclusion contain now more of the main results.

1 **Question 1: P2, L1-4: Despite the abundant literature on that topic, I recommend not to use wind speed ranges as a**
criterion to distinguish between drifting and blowing snow. As it is mentioned in the paper, the occurrence of
drifting and blowing snow is strongly related to surface snow properties, which make the characterization of wind
speed thresholds relative to the local climate conditions. For instance, low wind speeds can initiate erosion where
5 loose snow is frequently brought by snowfall, while high wind speeds are needed to erode consolidated snow. The
actual turbulent quantity involved in aerodynamic entrainment of surface snow particles is the friction velocity.
Erosion starts when the actual friction velocity (depending on atmospheric flow conditions and surface
aerodynamic properties) exceeds a threshold friction velocity (related to surface physical snow properties: density,
cohesion, grain size, etc.). In the context of this paper, using a more general classification by mentioning just the
10 height at which windborne snow is observed is a more convenient way to describe the drifting (< 2m) and blowing
snow (> 2m) processes. Besides, it is not correct to discriminate between suspension and blowing snow. Suspension
is a transport mode and refers to diffusion of snow particles in the atmosphere picked up at the top of the saltation
layer by turbulent eddies. For a given erosion event, the maximum elevation reached by suspended particles in
define the height of the blowing snow layer, which is thus not necessarily confined to a few meters above the surface.
15 Saltation is the other main transport mode, and describes ballistic trajectories and periodic rebounds of particles
at the surface. Drifting and blowing snow thus must be seen as differently balanced situations between these two
transport modes: drifting snow more generally refers to a situation where saltation is the dominant transport
mode, while blowing snow stands for the opposite

The paragraph in the paper has been changed accordingly, not referring to wind speeds thresholds, and with a more refined
20 reference to saltation and suspension modes in blowing and drifting snow.

*Snow particles can be dislodged from the snow surface, picked up by the wind and lifted from the ground into the near-
surface atmospheric layer. This phenomenon occurs approximatively on 70% of the Antarctic continent during winter (Palm
et al., 2011). Generally, drifting snow events are shallower than blowing snow events. Drifting snow typically stays below 2
25 m height whereas blowing snow can reach heights of several hundreds of meters. The transport involves a mix of suspension
and saltation transport modes (Leonard et al., 2011), with a dominance of saltating particles (Bagnold, 1974) in the case of
drifting snow, and suspended particles in blowing snow layers (Mellor, 1965).*

2 **Question 2: P2, L10: Similarly, the threshold speed of 11 m s⁻¹ given by Kodama et al. (1985) is relative to the**
30 **measurement period and location in Adelie Land and should not be presented as a general threshold above which**
the influence of snowdrift sublimation on SMB become significant.

The threshold wind speed has been removed.

5 However, blowing snow is crucial for the regional SMB (Lenaerts and van den Broeke, 2012; Déry and Yau, 2002; Gallée et al., 2001; Groot Zwaafink et al., 2013) through the displacement and relocation of the snow particles (Déry and Tremblay, 2004). In addition, sublimation contributes substantially to SMB (Takahashi et al., 1992; Thiery et al., 2012; Dai and Huang, 2014; Kodama et al., 1985). This process can even be more effective to remove mass than surface sublimation (van den Broeke et al., 2004).

3 Question 3: P2, L11: This is not always the case. Change for “can be more effective”.

The text has been adapted accordingly.

See question 2 above.

10 **4 Question 4: P2, L17: “Affecting [. . .] the surface energy balance”, not “affect [. . .] on surface . . .”.**

The text has been adapted accordingly.

Blowing snow also plays a role in determining snow surface characteristics (Déry and Yau, 2002), affecting the surface energy balance (Lesins et al., 2009; Mahesh et al., 2003; Yamanouchi and Kawaguchi, 1985).

15 **5 Question 5: P2, L34: You should refer to Trouvilliez et al. (2014), who also report drifting snow statistics in East Antarctica from ground-based measurements with Flow-Capt instruments, instead of Trouvilliez et al. (2015) who present an evaluation of the Flow-Capt in the French Alps. The paper of Barral et al. has been published in 2014.**

The references have been changed accordingly

20 *A number of measurement campaigns have been organized in various regions of the AIS, using different types of devices: nets, mechanical traps and rocket traps, photoelectric and single-beam photoelectric sensors. Various studies have also worked with Flow-Capt or piezoelectric devices (Leonard et al., 2011; Amory et al., 2015; Trouvilliez et al., 2014; Barral et al., 2014).*

6 Question 6: P5, L7 to P6, L2: These sentences belong to the methodology and should be moved in section 3.2

These sentences have been moved to section 3.2

25

Section 2.2

The Vaisala CL-31 ceilometer (firmware 1.72) was installed on the roof of the station in December 2009 and is operational at present. It emits laser pulses at a central wavelength of 910 ± 10 nm at 298 K. The measurement resolution is set to 10 m

and the reporting interval on 15 s. Several outages of the energy provision system limit the data mainly to Antarctic summer season (December to March is best represented). Only one year of continuous measurements was achieved (2015). The Metek vertically-profiling precipitation radar, set up since 2010, enables to retrieve snowfall rates, using the return from the vertically profiling Doppler radar operating at a frequency of 24 GHz. The raw Doppler spectra is post-processed following Maahn and Kollias (2012), to calculate radar reflectivity profiles which are then linked to snowfall rates using the newly developed Ze-Sr relation for PE by Souverijns et al. (2017) and has a sensitivity up to -14 and -8 dBz (Souverijns et al., 2017). A full description of micro-rain radars can be found in Klugmann et al. (1996) and the radar set up at Princess Elisabeth is described in Gorodetskaya et al. (2015).

10 Section 3.2

The information retrieved from the Micro Rain Radar (hourly precipitation rates) is collocated to ceilometer blowing snow detection, to determine the time (in hours) since the last precipitation event.

7 Question 7: P6, L3: How do you use this information in the study?

The cloud base temperature is used as an atmospheric variable. In the case of blowing snow, the measured cloud temperature is actually the blowing snow layer temperature. It was used in the cluster analysis, and in the PCA. However, it was not a determining variable. This information is left out in the new version of the paper.

8 Question 8: P7, L19: Distinguishing visually between pure blowing snow and mixed blowing snow-precipitation events seems far too subjective to me, even if “the blowing snow layer is not too dense”.

Yes, the visual detection of pure blowing snow versus mixed events is subjective. This method is applied by the visual observer at Neumayer station, following the procedure described by Gert König-Langlo (personal communication, 2016). This further reinforces our position of not treating the visual observations as "ground truth".

9 Question 9: P8, L31: the first “of” has to be removed. Change “layer. E.g.” for “layer, e.g.”

The text has been changed accordingly

Studies investigating the boundary-layer properties based on ceilometer attenuated backscatter make use of both properties of the signal (shape and intensity), to evaluate the presence and extent of a particular layer, e.g. in order to determine the height of the mixing layer (Wiegner et al., 2014).

- 10 **Question 10: P10, L5 and onwards: It is likely that I don't understand correctly the detection principle, but in its current form I have some reservations about your classification procedure, especially about the distinction between precipitation with and without blowing snow, and the omission of strong precipitation associated with heavy blowing snow. I tried to list them below. It is difficult to relate the profile features described in the text using heights and bin numbers to the plotted profiles in Fig. 5. You could, for instance, clearly indicate the discontinuity between the 4th and 5th bins, and specify to which bin the lowermost backscatter intensity value reported on the graph correspond to. This would facilitate the understanding of the description of the detection algorithm.**
- 5
- **The increase in the backscatter signal between the first and the second bins in the mixed blowing snow profile in Fig. 5 is of very small intensity compare to the one characterizing pure blowing snow. Except for this aspect, this profile seems very similar to the pure precipitation profile. Moreover, I suppose that a mixed profile should include both the signature of precipitation and blowing snow (strong signal close to the surface). Are you sure that this absence of the blowing snow signature does not simply imply that there is no blowing snow?**
 - **L14: "between 40 and 50 m": give the corresponding bin numbers.**
 - **L17: I don't understand why during strong precipitation associated with storms, the precipitation intensity might cover the blowing snow signal close to the ground. I'm wondering even further if the opposite would be true. The strong backscatter signal close to the surface in the typical blowing snow profile illustrates the influence of high particle density layers. This would be particularly amplified when abundant snowfalls provide a large supply of fresh snow that can be easily eroded by strong winds. By discarding these cases, you might omit an important part of the mixed blowing snow events, which can further affect all your statistics. This could be a major issue since you say latter in the paper that most of the blowing snow events occur simultaneously with precipitation. If the situation with strong precipitation and blowing snow is a clear limitation of your approach, you have to quantify it, especially since the occurrence of overcast conditions is also a limitation to satellite retrieval. You should give the relative proportion of each profile category (blowing snow, precipitation + blowing snow, precipitation, clear sky and omissions).**
- 15
- 20
- 25 **Figure 5 (Fig.6 in the new manuscript, Fig. 13 below) has been adapted to show both bin number and height (m agl). The discontinuity is clearly indicated in grey.**
- **Figure 5 is indeed not clear: it was based on only one day (24.04.2016) during which blowing snow was accompanied by clouds/precipitation at the end of the blowing snow event, hence, the lower intensities and the resemblance to the pure precipitation profile. Another day was therefore selected for the new version of the manuscript (10.02.2014), to illustrate the pure precipitation and the mixed event. In this new figure (Fig.1 below, Fig.6 in the new manuscript), the intensity of the profile in the lowermost bins is clearly indicative of blowing snow (red line), and the increase around the 15th bin indicates the presence of clouds/precipitations (arrow). In the case of precipitation/cloud without blowing snow, this low-level decrease is absent, and the increase around the 17th bin reflects the presence of a cloud/precipitation.**
- 30

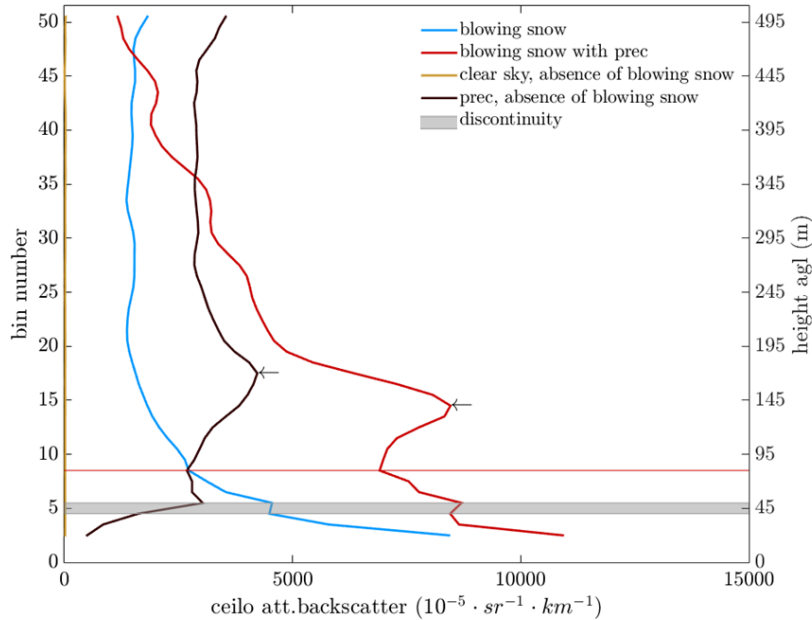


Figure 1. Different types of profiles relevant for blowing snow measured by the ceilometer at PE station: blue line - typical blowing snow signal with no precipitation nor clouds (24-04-2016); red line - blowing snow overlaid by precipitation (10-02-2016); black line - precipitation with no blowing snow (10-02-2014); yellow line - near-zero signal for clear sky conditions (24-04-2016). The height above ground is indicated on the right axis and the corresponding bin number on the left axis. All profiles exclude the lowermost bin, and start at the second bin (15 m agl.). The grey lines represent the discontinuity between bins 4 and 5 (35-45 m). The arrows indicate the presence of precipitation.

- The bin numbers have been added in Fig. 5 and in the text (see Fig.1 below, Fig.6 in the new manuscript).
- Given the specific conditions during heavy precipitation events, we treat these events differently in the improved manuscript. We know that most of the time, blowing snow happens together with storms and intense precipitation (the snowflakes rebound on the ground and are displaced by strong winds). Hence, in some cases the signal intensity is not decreasing with height, and the profile criterion could not be met. Therefore, we decided to create a new category "heavy mixed events" for the situation in which the signal in the second bin exceeds $1000 \cdot 10^{-5} \cdot \text{km}^{-1} \cdot \text{sr}^{-1}$ (threshold adapted from (Gorodetskaya et al., 2015)). Of those heavy mixed events, 45 % do not show an increase of the signal in the overlying bins at Neumayer III station, and would have therefore been discarded by the algorithm.

To conclude, a new method for precipitation/cloud detection based on the ceilometer profile only has been developed (see Fig.2): the algorithm searches upwards of the 7th bin (maximum limit for the profile criterion of the BSD algorithm) for a second increase in signal that is (1) above $100 \cdot 10^{-5} \cdot \text{km}^{-1} \cdot \text{sr}^{-1}$, which is the threshold for clouds detection (Van Tricht et al. (2014)), and (2) thicker than 9 bins (85m) (Van Tricht et al., 2014). This enables to detect overcast conditions, in the

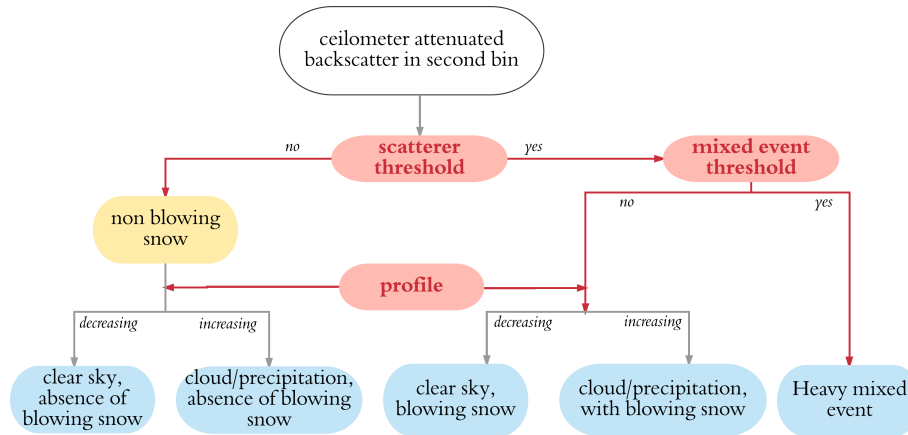


Figure 2. Chart of the method used to detect blowing snow from the attenuated backscatter signal of the ceilometer.

presence of blowing snow or not.

Regarding the intense mixed events, once the backscatter in the second range bin exceeds the blowing snow threshold, the algorithm evaluates if the threshold for intense mixed events is reached (above $1000 \cdot 10^{-5} \cdot \text{km}^{-1} \cdot \text{sr}^{-1}$, adapted from Gorodetskaya et al. (2015)). If it is the case, blowing snow is assumed present and the profile is not investigated.

5

The algorithm therefore investigates the shape of the profile in order to detect blowing snow. A condition is set, that a blowing snow profile implies that the mean of the overlying bins 3 to 7 (25 to 65 m) must be lower than the signal in the second range bin (15 m). In this way, the discontinuity, as described in section 3.1. (visible in Figures 1 and 5 between 35 and 45 m in the original manuscript, Fig.1 and 6 in the new manuscript), is not affecting our retrievals. In order to detect blowing snow occurring during clouds or precipitation, the profile shape is analyzed to identify a second increases in the signal intensity above the 7th bin (65 m height). A clear differentiation between clouds or precipitation cannot be made on the basis of the ceilometer alone, but the presence of clouds and/or precipitation can be identified. This analysis is carried out for both blowing snow and non blowing snow measurements. [...]

10

Inherent to this profile-based method, the detection of blowing snow during precipitating events is limited to cases when the blowing snow signal is preserved close to the ground. In case of precipitation associated with storms, there is always blowing snow due to the high wind displacing the snow, and no distinction between precipitation and blowing snow is possible, as the ceilometer signal is entirely attenuated near the surface (Gorodetskaya et al., 2015), it is not possible to get signal in the overlying bins, and the profile of the backscatter intensity might not decrease upwards. Such intense precipitating events mixed with snowfall are identified as having a second bin signal higher than $1000 \cdot 10^{-5} \cdot \text{km}^{-1} \cdot \text{sr}^{-1}$ (threshold adapted from Gorodetskaya et al. (2015)). In those cases, the events are classified as a heavy mixed blowing snow event, and the profile analysis is eluded by the algorithm.

20

11 **Question 11: P11, Section 4.1: There is a temporal discordance between visual observations (performed 6 times a day) and ceilometer measurements (hourly means). Have you re-sampled the ceilometer dataset to match the frequency of visual observations, or do you compare the ceilometer hourly output corresponding to the time at which the visual observations were performed? Are the visual observations continuous over the measurement period (2010-2015)?**

We have re-sampled ceilometer to hourly output, and selected the re-sampled data corresponding to the time at which visual observations are carried (1) if there are more than 140 measurements (35 mins) with a NaN value, the measurements within the hour are discarded. Else, if there is more than 20 mins of blowing snow detections, blowing snow is assumed for that measured hour (only to get rid of really short lived events). Then, we compare this with the visual observation.

10 Yes, the visual observation are continuous over the measurement period, but omit observations at 03 and 06:00 UTC.

In order to investigate the type of blowing snow detected by the BSD algorithm, we compare it to visual observations at Neumayer, carried out routinely at 09-12-15-18-21 and 24:00. All ceilometer measurements are considered over one hour, corresponding to the time at which visual observations are carried out. We identify a blowing snow event when blowing snow is present in at least 80 profiles (20 mins). The WMO visual observations are categorized in six classes of blowing and/or drifting snow events, ranging in intensity and whether there is precipitation or not (Table S3 in Supplements).

and section 2.3

20 *The measurements are carried out daily every 3 hours but visual observations are omitted at 03 and 06:00 UTC.*

12 **Question 12: P12, Figure 6: Indicate N for each category.**

The figure has been removed from the new version of the manuscript. Table 1 below (Table 3 in the new manuscript) lists the number of detections (N) for each category. The total number of event for each category is also displayed in the wind rose figures (Figs 3 and 4 below, Figs. 9 and 10 in the new manuscript).

25 13 **Question 13: P12, L16: Don't you think you could use the profile classification developed at PE (in terms of vertical variation in backscatter intensity) to discriminate the occurrence of precipitation at Neumayer?**

We have conducted this analysis (see Question 10), and similar trends as observed at PE station regarding blowing snow associated with precipitating events and synoptic disturbances.

30 *Further, we investigate the specific meteorological conditions (near-surface temperature inversion, relative humidity, surface temperature, wind speed and direction, in- and outgoing longwave fluxes, and the time since the last precipitation event)*

Table 1. Detection numbers and scores of the different categories of observations. The first 4 columns give N BS_{both} - stands for blowing snow detected by both the algorithm and the visual observations, N BS_{none} - when both methods agree that there is no blowing snow, N BS_{ceilo} and N BS_{vis} - represent detections by the algorithm and the observer only, respectively (the corresponding percentages are presented in table S4, in the supplement). The four last columns give the scores. B stands for blowing and D for drifting snow. The total number of measurements is 10584.

	N BS _{both}	N BS _{none}	N BS _{ceilo}	N BS _{vis}	accuracy	sensitivity	specificity	TSS
B and D snow, with or without prec	2404	5170	972	2308	0.70	0.51	0.84	0.35
B and D snow, without prec	992	6578	2373	897	0.70	0.52	0.73	0.26
heavy B snow, without prec	378	7406	2998	72	0.72	0.84	0.71	0.55
all B snow, without prec	822	6993	2554	485	0.72	0.63	0.73	0.36
all B snow, with or without prec	1856	6665	1520	813	0.78	0.69	0.81	0.51
heavy blowing snow, with or without prec	1114	7249	2262	229	0.77	0.83	0.76	0.59

during blowing snow events.

For all three categories of blowing snow events, the 2m wind direction shows a preferential easterly/north-easterly orientation at both Neumayer and PE, while the absence of blowing snow is characterized by a wider spectrum of wind directions (Figs.3 and 4 below, Figs. 9 and 10 in the new manuscript). Positive anomalies in wind speed and RH occur during blowing snow events. Cyclonic events are a common feature at Neumayer (König-Langlo and Loose, 2007), bringing easterly winds during which most of the drifting and blowing snow occur. Also at PE, most of the blowing snow events ($N = 1643$, 92 %) are associated with the warm synoptic and transitional regimes, when moist air is brought from the ocean, that precipitate inland (Gorodetskaya et al., 2013). Thiery et al. (2012) also showed that at PE drifting snow sublimation occurs mostly during transitional regimes. These regimes occur 41-48 % of the time (Gorodetskaya et al., 2013, 2014). Very few blowing snow events occur in cloudless cold conditions (cold katabatic regime), when the northerly winds blows from the interior towards the coast ($N = 139$; 8%).

Intense mixed events (Fig.1 above, Fig. 6 in the new manuscript) occur together with north-easterly strong winds : 87° to N, $10 \text{ m} \cdot \text{s}^{-1}$ at PE and 65° to N, $13 \text{ m} \cdot \text{s}^{-1}$ at Neumayer III , warmer surface temperatures and higher relative humidity. These are the signature of storms associated with synoptic events, during which the turbulent mixing reduces the vertical temperature gradient (Gorodetskaya et al., 2013). The majority (60 %) of the blowing snow events occur during storms or overcast conditions (with cloud and/or precipitation). These mixed events have generally a short time lag since the last precipitation event and reach high atmospheric levels. Dry blowing snow has a mean wind direction of 120° to N at PE and 77° at Neumayer III, lower wind speeds ($6\text{-}7 \text{ m} \cdot \text{s}^{-1}$) and a greater temperature inversion. The mean time lag since the last precipitation event at PE (23 hours) indicates that these events most likely occur after a storm, and that cloudless blowing snow (8 %) is mostly associated to katabatic winds.

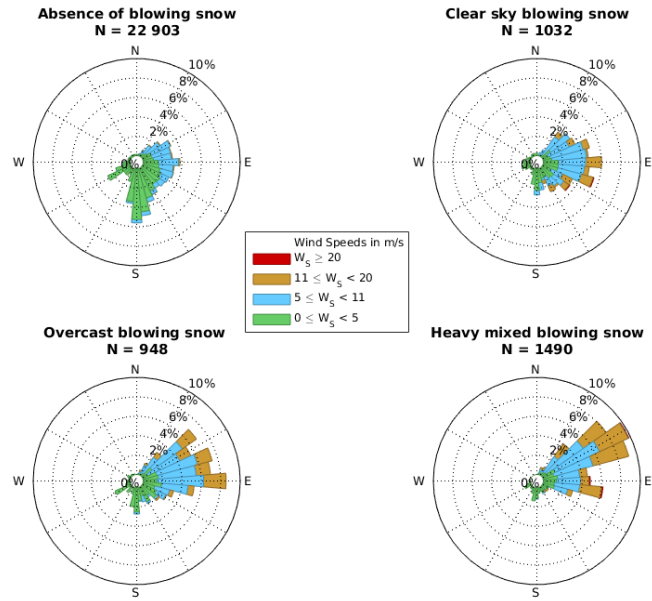


Figure 3. Wind rose at PE station, N = number of events

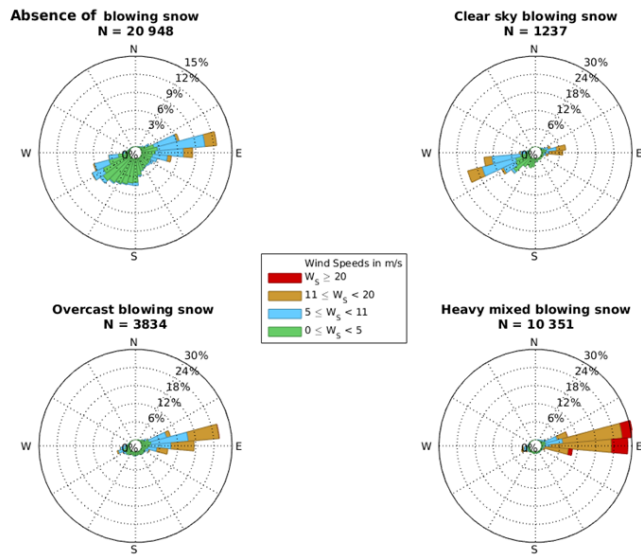


Figure 4. Wind rose at Neumayer station, N = number of events

14 Question 14 : P12, L19: An “r” is missing in the penultimate word.

The "r" has been added.

15 Question 15: P13, Fig. 7: How can you explain the apparently systematic discordance between visual observations and the detection algorithm in January?

Indeed, January fall completely outside the variability of the other months in the visual observations. We suspect that there is some issue with these data in January, as no visual observations are reported in January 2011, 2013, and only a few are available during January 2014 and 2015. Other months, such as February 2011-2013 and 2015, as well as November and December 2014 and 2015 have also a restricted number of visual reports. We suspect that the observers might have been away on the field or not available for reporting during those periods. However, the ceilometer was operating continuously during these months. In addition, by sub-sampling the ceilometer blowing snow detections to the corresponding visual observation hours, the frequencies retrieved are biased (if a storm occurred between midnight and 09:00 UTC, it is not reported, and therefore excluded from the frequencies calculation). The frequency distribution presented here (Fig.5 below, Fig. 7 in the new manuscript) is therefore calculated on ceilometer measurements only, which are continuous over time, and are not compared to visual observations. The total frequency is of 36 %, and the reason this frequency is higher than in the previous manuscript, is that we now include heavy mixed events.

16 Question 16 : P13, L7: Please indicate over which period of time the frequency is computed

The period (2011-2015) was indicated. The sentence has been adapted to make it clearer.

The frequency is calculated here by reporting the sum of all hours during which blowing snow occurs ($n = 2\,714\,164$) over the total number of observation hours ($n = 9\,742\,717$). Blowing snow at Neumayer III occurs on average 28% of the time for the 2011-2015 period, as detected by the BSD algorithm. [...] The overall blowing snow frequency is computed at PE for the 2010-2017 period. However, the limited availability of Antarctic winter data (due to power failures at the station) might lead to an underestimation of the blowing snow frequency. Total blowing snow frequency reaches 13 % at PE station, which is lower than at Neumayer [...]

17 Question 17: P13, Second paragraph: this paragraph is hard to follow and needs rearrangement:

- L9-11: You switch between annual and monthly time scales, and frequency and blowing snow rates. Move the sentence in which you describe the calculation of the frequencies at the beginning of the paragraph. Indicate the time period over which König-Langlo and Goose (2007) computed their frequencies. Remove “blowing snow

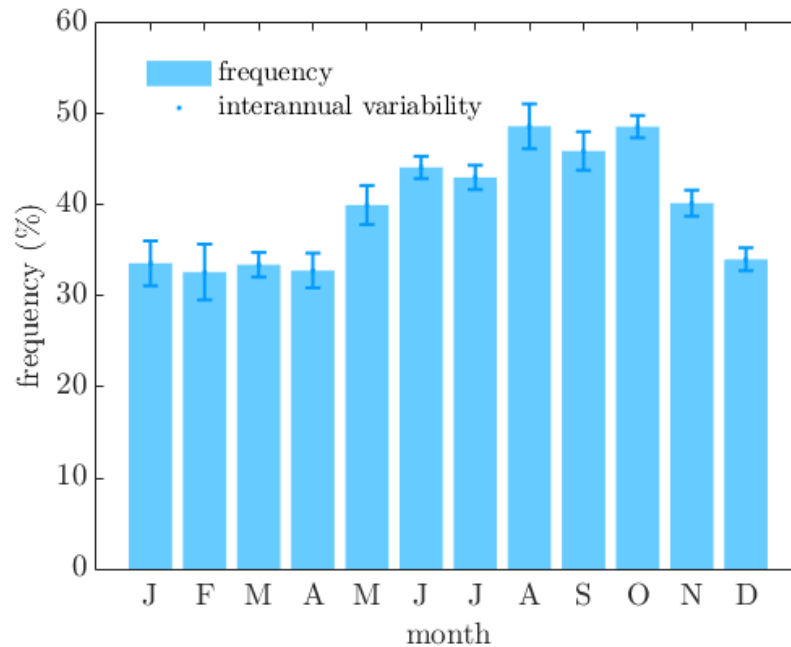


Figure 5. Yearly cycle of blowing snow at Neumayer III station (2011-2015). The error bars represent the interannual variations.

rates” and stay focus on frequencies to compare apples and apples. Indicate also the measurement period for the frequency computed at PE (and for this you also need to discuss the representativeness of the winter data due to power supply issues).

– the frequencies paragraph has been changed accordingly.

5 – **L13: See also Trouvilliez et al. (2014) and Amory et al. (2017) for similar statistics from ground-based measurements.**

– the references have been added and the text was modified.

– **L14: “Reasonable” is not rigorous. Please replace.**

– ‘reasonable’ has been rephrased

10 – **L16: In the previous sentence you give the frequency for two locations (Neumayer: 28% and PE: 9%): which one do you compare with Palm’s results? “Coherent” and “analogous” give no quantitative information, and are somewhat confusing when used together. Give directly the values from Palm et al. (2011) (and indicate the measurement period) and, then, discuss the particular geographical settings of PE to explain the contrast in wind speed and, ultimately, in blowing snow frequencies, with the other results/locations mentioned in the text. If the**

frequencies compare reasonably well with satellite measurements, does this mean that the hindering effect of clouds is not so influent? Again this appears contradictory with the apparently frequent occurrence of precipitation and overcast conditions during blowing snow events.

- The map present in (Palm et al., 2011) gives a range rather than a precise number. In the case of PE station, for instance, blowing snow frequency is 0-10 % while the BSD algorithm reaches 13 % of blowing snow (not 9 % since we include the heavy blowing snow events, the frequency increased). In this case, the BSD frequency is higher than the detection rate by the satellite method. This can be related to the number of blowing snow events occurring together with clouds/precipitation, missed by the satellite, and to the different spatial and temporal dimensions of the different methods. In addition, the geographical settings of PE station are discussed.

The frequency is calculated here by reporting the sum of all hours during which blowing snow occurs at Neumayer based on the BSD algorithm over the total number of observation hours. Blowing snow at Neumayer III occurs on average 36% of the time for the 2011-2015 period. This is consistent with König-Langlo and Loose (2007), who report 20 % of drifting and 40 % drifting and blowing snow for the 1981 - 2006 period. However, there is an inter-annual variability that reaches ± 5 % , also observed by Lenaerts et al. (2010). The pattern visible in Fig.5 above (Fig. 7 in the new manuscript) is common for blowing snow over Antarctica: a seasonal cycle peaking during the Antarctic winter (March - November) and displaying lower values for the rest of the year (Mahesh et al., 2003; Lenaerts et al., 2010; Scarchili et al., 2010; Palm et al., 2011; Amory et al., 2017). The overall blowing snow frequency is computed at PE for the 2010-2017 period and reaches 13%. This lower blowing snow frequency at PE can be explained by the location of the station: the station is shielded from the katabatic winds by the Utsteinen mountain range, making it a quieter zone between the flows diverged to the sides of the station (Parish and Bromwich, 2007), while Neumayer III station is located on the ice shelf and experiences higher wind speeds [...] and is more exposed to storms. In addition, the limited availability of Antarctic winter data (due to power failures at the station) leads to an underestimation of the blowing snow frequency as mostly extended summer period was used, and only one winter is taken into account.

The frequencies measured by the BSD algorithm are larger than those retrieved by satellite method: Palm et al. (2011) gives a range of 0-10 % blowing snow for both locations. This can be related to the number of blowing snow events occurring together with clouds/precipitation, missed by the satellite, and to the different spatial and temporal dimensions of the different methods. Of all blowing snow detected events, 67 % is mixed with intense events at Neumayer III, and 43 % at PE station. Cloudless blowing snow is very rare at Neumayer III station (8 % of the events), while it reaches 30 % at PE station.

18 Question 18: P14, Fig. 8 (legend): Non blowing snow (not “no”)

The figure is not displayed in the new version of the manuscript.

19 **Question 19: P14, section 4.2: This section could have been more organized. You alternate between katabatic and synoptic conditions, blowing snow and non-blowing snow conditions, PE and Neumayer, and results and theory. Some sentences are ambiguous, others contain syntax errors, irrelevant or incomplete information, and some conclusions seem a bit early. I think you could remove this section entirely without disturbing your global analysis. Moreover, this would avoid redundant information with section 4.3, in which you actually refer to the work of Gorodetskaya et al. (2013) to define the two meteorological regimes. Find more detailed comments below:**

This section has been removed, only parts are kept in section 4.3. Separate answers are given for the remarks still present in the new version of the paper:

- **L5: “Fig. 8 and 10”: an “s” is lacking**
- 10 – L5 : The figures are not displayed anymore
- **L5-7: You only use a wind direction criterion to distinguish katabatic from synoptic conditions. What about a combined influence of katabatic and synoptic conditions? Is the deflection due to the Coriolis force also an influent factor accounting for the easterly component of the surface flow?**
- L 5-7: There are three regimes: warm synoptic, cold katabatic, and transitional, when the situation evolves from synoptic to katabatic or the other way around as was defined by Gorodetskaya et al. (2013). While the wind direction was the dominant parameter in the PCA analysis, the parameters used to distinguish between these regimes are the wind direction, together with the temperature inversion and cloudiness, as well as the wind speed and relative humidity. Regarding the deflation to the East, ongoing analysis (Souverijns et al, in prep) showed that among the low pressure systems that are circling eastward around Antarctica over the Southern Ocean - mostly those centered to the north and to the northwest from PE determine the synoptic conditions at the PE station. As winds turn clockwise around the cyclone, air from oceanic areas is drawn towards the station. These oceanic air masses have the potential to take up a lot of moisture, and precipitate at the coastal areas of Dronning Maud Land, as winds are forced to rise against the Antarctic plateau. In those cases, winds at PE originate from the north east (when the cyclone is located to the northwest) or from the more inland areas at the east (when the low pressure system is located north of the station).
- 15
- 20
- 25 – **L8-10: This sentence is ambiguous. Please rephrase.**
- This sentence has been removed.
- **L11-13: Harsh construction. The colon (“:”) is misused. “wind speeds are high enough to be able to. . .and saltation” is clumsy: I guess “wind speeds are high enough to initiate snowdrift” is analogous but more concise.**
- The sentence has been rephrased accordingly.
- 30 – **L12: The increase in RH is (partly) caused by blowing snow, not a cause of, so it doesn’t “privilege” blowing snow.**

- The sentence has been removed.
- **L13-15: Mentioning the self-limiting process of blowing snow sublimation and the increase in roughness due to windborne snow particles is not relevant since i) they are not a result here and ii) they don't explain any described feature.**
- 5 – The sentence has been removed.
- **L15-16: This sentence needs rephrasing: “The increase in RH is both a result [. . .] and sublimation (not “due to”) of precipitating and blowing snow particles.”**
- The sentence has been removed.
- **P15, L1: “Those also have an impact on the radiative budget”: This is elusive. Illustrate and discussed further or remove.**
- 10 – The sentence has been removed.
- **P15, L2: Turbulent mixing generally occurs during strong winds, whatever their origin (synoptic or katabatic). How do you distinguish between synoptic and katabatic conditions?**
- PE station is shielded by the Utsteinen mountain range, therefore katabatic winds have the lowest wind speeds (see Fig.3 above and Fig. 10 in the new manuscript), compared to synoptic or transitional regimes.
- 15 – **P15, L4: “These variables”: You mean “trends” (?)**
- Yes, the sentence has been adapted accordingly

The near surface atmosphere changes, associated with blowing snow events, are investigated for both stations, and detailed means and standard deviation are displayed in Table S6 and S7, in supplements. We investigate how blowing snow hourly means relate to weather regimes, derived from the hierarchical cluster analysis applied in Gorodetskaya et al. (2013), which defines the weather regimes at PE station: "cold katabatic", "warm synoptic", and "transitional synoptic". The cold katabatic regime is characterized by slower wind speeds and lower humidity, reduced incoming long wave radiation, a slight surface pressure increase, and a substantial temperature inversion. Warm synoptic conditions involve higher wind speeds and specific humidity, strongly positive anomalies of incoming long wave radiation. The surface pressure is slightly lower, and the temperature inversion is strongly reduced than during average conditions. Finally, average wind speeds, humidity and incoming long wave radiation, as well as slightly lower surface pressure are observed during the transitional regime, when the situation evolves from synoptic to katabatic or the other way around (Gorodetskaya et al., 2013). Further, we investigate the specific meteorological conditions (near-surface temperature inversion, relative humidity, surface temperature, wind speed and direction, in- and outgoing longwave fluxes, and the time since the last precipitation event) during blowing snow events.

20

25

30 *For all three categories of blowing snow events, the 2m wind direction shows a preferential easterly/north-easterly orientation*

at both Neumayer and PE, while non-blowing snow takes place under a wider spectrum of wind directions (Figs. 9 and 10). Positive anomalies in wind speed and RH occur during blowing snow events. Cyclonic events are a common feature at Neumayer (König-Langlo and Loose, 2007), bringing easterly winds during which most of the drifting and blowing snow occur. Also at PE, most of the blowing snow events ($N = 1643$, 92 %) are associated with the warm synoptic and transitional regimes, when moist air is brought from the ocean, that precipitate inland (Gorodetskaya et al., 2013). These regimes occur 41-48 % of the time (Gorodetskaya et al., 2013, 2014). Very few blowing snow events occur in cloudless cold conditions (cold katabatic regime), when the northerly winds blows from the interior towards the coast ($N = 139$; 8%). Intense mixed events (see Fig.5) occur together with north-easterly strong winds : 87° to N, $10 \text{ m} \cdot \text{s}^{-1}$ at PE and 65° to N, $13 \text{ m} \cdot \text{s}^{-1}$ at Neumayer III , warmer surface temperatures and higher relative humidity. These are the signature of storms associated with synoptic events, during which the turbulent mixing reduces the vertical temperature gradient (Gorodetskaya et al., 2013). The majority (60 %) of the blowing snow events occur during storms or overcast conditions (with cloud and/or precipitation). These mixed events have generally a short time lag since the last precipitation event and reach high atmospheric levels. Dry blowing snow has a mean wind direction of 120° to N at PE and 77° at Neumayer III, lower wind speeds ($6\text{-}7 \text{ m} \cdot \text{s}^{-1}$) and a greater temperature inversion at. The mean time lag since the last precipitation event at PE (23 hours) indicates that these events most likely occur after a storm, and that cloudless blowing snow (8 %) is mostly associated to katabatic winds.

20 Question 20: P16, Fig. 10 (caption): Indicate the relative proportion of each category.

The proportions have been added to the Figs. 3 and 4 above (Figs.9 and 10 in the new manuscript).

21 Question 21: P16, L4: “as”, not “although”.

The sentence has been corrected

20

a great part of the events during the synoptic regime would be missed, as they represent more than half of the events observed at PE

22 Question 22: P16, L13: Remove “anymore”.

The sentence has been corrected

25

This is, however, not so obvious if we normalize the distribution of blowing snow events taking into account the total number of measurements within each time lag after precipitation.

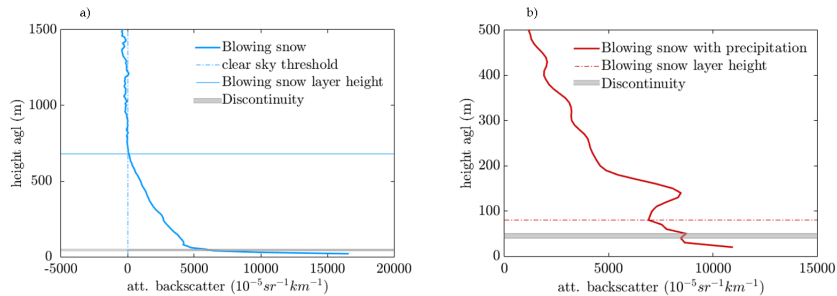


Figure 6. Determination of the height of the layer by the BSD algorithm. (a) in case of a cloud free blowing snow profile, the height of the layer is attained when the backscatter intensity reaches the clear sky threshold. (b) in case of precipitation, the height of the blowing snow layer is reached when the intensity of the backscatter signal re-increases.

23 Question 23: P17, section 4.3.2: It is not clear how the depth of the blowing snow layer is determined.

The explanation for the blowing snow depth determination lies in P11, L2-7, a reference to this section as been added. In addition, illustrations are added in the Supplements (Fig.6 above, Fig. S3 in supplements)

- 5 *The height of the blowing snow layer (algorithm explained in section 3.2.) varies according to different parameters: wind speed, and the size and density of the snow particles.*

and section 3.2.

- 10 *In addition to the detection of blowing snow, the BSD algorithm quantifies the height of the layer (see Fig. S3, supplements) This is done as follows; if the profile decreases steadily (indication of absence of precipitation), the range gate at which the intensity of β_{att} drops under the clear sky threshold value is the top of the layer. Anything above this height is considered clear sky. If there is precipitation or a cloud during the blowing snow event, the shape of the backscatter profile does not decrease monotonously, but shows an increase in higher levels. In that case, the range gate at which the profile increases again is the*
- 15 *top of the blowing snow layer, and the base of the cloud and/or precipitation.*

24 Question 24: P18, Fig. 11 (ordinate axis): Indicate the units.

The figure on page 18 is Figure 13, the figure label has been changed accordingly.

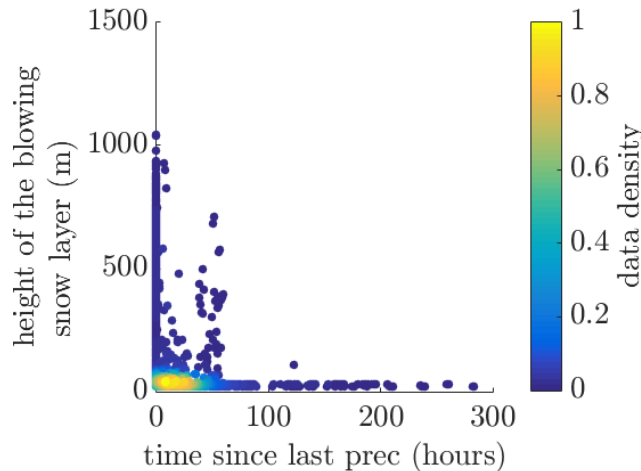


Figure 7. Scatter plot of the time since last precipitation event versus height of the blowing snow layer. Each point represents a blowing snow event. The colorbar represent the data density (number of observations divided by the entire sample size).

25 Question 25: P18, L10: If your algorithm is applied “successfully”, then you consider the visual observations as ground truth. Compare favorably with or something like that, would be more appropriate. Idem for “proved the applicability”.

Indeed, this suggests that we consider visual observations as ground truth, which is not the case. The text has been changed accordingly.

The BSD algorithm developed for the Vaisala CL-31 ceilometer at PE was applied to the Vaisala CL-51 ceilometer at Neumayer III station. Comparing the BSD algorithm detections to visual observations at Neumayer showed a good agreement and the ability of the BSD algorithm to detect (heavy) blowing snow events, both under dry and precipitating conditions.

10 26 Question 26: P19, L15: Metamorphism does not impact the friction velocity, only the threshold friction velocity (see comment 1).

The sentence has been changed accordingly

These parameters change with metamorphism and impact the threshold friction velocity, and thus the and minimum wind speed required for particles uplift from the ground.

27 Question 27: P19, L17: Can you give more examples of such (many) studies?

Giovinetto et al. (1992), Déry and Yau (1999), Déry and Yau (2002), Yang et al. (2010) and Palm et al. (2011).

5 *Here, we do not apply any wind speed threshold to the detection of blowing snow, whereas some modelling studies assume a drifting snow dependency on temperature and wind speed (Giovinetto et al., 1992; Déry and Yau, 1999, 2002; Yang et al., 2010). Palm et al. (2011) for instance, uses a minimum wind speed criterion to detect blowing snow from satellite backscatter, potentially leaving out some events.*

28 Question 28: P19, L19: a “the” is redundant. The properties listed in brackets are not complementary information of “freshly fallen snow”. Please rephrase.

10 The sentence has been adapted accordingly

We find that the presence of freshly fallen snow has a great impact on blowing snow occurrence and blowing snow layer height.

29 Question 29: P19, L29: Which role do you give to the turbulence during katabatic conditions in limiting the occurrence of blowing snow at PE?

15

The sentence was wrongly phrased. The 'limited ' was intended to be related to availability, but also to turbulence. During the katabatic regime, there is little turbulence at PE station, as the greater temperature inversion than for the synoptic regimes suggests. Less turbulence, therefore less particles lifted from the ground.

20 *At PE, the explanation for the limited occurrence of blowing snow under katabatic conditions might lie in the fact that the station is shielded by the Sør Rondane mountains: wind speeds are lower and turbulence is reduced due to the very stable conditions that are frequently present (Gorodetskaya et al., 2013). In addition, the availability of fresh snow is limited as the time lag since the last precipitation event is greater, compared to synoptic conditions.*

30 Question 30: P19, L29-31: Katabatic winds or conditions, not “katabatics”. Please clarify where and how the effect of katabatic winds on the occurrence of blowing snow has been overestimated? Do you actually mean that katabatic winds are not the main driven force behind blowing snow at PE, as usually considered? If so, you should limit this conclusion to the particular geographical settings of PE, which are likely non-representative of the general conditions in coastal East Antarctica.

5

Yes, The analysis of blowing snow occurrence at Princess Elisabeth station reveals that there are fewer blowing snow events during the cold katabatic regime : $N = 152$, 8%, than during the warm synoptic or transitional regimes. This is also illustrated in Fig.3 above: the wind roses show 1 to 2 % of blowing snow taking place during northerly winds. These special conditions at PE have been also described by Thiery et al. (2012) showing that most of the drifting snow sublimation occurs during transitional synoptic regime when the winds are strong due to the nearby cyclone, while air is undersaturated. Larger occurrences of katabatic winds are found in the absence of blowing snow. This indicates that blowing snow occurs predominantly under easterly and north easterly winds, and that the effect of katabatic winds are not the main driver for blowing snow occurrence at PE station. Regarding Neumayer III station, we find that blowing snow occurs mainly during synoptic disturbances, which is also stated by König-Langlo and Loose (2007): "blowing snow is limited to synoptic disturbances and advection from the east". Please note that we discuss significant blowing snow events (layers higher than 30 m height). Drifting snow might give different results, but is not investigated in this paper.

10

15

At PE, the explanation for the limited occurrence of blowing snow under katabatic conditions might lie in the fact that the station is shielded by the Sør Rondane mountains, but also due to the limited availability of fresh snow and the reduced turbulence during those events compared to synoptic conditions, maintaining particles aloft. This, together with the reduced number of blowing snow events occurring under katabatic winds (Fig. 10) might indicate that the effect of katabatic winds on blowing snow occurrence has been overestimated, and that synoptic events bringing fresh snow is a most possibly determining factor for blowing snow at Neumayer III and PE stations.

20

31 Question 31: P20, L7: Specify that this conclusion is only valid for PE.

The sentence has been adapted accordingly. However, this is also valid at Neumayer III station.

25

The presence of precipitation does not substantially limit the retrieval by the ceilometer. This is an improvement to satellite detection, limited to clear sky conditions and therefore missing a great part of the blowing snow as more than half of the blowing snow happens during a storm at PE and Neumayer III station.

32 Question 32: P20, L9: “mainly determines”.

the sentence has been changed accordingly

5 *The availability of fresh snow mainly determines the onset of blowing snow, and the available fresh snow can be lifted to higher heights than during katabatic conditions whose effect is likely to have been overestimated for lifting snow from the surface.*

33 Question 33: P20, L10-11: In which context this conclusion has been drawn?

10 The majority of the blowing snow events occur during transitional or warm regimes at both stations (around 92 %), and only a limited number of blowing snow events have been retrieved during katabatic conditions. In addition, 60 % of the blowing snow events happen together with precipitation, indicating synoptic or transitional events rather than katabatic conditions.

15 *We further conclude that most of the blowing snow events happen during or shortly after precipitation, brought to the continent by the easterly winds associated to synoptic systems. The availability of fresh snow mainly determines the onset of blowing snow, and the available fresh snow can be lifted to higher heights than during katabatic conditions at PE and Neumayer stations. This highlights again the limitation of wind speed thresholds, when applied to blowing snow retrieval methods. The properties of the snow particles, as well as the availability of fresh snow need to be taken into account in order to accurately initiate blowing snow in models.*

34 Question 34: P20, L12: “The availability”: you mean erodibility (availability of fresh snow is not a snow property)?

20 "Including" has been changed to "and".

This highlights again the limitation of wind speed thresholds, when applied to blowing snow retrieval methods. It also emphasizes the need to take into account the properties of the snow particles and the availability of fresh snow, in order to accurately initiate blowing snow in models.

25 **35 Question 35: P20, L15: Use “evaluate” rather than “validate”.**

the sentence has been changed accordingly

These can further be used to evaluate satellite retrieval and combined to produce blowing snow products over the ice sheets.

REVIEWER 2

General comments: The calibration of the ceilometer remains an issue and I wonder if it will be possible. This is important since the use of a ceilometer would start to be relevant for blowing snow studies if a quantitative retrieving of blowing snow characteristics (height of the blowing snow layer, amount of transported snow) may be done. Is it the intention of the authors to perform such a calibration in the future? This point must be considered in the discussion and the conclusion in order to advice the reader about the potentialities and weaknesses of the study. Nevertheless the paper represents a sufficient amount of work to be published. To my opinion the technical description should be improved for a TC reader, especially a modeller. In fact there is too much or not enough. An alternate possibility should be to shorten the technical description and to do it in an other more specialized journal. I had difficulties with a double meaning of some sentences (see specific comments below).

Thank you for your comments, we have replied to each of the comments below.

Calibration of the ceilometer to quantitatively retrieve the amount of transported snow is indeed an issue, as this can not be derived from the ceilometer attenuated backscatter signal. With the current instrumentation this is not possible. Furthermore, we derived a blowing snow algorithm for instruments already present at Princess Elisabeth station. Lidars can be used to define the lidar ratio, but these instruments are (1) more expensive and (2) less abundant than ceilometers. Even after ceilometer calibration, the amount of transported snow can not be derived from particles properties only. We would require to estimate the transport rate also.

We present here our novel BSD algorithm, designed to retrieve blowing snow events, but not drifting snow, from ground-based remote-sensing ceilometers. Ceilometers can retrieve the presence of blowing snow, but other properties such as size, shape and density measurement is only possible if the ceilometer is calibrated, which is very challenging for such a remote location, and not done in this paper.

The algorithm has been adapted to derive precipitation/cloud occurrences from the ceilometer profile directly, and the new version of the paper contains an improved technical description of the algorithm (containing the bin numbers and threshold values, text below), together with a scheme of the concept of the blowing snow algorithm (Fig.8 below, Fig. 5 in the new manuscript).

The approach used for the blowing snow detection (BSD) algorithm is similar, but there is no wind speed criterion in our analysis. In addition, the ceilometer is ground-based, allowing the detection of blowing snow during overcast conditions. The algorithm method is displayed in Fig.5. To detect blowing snow, the intensity of the backscatter signal at the lowest usable bin must exceed a certain threshold (section 3.3), and the intensity of the signal must decrease in the next range bins indicating a particles density greater in the lower levels than at the top of the layer. As previously highlighted, clean air molecules cannot be distinguished because the signal associated with it is smaller than the noise generated by the hardware (Wiegner et al., 2014; Kotthaus et al., 2016) and by the background light (Vande Hey, 2015), polluting the signal in the lowest bins. To distinguish

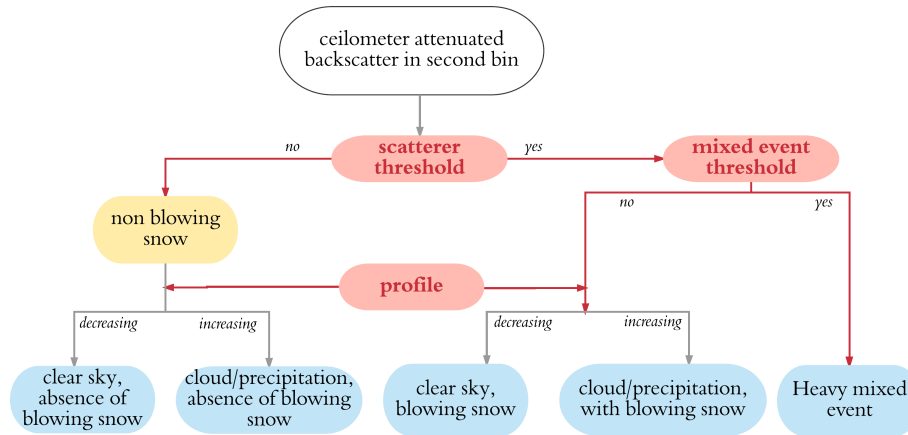


Figure 8. Chart of the blowing snow detection method

the presence of scatterers (aerosols, blowing snow particles, cloud particles...) present in the atmosphere from these artifacts, we need to investigate the signal intensity representative for cloudless conditions. I.e., the average β_{att} of the second range bin received by the ceilometer during scatterer-free conditions. Clear sky days are manually selected for the whole period using the daily quicklooks (Fig.1) and are days where the quicklook background is uniform and without precipitation or clouds, and

5 where the time series of the signal in the second range bin is stable around a low value (corresponding to hardware and background noises), to avoid low-level disrupting signal. Next, we compute the 99th percentile of all clear-sky β_{att} signal in the second range bin as threshold value (for calculation, see section 3.3). As such, it is representative of the presence of scatterers exceeding the value for clear sky. Since the noise is instrument-dependent, individual pre-processing and thresholds have to be defined for each instrument the BSD algorithm is applied to.

10

After comparing the backscatter signal in the second range bin to the clear-sky threshold, the BSD algorithm investigates the shape of the β_{att} profile. A regular clear sky ceilometer profile (signal intensity versus height) does not show intense vertical variations (Fig.6): in the infrared, the transmission term is close to one and decreases only slightly with height. This implies that any important variation in the β_{att} signal can be attributed to the particles backscatter. The blowing snow and

15 blowing snow with precipitation lines in Fig. 6 shows a typical sharp decrease until bin 8-10 (75 - 95 m height), above which the signal keeps decreasing steadily (blue line): this is the signature of clear sky blowing snow. The red profile, on the other hand, shows a re-increase in intensity around the 15th bin (145 m height), overlying the blowing snow signal: this indicates the presence of scatterers interpreted as precipitation (denoted by the arrow on the graph). If there is no blowing snow while precipitation is present, the profile does not decrease prior to the increase at higher levels (black line in Fig.6). The algorithm

20 therefore investigates the shape of the profile in order to detect blowing snow. A condition is set, that a blowing snow profile implies that the mean of the overlying bins 3 to 7 (25 to 65 m) must be lower than the signal in the second range bin (15 m). In this way, the discontinuity, as described in section 3.1. (visible in Figures 1 and 6 between 35 and 45 m), is not affecting our

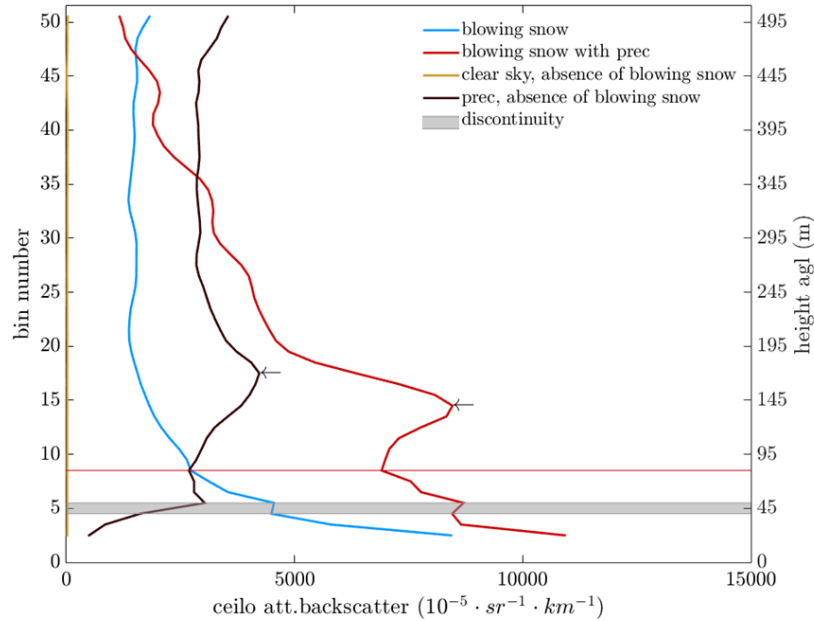


Figure 9. Different types of profiles relevant for blowing snow measured by the ceilometer at PE station: blue line - typical blowing snow signal with no precipitation nor clouds (24-04-2016); red line - blowing snow overlaid by precipitation (10-02-2016); black line - precipitation with no blowing snow (10-02-2014); yellow line - near-zero signal for clear sky conditions (24-04-2016). The height above ground is indicated on the right axis and the corresponding bin number on the left axis. All profiles exclude the lowermost bin, and start at the second bin (15 m agl.). The grey lines represent the discontinuity between bins 4 and 5 (35-45 m). The arrows indicate the presence of precipitation.

retrievals. In order to detect blowing snow occurring during clouds or precipitation, the profile shape is analyzed to identify a second increases in the signal intensity above the 7th bin (65 m height). A clear differentiation between clouds or precipitation cannot be made on the basis of the ceilometer alone, but the presence of clouds and/or precipitation can be identified. This analysis is carried out for both blowing snow and the absence of blowing snow measurements. The information retrieved from the Micro Rain Radar (hourly precipitation rates) is collocated to ceilometer blowing snow detection, to determine the time (in hours) since the last precipitation event at PE station.

Inherent to this profile-based method, the detection of blowing snow during precipitating events is limited to cases when the blowing snow signal is preserved close to the ground. In case of precipitation associated with storms, there is always blowing snow due to the high wind displacing the snow, and no distinction between precipitation and blowing snow is possible, as the ceilometer signal is entirely attenuated near the surface (Gorodetskaya et al., 2015), it is not possible to get signal in the overlying bins, and the profile of the backscatter intensity might not decrease upwards. Such intense precipitating events mixed with snowfall are identified as having a second bin signal higher than $1000 \cdot 10^{-5} \cdot \text{km}^{-1} \cdot \text{sr}^{-1}$ (threshold adapted from Gorodetskaya et al. (2015)). In those cases, the events are classified as a mixed blowing snow event, and the profile analysis is

eluded by the algorithm.

In addition to the detection of blowing snow, the BSD algorithm quantifies the height of the layer (see Fig. S3, supplements) This is done as follows; if the profile decreases steadily (indication of absence of precipitation), the range gate at which the intensity of β_{att} drops under the clear sky threshold value is the top of the layer. Anything above this height is considered clear sky. If there is precipitation or a cloud during the blowing snow event, the shape of the backscatter profile does not decrease monotonously, but shows an increase in higher levels. In that case, the range gate at which the profile increases again is the top of the blowing snow layer, and the base of the cloud and/or precipitation (around the 7th bin in Fig.6, for the black and the red profiles). Layer height definition is illustrated in Fig. S3 in the supplements.

36 **Question 1: p. 2, line 5. : the word “suspension” is defined here but is no used in the rest of the paper (see e.g., line 18 p.7), so that its introduction here is not clear.**

Indeed. I have re-worked this part of the introduction.

This phenomenon occurs approximatively on 70 % of the Antarctic continent during winter (Palm et al., 2011) and snow is transported as "drifting snow" (if the vertical extend of the layer is lower than 2 m), or as "blowing snow" (layers more than 2 m height). These transport involve a mix of suspension and saltation transport modes (Leonard et al., 2011), with a dominance of saltating particles (Bagnold, 1974) in the case of drifting snow, and suspended particles in blowing snow layers (Mellor, 1965).

37 **Question 2: p.2, line 24, note that the precipitation process is also poorly constrained in Antarctica so that the authors have to face to one equation on SMB with at least two unknowns: precipitation and snow erosion by the wind.**

Indeed, although there are products available such as stake measurements (SAMBA dataset (Favier et al., 2013), and observations from the Cloudsat satellite (Palerme et al., 2014)) which allow precipitation estimates on large areas over the continent. In addition, at the Princess Elisabeth station, we have a micro-rain radar that enables to measure precipitation rates. Erosion by the wind is much more difficult to predict there, and is treated as a residual term, containing all the uncertainties on the other terms.

25 *Currently, simulations of the AIS SMB are highly uncertain since both precipitation and blowing snow processes are poorly constrained and probably lead to inconsistencies between the atmospheric modeled precipitations and the measured snow accumulation value (Frezzotti et al., 2004; Scarchili et al., 2010; Groot Zwaaftink et al., 2013; Gorodetskaya et al., 2015; van de Berg et al., 2005).*

Table 2. Climatic conditions at Princess Elisabeth , and Neumayer III stations. For extended climatology, see Gorodetskaya et al. (2013) for PE station and König-Langlo and Loose (2007) for Neumayer station.

variable	Princess Elisabeth	Neumayer III
coordinates	71 °57' S; 23 °21' E	71 °56' S; 23 °20' E
distance from the coast	173 km	approx. 7 km
elevation	1392 m asl	43 m asl
average air temperature	-18 °C	-16 °C
average wind speed	5 m · s ⁻¹	9 m · s ⁻¹
average wind direction		
• synoptic disturbances	90 °to N	100 °to N
• katabatic conditions	180 °to N	170 °to N
relative humidity	56 %	90 %
pressure	827 hPa	986.5 hPa

38 Question 3: p.3, section 2. What are the altitude of both stations PE and Neumayer. Is their climate (e.g., SMB, summer temperature, ...) different? This will help the reader when considering the development of the BSD by using observations at Neumayer and using it for another location.

A table has been added in the new manuscript (Table 2), presenting the climate at both stations (see Table 2 above).

- 5 PE station is located on Utsteinen ridge, 1392 m a.s.l. and 173 km inland. Neumayer station is located on the ice shelf at 43 m a.s.l. Their climate is indeed different. Neumayer is subject to higher wind speeds (9 m · s⁻¹) than PE station (5 m · s⁻¹) and higher relative humidity. PE is located further from the ocean, and is shielded from the katabatic winds by the Sør Rondane mountains. Accumulation is lower due to the distance to the coast. Surface temperature are similar, around -16 / -17 °C. For extended information on Neumayer III and PE meteorology, see König-Langlo and Loose (2007) and Gorodetskaya et al. (2013).

39 Question 4: p.3, section 2.1. An introductory sentence stating that the ceilometer was not initially set up for measuring blown snow events would clarify the section. More generally the description here should contain more information related to a possible use of the measurements for a determination of blown snow characteristics.

- 15 Indeed, although it is already stated at the end of the introduction (previous section), the paragraph has been adapted accordingly. The ceilometer measurement can not be used to determine anything else than blowing snow occurrence. Quantification of blowing snow displacement, and the determination of blowing snow properties such as particles density, shape or number can not be derived from the ceilometer attenuated backscatter signal.

Initially set up to measure cloud base height, ceilometers are rather simple and robust instruments. The algorithm described in this paper was built to derive blowing snow occurrence from the signal received by these devices.

and section 2.1.

5

The quantitative information that can be derived from the ceilometer measurements, is the attenuated backscatter intensity at defined heights (Wiegner et al., 2014; Madonna et al., 2015). Other properties such as optical depth, size and density would require to know the lidar ratio, and a reliable estimate of lidar ratio is complicated (Wiegner et al., 2014). In addition, this is only possible if the ceilometer is calibrated, which is very challenging since the signal to noise ratio has to be large enough in the troposphere (Wiegner et al., 2014) and is not done in the present study. This implies that quantification of blowing snow displacement, and the determination of blowing snow properties such as particles density, shape or number can not be derived from the ceilometer attenuated backscatter signal at Neumayer III and PE stations

10

40 Question 5: p.4, line 1. : what is the raw resolution in time of the ceilometer?

The reporting interval is of 2 s. This is stated in Table 1 in the original manuscript, and the sentence has been removed, for clarity.

15

41 Question 6: p.4, line 2. : “spatial resolution”: do you mean “vertical”?

Yes indeed. The sentence has been adapted accordingly

20

The ceilometer measures continuously and the standard output, β_{att} is displayed in a time-height cross section, with a 10m vertical resolution and 15 s temporal resolution.

42 Question 7: p.4, line 20. : please indicate for each instrument which measurement you intend to use in the paper, especially concerning the infrared pyrometer (see also p.6, line 2 where it is not said there for which purpose the cloud base height deduced from the brightness temperature is used). As for the next comment it is preferable to describe the use of an instrument in a single paragraph.

25

The cloud base temperature is used as a near-atmospheric variable. In the case of blowing snow, the measured cloud temperature is actually the blowing snow layer temperature. It was used in the cluster analysis, and in the PCA. However, it was not a determining variable. This information is left out in the new version of the paper. Only the micro-rain-radar is used to retrieve precipitation rates, in addition to the meteorological variables measured by the automatic weather station.

30

The Metek vertically-profiling precipitation radar, set up since 2010, enables to retrieve snowfall rates, using the return from the vertically profiling Doppler radar operating at a frequency of 24 GHz.

43 Question 8: p. 5, lines 4-6. The ceilometer is described twice. Please rearrange the text.

The text has been rearranged accordingly.

5

A cloud and precipitation observatory was set up on the roof of the station (approx. 10 m above the ridge) during the summer season of 2009-2010 and is still operational under the Hydrant/Aerocloud project (www.aerocloud.be). The observatory contains an automatic weather station (AWS) and a set of ground-based remote sensing instruments. The observatory was designed to be operated year-round, including the winter period when PE is unmanned. The station and the set of instruments

10

are controlled remotely via a satellite connection.
The Vaisala CL-31 ceilometer (firmware 1.72) was installed on the roof of the station in December 2009 and is operational at present. It emits laser pulses at central wavelength of 910 ± 10 nm at 298 K. The measurement vertical resolution is set to 10 m and the reporting interval on 15 s. Several outages of the energy provision system limit the data mainly to Antarctic summer season (December to March is best represented). Only one year of continuous measurements was achieved (2015).

15

The Metek vertically-profiling precipitation radar, set up since 2010, enables to retrieve snowfall rates, using the return from the vertically profiling Doppler radar operating at a frequency of 24 GHz. The raw Doppler spectra is post-processed following Maahn and Kollias (2012), to calculate radar reflectivity profiles which are then linked to snowfall rates using the newly developed Ze-Sr relation for PE by Souverijns et al. (2017) and has a sensitivity up to -14 and -8 dBz (Souverijns et al., 2017). A full description of micro-rain radars can be found in Klugmann et al. (1996) and the radar set up at Princess Elisabeth is

20

described in Gorodetskaya et al. (2015).
The monitoring of the instruments set up on the roof of the station is done via a webcam. Specifications of the instruments are given in Table 2 (see also Gorodetskaya et al. (2013, 2015)).

44 Question 9: p.5, lines 8-9. Please clarify the description of the MRR.

The description of the MRR has been adapted, and references to MRR description (Klugmann et al., 1996) and the specific

25

see question 8 above.

45 Question 10: p.8, line 4. Please indicate the reason of the turning on/off of the heater.

The heater is used to stabilize the laser temperature in cold environments (Kotthaus et al., 2016). The heater is turned on until

30

the device attains the temperature, then is switched off. The temperature of the instrument decreases then, due to the cold

surroundings, and when a minimum temperature is reached, the heater is turned on again.

5 *There are two sources of noise and artifacts affecting the ceilometer backscatter signal: the hardware of the Vaisala ceilometers, and the internal processing of the data (Kotthaus et al., 2016). Firstly, a heater is incorporated in the device to stabilize the laser temperature in cold environments. This heater is placed close to the laser transmitter and the periodic turning on (when a minimum temperature is reached by the instrument) and off (when the laser temperature is high enough) of the heater introduces a small periodic variation in the stability of the emitted signal (and therefore of the detected signal). This effect is stronger in the first range bins, closest to the device.*

46 Question 11: p.14, line 13. What about the role of sastrugi in the evolution of blowing snow intensity?

10 Indeed, the presence of sastrugis has an impact on blowing snow intensity evolution. However, in this section we investigate the changes in near-surface atmospheric variables during blowing snow conditions. Despite their possible impact, sastrugis are not measured either at PE nor at Neumayer III station.

15 *Apart from these factors, sastrugis might also have an impact on blowing snow (Amory et al., 2017) but are not measured here.*

47 Question 12: p.14 – 15, fig. 8 and 9. How do you quantify from a statistical point of view the differences between blowing snow and non blowing snow wind speed and relative humidity? What is your interpretation of the differences for the other variables?

20 By means of a t-test significant at the 95 % level. The difference for the other variables is not significant, meaning that blowing snow or non blowing snow conditions give similar distributions for these variables. However, due to the comments received on this section, it has been removed together with Figs. 8 and 9.

48 Question 13: p.16, line 2. What is the advantage of satellite detection?

25 The advantage of satellite detection is the spatial coverage of blowing snow. This enables Palm et al. (2011) to produce a map of blowing snow frequencies over the whole of the Antarctic continent. A sentence has been added, and the paragraph has been moved to section 5.1 (discussion).

30 *Satellite detections of blowing snow, although covering the whole continent, are limited to clear sky conditions. The BSD algorithm, however, is able to detect blowing snow during most of the storms, which is an improvement compared to satellite detection, as the majority of blowing snow occur together with cloud/precipitation.*

49 Question 14: p.16, line 14. Clarify “observations”

Observations referred to the number of measurements ; i.e. the number of times during the measurement period, that a certain time lag after precipitation is reached.

5 *A possible explanation is that the number of measurements decreases with time, and that blowing snow occurred during those measurements.*

50 Question 15: p.18, lines 17 – 18: “commission errors”: please clarify.

"Commission error" was stated twice, and should only appear once. The second mention should have been "ommission error". In our case, a commission error is a BSD detection that is not reported by the visual observer. It is similar to a "false alarm",
10 but since we do not consider visual observations as ground truth, but as another means of measuring blowing snow, we chose the omission/commission terms. The omission error refers to missing a blowing snow occurrence that is reported by the visual observer.

*Furthermore, the hourly time filtering applied leads to commission errors (events detected by the algorithm, but not reported
15 by the visual observations) and ommission errors (short-lived events are likely removed from the running mean).*

51 Question 16: p.19, line 2. Is it possible to improve the set-up of the ceilometers on the field, and how?

Indeed, however, most of the ceilometers are intended to forecast the weather for planes landing. Depending on the purpose of ceilometer measurements, the ceilometer could be placed closer to the ground to measure lower level blowing snow, and reporting resolution can be adapted (10 m vertical resolution).

20

If setting up a ceilometer in the aim of measuring blowing snow, the device should be placed as close to the ground as possible to also retrieve shallower blowing snow events. The BSD algorithm can be applied to any ceilometer located in Antarctica, but we recommend to use a bin width of 10 m for operating ceilometers to detect blowing snow, which is the case at PE and Neumayer III.

25 52 Question 17: p.20, line 3. : ... designed to retrieve blowing snow events but no drifting snow from ground-based ...

The sentence has been adapted accordingly.

We present here our novel BSD algorithm, designed to retrieve blowing snow events, but not drifting snow, from ground-based remote-sensing ceilometers.

REVIEWER 3 General comments:

1. The evaluation of the performance of the detection algorithm is based on the comparison with human observations at Neumayer III. The different classes (occurrence or not) may be unbalanced (much more cases without blowing snow than with, as suggested on l.14, p.13) requires more robust statistics than the one used. There is a lot of literature about what criteria can be employed for such confusion matrices. See for instance Allouche et al. (2006). I suggest the authors to sue such commonly used statistics (e.g. Cohen's kappa, true skill statistics) for the evaluation of the algorithm. The estimated depth is not really evaluated, what would be needed to do so.

Thank you for this excellent remark. I have used the statistics indicated in Allouche et al. (2006) (see answer to Question 6 below). Regarding the depth of the layer measured by the ceilometer, it is likely underestimated, due to the attenuation of the signal. A way to evaluate the layer height, is to compare height measured by the BSD to satellite detections (data from Palm et al. (2011)), when concurrent. This is part of an ongoing work and not included in this paper.

2. The statistics derived from the outcome of the blowing snow detection algorithm are informative and relevant, but they could be more complete, by including data and analysis about the inter- and intra-event variability of the blowing snow occurrence and depth.

We have performed this analysis on the blowing snow depth, and time versus last precipitation (Figs. 11 and 13 in the original manuscript), but the results showed no real inter variability between the events: Fig.11 was similar. The intra-variability in the layer height versus time since last precipitation (Fig. 10 below) shows two types of events: a majority of blowing snow layers of stable height, and a few events display an increase/decrease in layer heights. Given the limited amount of data and the focus of the paper, we decided to leave this out of the manuscript.

53 Question 1: P.7, l.28: the choice of smoothing the signal over 1 h should be better justified (why 1 h and not 30 min or 2 h?). The typical variability of the BS layer features should be commented (if there is a lot of dynamics within 1 h, one may loose relevant information by smoothing over 1 h).

The reason the running mean was set to 1 hour was to (1) smooth out effects of turbulence, but (2) mainly to get rid of the periodic fluctuation in the signal due to the heater switching on and off. 30 mins is not enough to smooth this out (see figure 11 below), and one hour was chosen since it is the lowest time period at which the heater artifact was substantially smoothed out. This was indeed not mentioned in the original manuscript.

We average every 15s- β_{att} profile over one hour using a running mean, to create mean attenuated backscatter profiles at every time step and avoid the variability due to turbulence and hardware noise. Figure 4. shows the resulting β_{att} at 09:30 UTC, based on the average of 240 profiles (120 preceding and 120 following 09:30 UTC). An additional reason for the integration

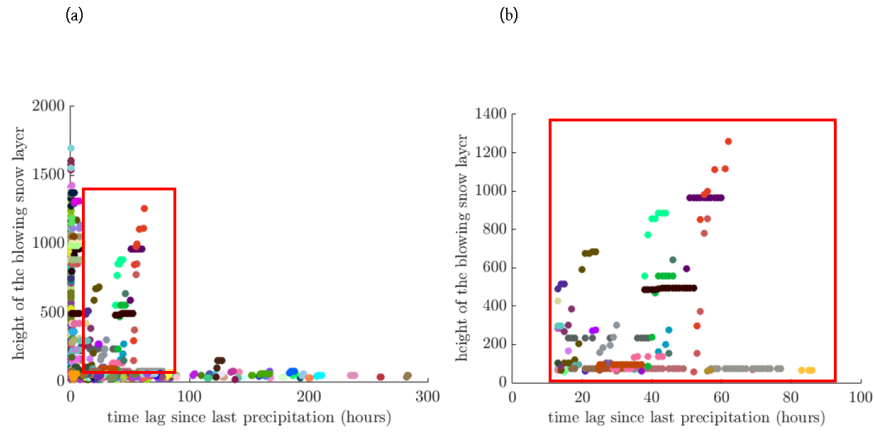


Figure 10. Inter- and intra variability of blowing snow layer height. Each color represents a distinct blowing snow event.

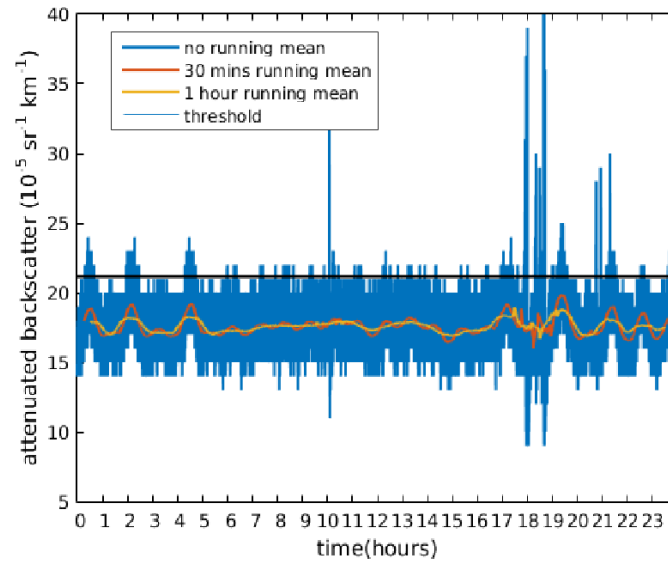


Figure 11. analysis of the periodic fluctuation visible in the ceilometer signal. Second range bin, 06.02.2013, clear sky day.

of the signal over longer time periods, is that it improves the signal to noise ratio (SNR). No additional SNR correction is performed on the raw data, as we found that a temporal SNR higher than 0.3 would remove parts of the blowing snow signal (Gorodetskaya et al., 2015).

There are two sources of noise and artifacts affecting the ceilometer backscatter signal: the hardware of the Vaisala ceilometers, and the internal processing of the data (Kotthaus et al., 2016). Firstly, a heater is incorporated in the device to stabilize the laser temperature in cold environments. This heater is placed close to the laser transmitter and the periodic turning on (when a minimum temperature is reached by the instrument) and off (when the laser temperature is high enough) of the heater introduces a small periodic variation in the stability of the emitted signal (and therefore of the detected signal). This effect is stronger in the first range bins, closest to the device, and the hourly running mean enables to smooth out most of this signal variation.

54 Question 2:P.8, l.1: “SNR higher than 0.3”: I guess it is expressed in dB. If so, it should be clearly mentioned.

The SNR is the signal-to-noise ratio, and is unteless. It is calculated at each height range bin j at time step i as :

$$10 \quad SNR_{i,j} = \frac{\overline{\beta_{i,j}}}{\sqrt{\frac{1}{2M} \sum_{k=-M}^{+M} (\beta_{i+k,j} - \overline{\beta_{i,j}})^2}} \quad (1)$$

which is the ratio of the temporal mean $\overline{\beta_{i,j}}$ and standard deviation of the attenuated backscatter over $\pm M$ time steps around time step i and range bin j (Van Tricht et al., 2014).

No additional SNR correction is performed on the raw data, as we found that a temporal SNR higher than 0.3 would remove parts of the blowing snow signal (Gorodetskaya et al., 2015).

55 Question 3: P.10, Fig.5: I probably missed something, but I do not understand why the backscatter signal from BS+precip is so much smaller (below 100 m alt) than the one from BS only (red vs blue). I would expect the two signals to sum up somehow... Or is the concentration in BS particles much smaller when there is precip? If so, what could be the explanations?

20 Figure 5 (Fig. 6 in the new manuscript) is indeed not clear, as we chose one day (24.04.2016) where the different typical events occur. During that day, blowing snow accompanied with cloud/precipitation unfortunately occurred at the end of the blowing snow event. Hence, the lower intensities and the resemblance to the pure precipitation profile. We have therefore selected another day (10.02.2014) to illustrate the pure precipitation, and the mixed event. In this new figure (Fig.12 below, Fig.6 in the new manuscript), the intensity of the profile in the lowermost bins is clearly indicative of blowing snow (red line), and the increase around the 15th bin indicates the presence of clouds/precipitations (arrow). In the case of precipitation/cloud without blowing snow, this low-level decrease is absent, and the increase around the 17th bin reflects the presence of a cloud/precipitation.

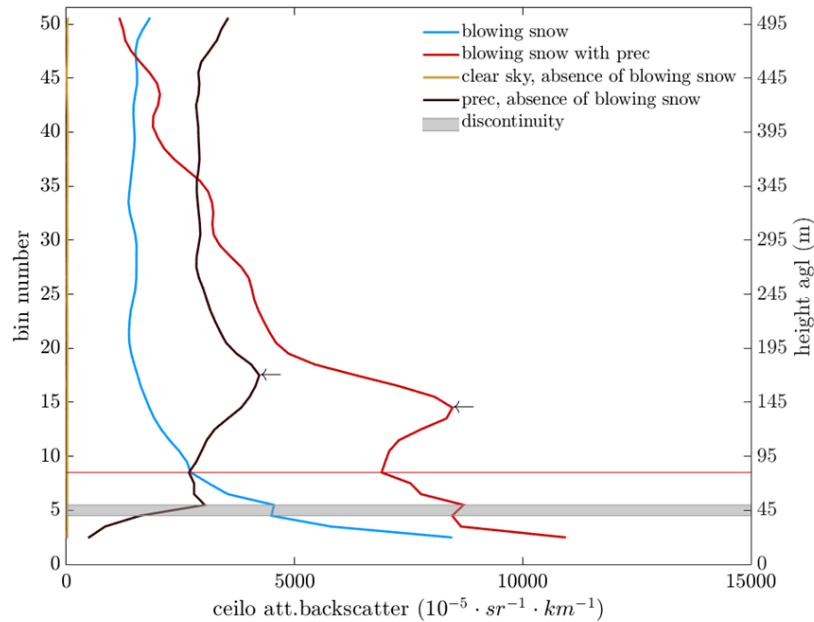


Figure 12. Different types of profiles relevant for blowing snow measured by the ceilometer at PE station: blue line - typical blowing snow signal with no precipitation nor clouds (24-04-2016); red line - blowing snow overlaid by precipitation (10-02-2016); black line - precipitation with no blowing snow (10-02-2014); yellow line - near-zero signal for clear sky conditions (24-04-2016). The height above ground is indicated on the right axis and the corresponding bin number on the left axis. All profiles exclude the lowermost bin, and start at the second bin (15 m agl.). The grey lines represent the discontinuity between bins 4 and 5 (35-45 m). The arrows indicate the presence of precipitation.

56 Question 4: P.10, l.19: related question: it is written “The precipitation intensity might cover the blowing snow signal”, which I find confusing with the curves in Fig.5 (for the lower altitudes). To be clarified...

We know that most of the time, blowing snow happens together with storms and intense precipitation (the snowflakes rebound on the ground and are displaced by strong winds). Hence, in some cases the signal intensity is not decreasing with height, and the profile criterion is not met. In those cases, blowing snow during very intense events was discarded by the algorithm. Fig 13 (below) presents a case of blowing snow around 23:00 UTC (intense coloration). From the profiles for 23:00 UTC it is clear that the signal of the cloud eclipses that of blowing snow, even though the threshold is largely exceeded in the second bin, and the decrease in bins 2-3 is visible. As the intensity of the signal in bins 3 to 7 is larger than in the second bin, the BSD algorithm does not detect blowing snow. We therefore adapted the method, applied in the new version of the manuscript. This improved algorithm limits the decrease of the profile to cases where the precipitation signal is not intense. In cases of signal in the second bin exceeding $1000 \cdot 10^{-5} \cdot \text{km}^{-1} \cdot \text{sr}^{-1}$ (threshold adapted from (Gorodetskaya et al., 2015)), the algorithm reports

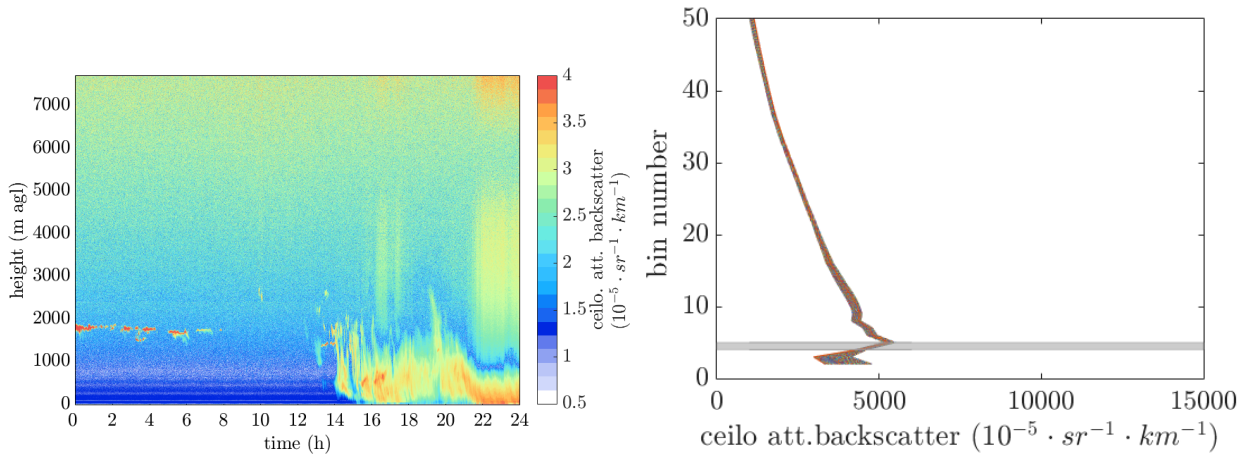


Figure 13. Quicklook presenting a mixed blowing snow event : clouds and precipitation occurring together with blowing snow around 23:00 UTC (left), and ceilometer attenuated backscatter profiles (intensity versus height) around 23:00 UTC (right).

a heavy precipitation event mixed with blowing snow in all cases. A chart presenting the blowing snow detection algorithm has been added to the paper (Fig. 14 below, Fig.5 in the new manuscript).

The algorithm therefore investigates the shape of the profile in order to detect blowing snow. A condition is set, that a blowing snow profile implies that the mean of the overlying bins 3 to 7 (25 to 65 m) must be lower than the signal in the second range bin (15 m). In this way, the discontinuity, as described in section 3.1. (visible in Figures 1 and 6 between 35 and 45 m), is not affecting our retrievals. In order to detect blowing snow occurring during clouds or precipitation, the profile shape is analyzed to identify a second increase in the signal intensity above the 7th bin (65 m height). A clear differentiation between clouds or precipitation cannot be made on the basis of the ceilometer alone, but the presence of clouds and/or precipitation can be identified. This analysis is carried out for both blowing snow and non blowing snow measurements. The information retrieved from the Micro Rain Radar (hourly precipitation rates) is collocated to ceilometer blowing snow detection, to determine the time (in hours) since the last precipitation event at PE station.

Inherent to this profile-based method, the detection of blowing snow during precipitating events is limited to cases when the blowing snow signal is preserved close to the ground. In case of precipitation associated with storms, there is always blowing snow due to the high wind displacing the snow, and no distinction between precipitation and blowing snow is possible, as the ceilometer signal is entirely attenuated near the surface (Gorodetskaya et al., 2015), it is not possible to get signal in the overlying bins, and the profile of the backscatter intensity might not decrease upwards. Such intense precipitating events mixed with snowfall are identified as having a second bin signal higher than $1000 \cdot 10^{-5} \cdot \text{km}^{-1} \cdot \text{sr}^{-1}$ (threshold adapted from Gorodetskaya et al. (2015)). In those cases, the events are classified as a mixed blowing snow event, and the profile analysis is eluded by the algorithm.

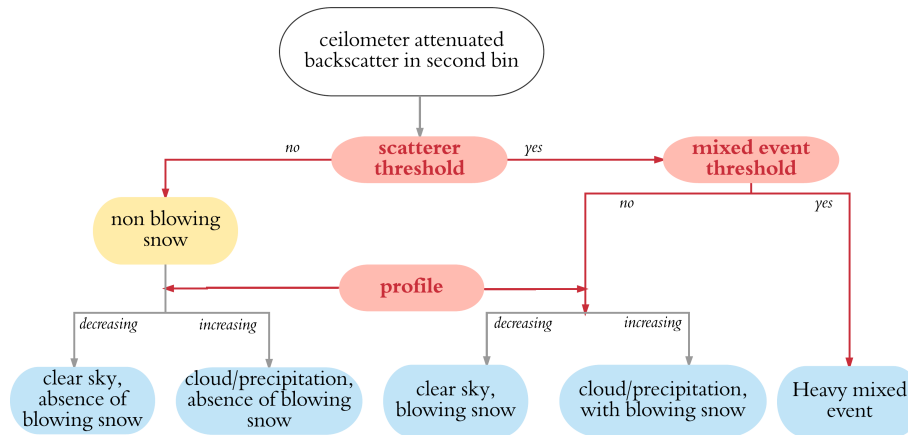


Figure 14. Chart of the blowing snow detection method

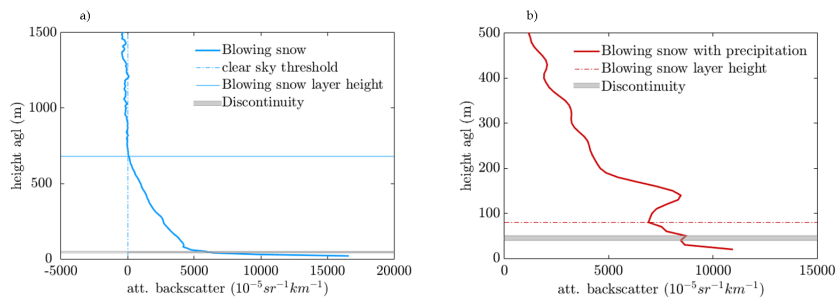


Figure 15. Determination of the height of the layer by the BSD algorithm. (a) in case of a clear sky blowing snow profile, the height of the layer is attained when the backscatter intensity reaches the clear sky threshold. (b) in case of precipitation, the height of the blowing snow layer is reached when the intensity of the backscatter signal re-increases.

57 Question 5: P.11, l.6-7: about the estimation of the top of the BS layer: it would help the reader to indicate in Fig.5 where is this limit. And how reliable would be the outcome in case of virgas?

Indeed. The graphs have been added (Fig. 15 above) to the Supplements (Fig. S3 in the new manuscript)

5 In our case, no distinction is made between clouds, precipitation and virga. this means that any re-increase in the profile is treated as the presence of clouds and/or precipitation.

If there is precipitation or a cloud/virga during the blowing snow event, the range gate at which the profile increases again is the top of the blowing snow layer, and the base of the cloud and/or precipitation layer (around the 7th bin in Fig.14, for the black and the red profiles). Layer height definition is illustrated in Fig. S3 in the supplements.

10

Table 3. Detection numbers and scores of the different categories of observations. The first 4 columns give N BS_{both} - stands for blowing snow detected by both the algorithm and the visual observations, N BS_{none} - when both methods agree that there is no blowing snow, N BS_{ceilo} and N BS_{vis} - represent detections by the algorithm and the observer only, respectively (the corresponding percentages are presented in table S4, in the supplement). The four last columns give the scores. B stands for blowing and D for drifting snow. The total number of measurements is 10584.

	N BS _{both}	N BS _{none}	N BS _{ceilo}	N BS _{vis}	accuracy	sensitivity	specificity	TSS
B and D snow, with or without prec	2404	5170	972	2308	0.70	0.51	0.84	0.35
B and D snow, without prec	992	6578	2373	897	0.70	0.52	0.73	0.26
heavy B snow, without prec	378	7406	2998	72	0.72	0.84	0.71	0.55
all B snow, without prec	822	6993	2554	485	0.72	0.63	0.73	0.36
all B snow, with or without prec	1856	6665	1520	813	0.78	0.69	0.81	0.51
heavy blowing snow, with or without prec	1114	7249	2262	229	0.77	0.83	0.76	0.59

58 Question 6: P.12, 1.7-14: better metrics could be computed to evaluate the performance of the algorithm, see General comments above.

Indeed, thank you for this excellent remark. I have used the statistics indicated in Allouche et al. (2006).

5 *The results (Table 3 and table S4, in supplements) show a very good match in the blowing snow detection (Table. 3) and the optimum, 78 %, is reached for events classified as (heavy) blowing snow with or without precipitation. The lowest match (70 %) is found when all blowing and drifting snow is taken into account: the number of visually detected events strongly increases since more categories are included, whereas the number of detections by the BSD algorithm is fixed. In 21 % of the time, the visual observer reports something (blowing or drifting snow) that is not detected by the BSD algorithm. This is related to*
10 *the fact that the ceilometer points upwards and is elevated at a height of 12-15 m above the surface, which prevents it from detecting shallow layers of drifting snow.*

A fraction of 84 % visually observed heavy blowing snow events is detected by the BSD algorithm:

$$\frac{NBS_{both}}{NBS_{both} + NBS_{vis}} \quad (2)$$

In this case, we consider visual observations reported as 'heavy blowing snow' only. For 95 % of the N BS_{ceilo} events not
15 *reported as 'heavy blowing snow' by the observer, intensities of the backscatter signal are below $1000 \cdot 10^{-5} \cdot \text{km}^{-1} \cdot \text{sr}^{-1}$; it is therefore likely that those events are classified as 'slight' or 'moderate' by the visual observer instead of being considered heavy. For the N BS_{vis}, 54 % do not attain the threshold indicating the presence of scatterers and in 46 % of the cases the ceilometer attenuated backscatter profile does not decrease with height.*

We also compare the skills of the BSD algorithm to different evaluation metrics (Allouche et al., 2006) (the equations for
20 *each of the metrics are presented in Supplements). The accuracy, highest for the category collecting all blowing snow events,*

is the proportion of correctly detected events. To take into account omission errors, sensitivity is used and the best score is attained by both heavy blowing snow categories. Specificity reflects commission errors, and the categories encompassing most events (blowing and drifting snow) perform best. Finally, since the N_{BSnone} is larger than the other categories, the matches are likely biased, and we therefore use the true skill statistics (TSS, (Allouche et al., 2006)), which is a method enabling to
5 measure the overall accuracy and correct for the accuracy expecting to occur by chance, which also accounts for commission and omission errors, while being independent of prevalence in the data. TSS statistics range from -1 to +1, where values under zero indicate no better performance than random, and the closest the result to 1, the better the agreement. This metric clearly indicates that heavy blowing snow is the best detected category of events.

10 **59 Question 7: P.14, l.3: Which statistical tests have been used to check if there are “statistically significant differences”?**

By means of a t-test, at the 95 % significance level. The difference for the other variables is not significant, meaning that blowing snow or non blowing snow conditions give similar distributions for these variables. However, due to the comments received, this section has been removed from the new version of the manuscript, together with Figs. 8 and 9.

15 **60 Question 8: P.15, l.16: a minimum of description should be provided about the clustering method employed, so the reader does not have to check the reference to know what type of clustering method has been used for instance...**

Some information has been added. However, since the ceilometer profile classification is also useful to discriminate between the different types of events, less emphasis is put on the cluster analysis.

20 *The near surface atmosphere changes, associated with blowing snow events, are investigated for both stations, and detailed means and standard deviation are displayed in Table S6 and S7, in supplements. We investigate how blowing snow hourly means relate to weather regimes, derived from the hierarchical cluster analysis using PE AWS data following Gorodetskaya et al. (2013), which defines the weather regimes at PE station: "cold katabatic", "warm synoptic", and "transitional synoptic". The cold katabatic regime is characterized by slower wind speeds and lower humidity, reduced incoming long wave radiation, a slight surface pressure increase, and a substantial temperature inversion. Warm synoptic conditions involve higher wind
25 speeds and specific humidity, strongly positive anomalies of incoming long wave radiation. The surface pressure is slightly lower, and the temperature inversion is strongly reduced than during average conditions. Finally, average wind speeds, humidity and incoming long wave radiation, as well as slightly lower surface pressure are observed during the transitional regime, when the situation evolves from synoptic to katabatic or the other way around (Gorodetskaya et al., 2013).*

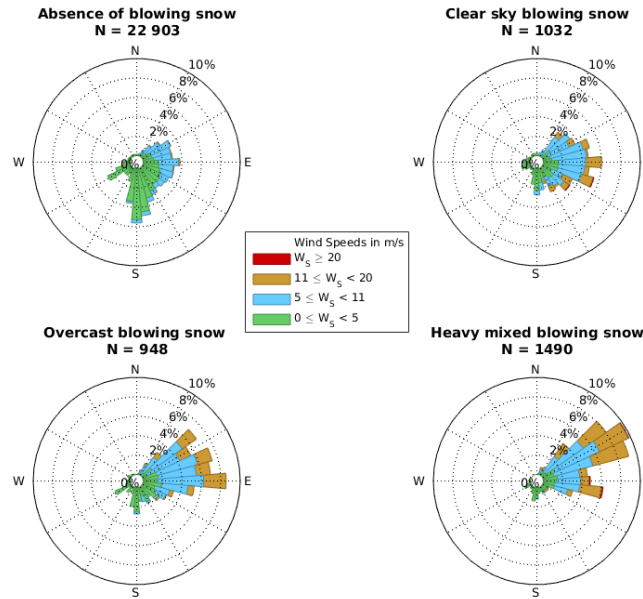


Figure 16. Wind roses presenting the wind direction for all blowing snow, blowing snow with or without precipitation, and non-blowing snow conditions at Princess Elisabeth station.

61 Question 9: P.16, Fig.10: the font size of the text in the figure should be increased.

The font size has been adapted accordingly (see Fig.16 above).

62 Question 10: P.16, l.14: I do not understand why the number of observations would decrease... The ceilometer is collecting data every 15s, no? The explanation should be clarified.

- 5 The sentence was wrongly phrased. "Observations" has been replaced by "measurements". The number of "observations/measurements" decreases because it is rare that there is no precipitation for a dozen of days continuously.

This is, however, not so obvious if we normalize the distribution of blowing snow events taking into account the total number of measurements within each time lag after precipitation [...]. A possible explanation is that there are less measurements as we go in time, and that blowing snow occurred during those measurements.

63 Question 11: P.18, Fig.13: are these distributions for the two stations (Neumayer and PE) or only one location?

This is for PE station only, since the time since the last precipitation event is only available using the micro-rain radar. The text and legend have been adapted accordingly.

5 *We further tested the hypothesis that the height of the blowing snow layer is related to wind speed at PE station. While there is no correlation, (also found by Mahesh et al. (2003)), the height of the blowing snow layer is related to the time since last precipitation (Fig. 13). The height of the blowing snow layer can reach up to 1000 m within 24 to 48 h after precipitation, and 95 % of the blowing snow layers thicker than 500 m occur shortly after the last precipitation event at PE. Blowing snow events taking place much later after the precipitation event are limited to a vertical extend lower than 100 m thick.*

10

and legend :

Scatter plot of the time since last precipitation event versus height of the blowing snow layer at PE station. Each point represents a blowing snow event. The colorbar represent the data density (number of observations divided by the entire sample size).

15

64 Question 12. P.18, l.17: "commission errors" is repeated twice.

"Commission error" was stated twice, and should only appear once. The second mention should have been "ommission error". In our case, a commission error is a BSD detection that is not reported by the visual observer. It is similar to a "false alarm", but since we do not consider visual observations as ground truth, but as another means of measuring blowing snow, we chose the omission/commission terms. The omission error refers to missing a blowing snow occurrence that is reported by the visual observer.

20

Furthermore, the hourly time filtering applied leads to commission errors (events detected by the algorithm, but not reported by the visual observations) and ommission errors (short-lived events are likely removed from the running mean).

25 **65 Question 13. P.19, l.9: I guess the same algorithm could be applied to lidar systems, no?**

Indeed, the algorithm could be adapted to lidars. However, we developed the algorithm for existing instruments at PE station, which is not equipped with a lidar. Moreover, such instruments are more expensive, and less widespread as ceilometers (low-cost networks).

References

- Allouche, O., Tsoar, A. and Kadmon, R.: Assessing the accuracy of species distribution models: prevalence, kappa and the true skills statistics (TSS), *Journal of applied Ecology*, 43, 1223–1232, 2006.
- Amory, C., Gallée, H., Naaim-Bouvet, F., Favier, V., Vignon, E., Picard, G., Trouvilliez, A., Piard, L., Genthon, C., Bellot, H.: Seasonal
5 Variations in Drag Coefficient over a Sastrugi-Covered Snowfield in Coastal East Antarctica, *Boundary-Layer Meteorol.*, 164, 107–133, 2017.
- Amory, C., Trouvilliez, A., Gallée, H., Favier, V., Naaim-Bouvet, F., Genthon, C., Agosta, C., Piard, L., and Bellot, H.: Comparison between observed and simulated eolian snow mass fluxes in Adélie Land, East Antarctica, *The Cryosphere*, 9, 1373–1383, 2015.
- Bagnold, R. A.: *The Physics of Blown Sand and Desert Dunes*, Mathuen, London, 265 pp., 1954.
- 10 Barral, H., Genthon, C., Trouvilliez, A., Brun, C., Amory, C.: Blowing snow in coastal Adélie Land, Antarctica: three atmospheric-moisture issues, *The Cryosphere*, 8, 5, 1905–1919, 2014.
- Dai, X., and Huang, N.: Numerical simulation of drifting snow sublimation in the saltation layer, *Scientific Reports*, 4 (6611), 1–5, doi: 10.1038, 2014.
- Déry, S. J., and Tremblay, L. B.: Modeling the Effects of Wind Redistribution on the Snow Mass Budget of Polar Sea Ice, *J. Phys. Oceanogr.*,
15 34, 258–271, 2004.
- Déry, S. J., and Yau, M. K.: A climatology of adverse winter-type weather events, *J. Geophys. Res.*, 104, 16,657–16,672, 1999.
- Déry, S. J., and Yau, M. K.: Large-scale mass balance effects of blowing snow and surface sublimation, *J. Geophys. Res.*, 107(D23), doi:10.1029/2001JD001251, 8-1 – 8-17, 2002.
- Favier, V., Agosta, C., Parouty, S., Durand, G., Delaygue, G., Gallée, H., Drouet, A. S., Trouvilliez, A., and Krinner, G.: An updated and
20 quality controlled surface mass balance dataset for Antarctica, *The Cryosphere*, 7, 583–597, doi:10.5194/tc-7-583-2013, 2013.
- Frezzotti M., Pourchet, M., Flora, O., Gandolfi, S., Gay, M., Urbini, S., Vincent, C., Becagli, S., Gagnani, R., Proposito, M., Severi, M., Traversi, R., Udisti, R., and Fily, M.: New estimations of precipitation and surface sublimation in East Antarctica from snow accumulation measurements, *Clim. Dyn.*, 23, 803–813, 2004.
- Gallée, H., Guyomarc’h, G., and Brun, E.: Impact of snow drift on the Antarctic ice sheet surface mass balance : possible sensitivity to
25 snow-surface properties, *Boundary Layer Meteorol.*, 99, 1–19, 2001.
- Giovinetto, M.B., Bromwich, D.H., and Wendler, D.: Atmospheric Net Transport of Water Vapor and Latent Heat Across 70°S, *J. Geophys. Res.*, 97, 917–930, 1992.
- Gorodetskaya, I. V., Tsukernik, M., Claes, K., Ralph, M. F., Neff, W. D., and van Lipzig, N. P. M.: The role of atmospheric rivers in anomalous snow accumulation in East Antarctica, *Geophys. Res. Lett.*, 16, 6199-6206, 2014.
- 30 Gorodetskaya I. V., Kneifel, S., Maahn, S., Van Tricht, K., Thiery, W., Schween, J. H., Mangold, A., Crewell, S., and van Lipzig, N. P. M.: Cloud and precipitation properties from ground-based remote-sensing instruments in East Antarctica, *The Cryosphere*, 9, 286–304, 2015.
- Gorodetskaya, I. V., van Lipzig, N. P. M., van den Broeke, M. R., Mangold, A., Boot, W., and Reijmer, C. H.: Meteorological regimes and accumulation patterns at Utsteinen, Dronning Maud Land, East Antarctica: Analysis of two contrasting years, *J. Geophys. Res.*, 118, 4, 1700–1715, 2014.
- 35 Groot Zwaafink, C. D., Cagnati, A., Crepaz, A., Fierz, C., Macelloni, G., Valt, M., and Lehning, M.: Event-driven deposition of snow on the Antarctic Plateau: analyzing field measurements with SNOWPACK, *The Cryosphere*, 7(1), 333–347, 2013.

- Klugmann, D., Heinsohn, K., Kirtzel, H.J.: A low cost 24 GHz FM-CW Doppler radar rain profiler, *Contributions to Atm. Phys.*, 69, 247–253, 1996.
- Kodama, Y., Wendler, G., and Gowink, J.: The effect of blowing snow on katabatic winds in Antarctica, *Ann. Glaciol.*, 6, 59–62, 1985.
- König-Langlo, G., and Loose, B.: The Meteorological Observatory at Neumayer Stations (GvN and NM-II) Antarctica, *Polarforschung*, 76 (1-2), 25-38, 2007.
- Kotthaus, S., O'Connor, E., Muenkel, C., Charlton-Perez, C., Gabey, M. G, and Grimmond, C. S. B.: Recommendations for processing atmospheric attenuated backscatter profiles from Vaisala CL31 Ceilometers, *Atmos. Meas. Tech. Discuss.*, 9.8, 3769–3791, 2016.
- Lenaerts, J. T. M., and van den Broeke, M. R.: Modeling drifting snow in Antarctica with a regional climate model: 2. Results, *J. Geophys. Res.*, 117(D5), D05109, 2012.
- 10 Lenaerts, J. T. M., van den Broeke, M.R., Déry, S.J., König-Langlo, G., Ettema J., and Munneke, P.K.: Modelling snowdrift sublimation on an Antarctic ice shelf, *The Cryosphere*, 4, 179–190, 2010.
- Leonard, K. C., Tremblay, L. B., Thom, J. E., and MacAyeal, D. R.: Drifting snow measurements near McMurdo station, Antarctica: A sensor comparison study, *Cold Regions Science and Technology*, 70, 71–80, 2011.
- Lesins, G., Bourdages, L., Duk, T. J., Drummond, J. R., Eloranta, E. W., and Walden, V. P.: Large surface radiative forcing from topographic blowing snow residuals measured in the High Arctic at Eureka, *Atm. Chem. Phys.*, 9(6), 1847–1862, 2009.
- 15 Maahn, M., and Kollias, P.: Improved Micro Rain Radar snow measurements using Doppler spectra post-processing, *Atm. Meas. Tech.*, 5, 2661-2673, 2012.
- Madonna, F, Amato, F, Vande Hey, J., and Pappalardo, G.: Ceilometer aerosol profiling versus Raman lidar in the frame of the INTERACT campaign of Actris, *Atmos.Meas.Tech.*, 8, 2207–2223, 2015.
- 20 Mahesh, A., Eager, R., Campbell, J. R., and Spinhirne, J.D.: Observations of blowing snow at South Pole, *Journal of Geophysical Research*, 108 (D22), 4707, 2003.
- Mellor, M.: *Blowing Snow*, Cold Regions Science and Engineering: Part II, section A3c., 78pp., 1965.
- Palermé, C., Kay, J. E., Genthon, C., L'Ecuyer, T., Wood, N. B., and Wood, C.: How much snow falls on the Antarctic ice sheet?, *The Cryosphere*, 8, 1577–1587, doi: 10.5194/tc-8-1577-2014, 2014.
- 25 Palm, S. P., Yang, Y. Spinhirne, J. D., and Marshak, A.: Satellite remote sensing of blowing snow properties over Antarctica, *J. Geophys. Res.*, 116, D16123, 2011.
- Parish, T. R. and Bromwich, D. H.: Reexamination of the Near-Surface Airflow over the Antarctic Continent and Implications on Atmospheric Circulations at High Southern Latitudes, *Mon. Wea. Rev.*, 135, 5, 961–1973, doi:10.1175/MWR3374.1, 2007.
- Scarchili, C., Frezzotti, M., Grigioni, P., De Silvestri, L., Agnoletto, L., and Dolci, S.: Extraordinary blowing snow transport events in East Antarctica, *Clim. Dyn.*, 34, 1195–1206, 2010.
- 30 Souverijns, N., Gossart, A., Lhermitte, S., Gorodetskaya, I.V., Kneifel, S., Maahn, M., Bilven, F.L., and van Lipzig, N.P.M.: Estimating radar reflectivity - snowfall rate relationships and their uncertainties over Antarctica by combining disdrometer and radar observations, *Atmos. Res.*, accepted.
- Takahashi, S., Endoh, T., Azuma, N., and Meshida, S.: Bare ice fields developed in the inland part of Antarctica, *Proc. NIPR Symp. Polar Meteorol. Glaciol.*, 5, 128–139, 1992.
- 35 Thiery, W., Gorodetskaya, I.V., Bintanja, R., van Lipzig, N. M. P., van den Broeke, M.R., Reijmer, C. H., and Kuipers Munneke, P.: Surface and snowdrift sublimation at Princess Elisabeth station, East Antarctica, *The Cryosphere*, 6(4), 841–857, 2012.

- Trouvilliez, A., Naim-Bouvet, F., Genthon, C., Piard, L., Favier, V., Bellot, H., Agosta, C., Palerme, C., Amory, C., and Gallée, H.: A novel experimental study of aeolian snow transport in Adelie Land (Antarctica), *Cold Regions Science and Technology*, 108, 125–138, 2014.
- van de Berg, W., van den Broeke, M. R., Reijmer, C. H., and van Meijgaard, E.: Characteristics of the Antarctic surface mass balance, 1958-2002, using a regional atmospheric climate model, *Ann. Glaciol.*, 41(1), 97–104, 2005.
- 5 Vande Hey, J. D.: *A Novel Lidar Ceilometer: Design, Implementation and Characterisation*, Springer Theses, ISBN: 978-3-319-12612-8 (Print) 978-3-319-12613-5 (Online), Springer International Publishing, 2015.
- van den Broeke, M. R., Reijmer, C. H., and van de Wal, R. S. W.: A study of the surface mass balance in Dronning Maud Land, Antarctica, using automatic weather stations, *J. Glaciol.*, 50 (171), 565–581, 2004.
- Van Tricht, K., Gorodetskaya, I.V., Lhermitte, S., Turner, D.D., Schween, J.H., and van Lipzig, N.P.M.: An improved algorithm for polar
10 clouds-base detection by ceilometer over the ice sheets, *Atmos.Meas.Tech.*, 7, 1153–1167, 2014.
- Wiegner, M., Madonna, F., Biniotoglou, I., Forkel, R., Gasteiger, J., Geiß, A., Pappalard, G., Schäfer, K., and Thomas, W.: What is the benefit of ceilometers for aerosol remote sensing? An answer from EARLINET, *Atmos. Meas. Tech.*, 7, 1979–1997, 2014.
- Yamanouchi, T., and Kawaguchi, S.: Effects of drifting snow on surface radiation budget in the katabatic wind zone, Antarctica, *Ann. Glaciol.*, 6, 238–241, 1985.
- 15 Yang, J., Yau, M.K., Fang, X., and Pomeroy, J.W.: A triple-moment blowing snow-atmospheric model and its application in computing the seasonal wintertime snow mass budget, *Hydrol. Earth Syst. Sci.*, 14, 1063–1079, 2010.

Blowing snow detection from ground-based ceilometers: application to East Antarctica

Alexandra Gossart¹, Niels Souverijns¹, Irina V. Gorodetskaya^{2,1}, Stef Lhermitte^{3,1}, Jan T.M. Lenaerts^{4,1,5}, Jan H. Schween⁶, Alexander Mangold⁷, Quentin Laffineur⁷, and Nicole P.M. van Lipzig¹

¹Department of Earth and Environmental Sciences, KU Leuven, Leuven, Belgium

²Centre for Environmental and Marine Sciences, Department of Physics, University of Aveiro, Aveiro, Portugal

³Department of Geosciences and Remote Sensing, Delft University of Technology, Delft, the Netherlands

⁴Institute for Marine and Atmospheric research Utrecht, Utrecht University, Utrecht, The Netherlands

⁵Departement of Atmospheric and Oceanic Sciences, University of Colorado, Boulder CO, USA

⁶Institute of Geophysics and Meteorology, Koeln University, Koeln, Germany

⁷Royal Meteorological Institute of Belgium, Brussels, Belgium

Correspondence to: Alexandra Gossart (alexandra.gossart@kuleuven.be)

Abstract. Blowing snow impacts Antarctic ice sheet surface mass balance by snow redistribution and sublimation. Yet, numerical models poorly represent blowing snow processes, while direct observations are limited in space and time. Satellite retrieval of blowing snow ~~are is~~ hindered by clouds and only ~~consider~~ the strongest events ~~are considered~~. Here, we develop a blowing snow detection (BSD) algorithm for ground-based remote sensing ceilometers in polar regions, and apply it to ceilometers at Neumayer III and Princess Elisabeth (PE) stations, East Antarctica. The algorithm is able to detect (heavy) blowing snow layers reaching 30 m high. Results show that ~~79-78%~~ of the detected events are in agreement with visual observations ~~-.The at Neumayer. The BSD detects heavy blowing snow 36% of the time at Neumayer (2011-2015) and 13% at Princess Elisabeth station (2010-2017). Blowing snow occurrence peaks during the austral winter, and shows around 5% inter-annual variability.~~ The BSD algorithm is capable to detect both blowing snow lifted from the ground and occurring during precipitation, which is an added value since ~~most results indicate that 92%~~ of the blowing snow ~~occurs-takes place~~ during synoptic events, often combined with precipitation. ~~Our analysis-Analysis~~ of atmospheric meteorological variables ~~during blowing snow~~ shows that blowing snow occurrence strongly depends on fresh snow availability in addition to wind speed, ~~while~~. This finding challenges the commonly used parametrizations, where the threshold for snow particles to be lifted is ~~commonly parametrized as~~ a function of wind speed only. Blowing snow occurs predominantly during storms and overcast conditions, shortly after precipitation events, and can reach up to 1300 m in case of heavy mixed events (precipitation and blowing snow together). These results suggest ~~that the effect of katabatics and wind speed might have been overestimated~~ an important role of synoptic conditions in generating blowing snow events, and that fresh snow availability should be considered in determining the blowing snow onset.

1 Introduction

Understanding the Antarctic ice sheet (AIS) response to atmospheric and oceanic forcing is crucial given its large potential impact on sea level rise (Rignot and Thomas, 2002; Rignot and Jacobs, 2002; Rignot et al., 2011; Shepherd et al., 2012).

AIS mass balance is governed by the difference between surface mass balance (SMB) and solid ice discharging into the ocean. Solid precipitation is the only source term for the SMB. Meltwater runoff and surface sublimation are processes removing mass at the surface of the AIS, as well as the sublimation of the suspended snow particles. A fourth process is the wind-induced erosion or re-deposition of transported snow particles from one location to another (Takahashi et al., 1988):

5 Snow particles can be dislodged from the snow surface and picked up by high wind speeds, the wind and lifted from the ground into the near-surface atmospheric layer. ~~This phenomenon occurs approximately on 70% of the Antarctic continent during winter (Palm et al., 2011) and snow is transported (1) by saltation, which is usually called "drifting snow" (0-0.3 height, wind speeds from 2 to 5); (2) in suspension (layers up to~~ Generally, drifting snow events are shallower than blowing snow events. Drifting snow typically stays below 2 m high, wind speeds over 5), and (3) height whereas

10 blowing snow can reach heights of several hundreds of meters. The transport involves a mix of suspension and saltation transport modes (Leonard et al., 2011), with a dominance of saltating particles (Bagnold, 1974) in the case of drifting snow, and suspended particles in blowing snow ~~(wind speeds above 7 to 11, layers more than 2 height (Frezzotti et al., 2004)). layers (Mellor, 1965)~~. Despite its importance, the role of blowing snow on ~~local~~ SMB and surface melt on the AIS is currently poorly quantified. If we consider the ice sheet in its whole, the contribution of blowing snow is rather small: around 0-6% (Loewe,

15 1970; Déry and Yau, 2002; Lenaerts and van den Broeke, 2012). However, blowing snow is crucial for the ~~local AIS SMB (Lenaerts and van den Broeke, 2012; Déry and Yau, 2002; Gallée et al., 2001; Groot Zwaafink et al., 2013)~~ regional SMB (Gallée et al., 2001; Déry and Yau, 2002; Lenaerts and van den Broeke, 2012; Groot Zwaafink et al., 2013) through the displacement and relocation of the snow particles (Déry and Tremblay, 2004) ~~but also through sublimation (Takahashi et al., 1992; Thiery et al., 2012) (Dai and Huang, 2014), an ablation process that~~. This phenomenon occurs

20 approximately on 70% of the Antarctic continent during winter (Palm et al., 2011). In addition, sublimation contributes substantially to SMB ~~above a threshold wind speed of 11 (Kodama et al., 1985) and (Kodama et al., 1985; Takahashi et al., 1992) (Thiery et al., 2012; Dai and Huang, 2014)~~. This process can even be more effective to remove mass than surface sublimation (van den Broeke et al., 2004). The combination of blowing snow sublimation and transport is estimated to remove from 50 to 80% ~~(van den Broeke et al., 2008; Sarchili et al., 2010; Frezzotti et al., 2004; van den Broeke, 1997) (van den Broeke, 1997)~~

25 ~~(Frezzotti et al., 2004; van den Broeke et al., 2008; Scarchili et al., 2010)~~ (Frezzotti et al., 2004; van den Broeke et al., 2008; Scarchili et al., 2010) of the accumulated snow on coastal areas. Moreover, removal of the snow by the wind can locally lead to the formation of blue ice areas (Takahashi et al., 1988; Bintanja et al., 1995), which have a lower albedo and therefore enhance surface melt, and could affect ice shelf stability and collapse (Lenaerts et al., 2017). Blowing snow also plays a role in determining snow surface characteristics (Déry and Yau, 2002), affecting ~~snow density and wind velocity threshold (Lenaerts and van den Broeke, 2012), and on surface energy balance (Lesins et al., 2009)~~

30 ~~(Mahesh et al., 2003; Yamanouchi and Kawaguchi, 1985) (Yamanouchi and Kawaguchi, 1985; Mahesh et al., 2003) (Lesins et al., 2009)~~.

Many studies have focused on a minimum wind speed as a threshold to dislodge snow particles, depending on the snow surface properties (Budd et al., 1966). Schmidt (1980, 1982) explained that cohesion between snow particles requires higher wind speeds, or a higher impacting force of particles on the snow pack. In addition, the presence of liquid water in the snow

35 and enhanced snow metamorphism with the higher atmospheric temperatures in the summer induce varying wind thresholds

throughout the year (Bromwich, 1988; Li and Pomeroy, 1997).

Currently, simulations of the AIS SMB are highly uncertain since both [precipitation and](#) blowing snow processes are poorly constrained and probably lead to inconsistencies between the atmospheric modeled precipitations and the measured snow accumulation value ([Frezzotti et al., 2004](#); [Scarchili et al., 2010](#); [Groot Zwaaftink et al., 2013](#); [Gorodetskaya et al., 2015](#))

5 ~~(van de Berg et al., 2005)~~ ([Frezzotti et al., 2004](#); [van de Berg et al., 2005](#); [Scarchili et al., 2010](#); [Groot Zwaaftink et al., 2013](#)) ([Gorodetskaya et al., 2015](#)). In addition, strong blowing snow also hampers ground detection from satellites, and biases can be induced in efforts to study the Antarctic surface elevation due to the presence and radiative properties of blowing snow (Mahesh et al., 2002, 2003).

Efforts have been made to retrieve blowing snow from satellite data, but while it offers a large area coverage, the detection
10 is limited to clear-sky conditions and blowing snow layers thicker than 30 m (Palm et al., 2011), and make use of a wind threshold criterion. Moreover, ground validation remains essential to ~~validate~~ [evaluate](#) satellites measurements. A number of measurement campaigns have been organized in various regions of the AIS ~~and used~~, [using](#) different types of devices (nets, mechanical traps and rocket traps, photoelectric and ~~single-beam photoelectric sensors, and various studies have also worked with Flow-Capts~~ [acoustic sensors](#), or piezoelectric devices ~~,~~ ([Leonard et al., 2011](#); [Amory et al., 2015](#); ?)

15 ~~(?)~~ ([Leonard et al., 2011](#); [Barral et al., 2014](#); [Trouvilliez et al., 2014](#); [Amory et al., 2015](#)). However, custom-engineered sensors are rather expensive and scarce (Leonard et al., 2011), and both the remoteness of the continent and the harshness of the climate are limitations to widespread use of these devices.

In this study we propose a new method to detect blowing snow by the use of ground-based remote sensing ceilometers. Ceilometers are robust cloud base height detection devices. ~~Initially located~~ [Frequently used](#) in airports and designed to report visibility
20 for pilots, the backscatter signal of these ground-based low-power lidars contain further information. ~~These have been~~ widely used for scientific purposes regarding boundary layer investigation ([Thomas, 2012](#); [Mareowicz et al., 1997](#); [Eresmaa et al., 2006](#)) ([Heese et al., 2010](#)): ~~detection and~~ ([Marcowicz et al., 1997](#); [Eresmaa et al., 2006](#); [Heese et al., 2010](#); [Thomas, 2012](#)). ~~They have been used to detect the~~ vertical extent of aerosol layers below 5 km, ~~and~~ mixing height layers (Haeffelin et al., 2012), as well as the detection of the early stage of radiation fog (Haeffelin et al., 2016). Several algorithms have been developed to detect cloud
25 base height in specific areas, at the polar regions using the polar threshold algorithm (Van Tricht et al., 2014) or at temperate latitudes with the temporal height tracking algorithm (Martucci et al., 2010) ~~and the standard Vaisala algorithm~~ ([Flynn, 2004](#)). Ceilometer networks are also developed as a potential to cover larger regions (Illingworth et al., 2015). Over the Antarctic continent, the environmental conditions imply that research stations are usually equipped with robust instruments, that are able to withstand ~~cold and difficult circumstances~~ [low temperatures and high winds](#). Ceilometers can be operated autonomously and
30 continuously in ~~climatic environmental~~ conditions between -40 and +60 °C, up to 100% relative humidity, and ~~up to~~ 50 m · s⁻¹ [wind speeds](#) (Vaisala User's guide, 2006). Compared to lidars, ceilometers have numerous advantages: ~~e.g.,~~ [such as](#) eye-safe operation, low first range gate and ~~relative~~ [relatively](#) low price, making it one the most abundant cloud detection device on the ice sheets (Van Tricht et al., 2014; Wiegner et al., 2014).

The goal of this paper is to present a new methodology for blowing snow detection (BSD) using the ceilometer attenuated
35 backscatter profile, and estimate the frequency of blowing snow at Neumayer III and Princess Elisabeth stations. Subse-

quently, we apply the BSD algorithm ~~and investigate the near surface atmospheric changes during blowing snow, and we discuss blowing snow and the associated meteorological regimes~~ to infer various blowing snow statistics (occurrence, depth) and investigate meteorological conditions during blowing snow events. We conclude by examining the applicability of the BSD algorithm to other Antarctic sites.

5 2 Instrumentation and location

2.1 Ceilometers

Ceilometers ~~are rather simple and robust instruments. They~~ consist of a single-wavelength, eye-safe active laser transmitter that emits pulses in the vertical direction, and an avalanche diode receiver that collects the pulse signal. The laser pulse backscattered by molecules, aerosols, precipitation and cloud particles present in the atmosphere at height z , is detected by the ceilometer receiver. Typically, the backscatter intensity depends on the concentration or size of particles in the air, but the ceilometer receiver also detects noise induced by the device's electronics and the background light. The lidar equation enables to get the return signal strength from the emitted laser pulse (Münel et al., 2006). As equation 1 displays:

$$\beta_{att}(a) = \beta(z) \cdot \tau^2(z) \quad (1)$$

the attenuated backscatter profile at the range a , β_{att} ($\text{sr}^{-1} \cdot \text{m}^{-1}$) is a product of the true backscatter coefficient β at ~~distance~~ height z , taking into account the two way attenuation of the lidar due to the transmittance of the atmosphere (τ^2), ~~and a~~. A height normalization is applied to the retrieved signal ~~to remove the excessive decrease in backscatter intensity in the presence of fog or precipitation between the instrument and the cloud base (Gorodetskaya et al., 2015).~~ Finally, the detected signal is summed to a resolution of 15 (to increase signal-to-noise ratio, Vaisala User's guide (2006)) at a spatial resolution of ~~10~~. The detected signal is reported at the centre-center of the 10 m range gate (i.e. for a signal measured between 50 and 60 m, the value of the range gate will be attributed to a height of 55 m (range bin 56)). The ceilometer measures continuously and the standard output, β_{att} is displayed in a time-height cross section, with a 10m vertical resolution and 15 s temporal resolution (Fig. 1).

The cloud-base height is the standard ceilometer output determined from the backscattered signal: ~~using the time delay between the launch of the pulse and its reception, and knowing the speed of displacement (the speed of light).~~ Secondly, In addition, the instantaneous magnitude of the signal received by the diode provides information on the backscattering properties of the atmosphere, at determined heights. The ~~only quantitative particle property~~ quantitative information that can be derived from the ceilometer measurements is the attenuated backscatter intensity at defined heights (Wiegner et al., 2014; Madonna et al., 2015). Other properties such as optical depth, size and density would require to know the lidar ratio. ~~This, and a reliable estimate of lidar ratio is complicated (Wiegner et al., 2014).~~ In addition, this is only possible if the ceilometer is calibrated, which is very challenging since the signal to noise ratio has to be large enough in the troposphere (Wiegner et al., 2014) and is not done in the present study. This implies that quantification of blowing snow displacement, and the determination of blowing

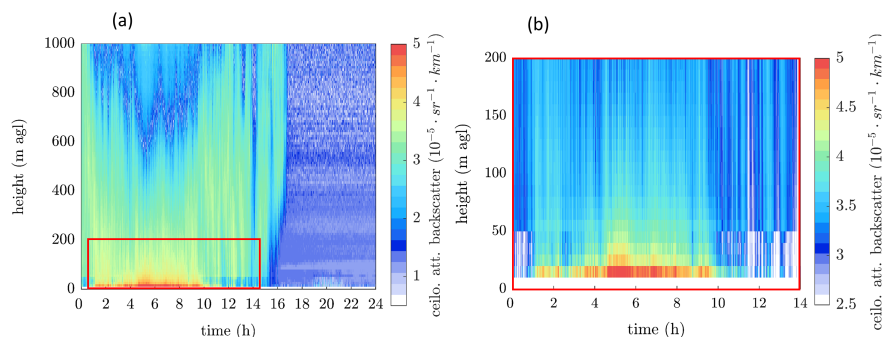


Figure 1. (a) Time (x-axis, in h)- height (y-axis, m agl) cross section of an attenuated backscatter profile for the CL-31 ceilometer at PE station, on April 24, 2016. The colour of the profile represents the intensity of the returned backscattered signal at a certain range bin. (b) Zoom onto blowing snow between 1:00 and 10:00 UTC, denoted by the red and yellow color in the range bins closest to the ground. The ~~artefact~~artifact discussed in section 3.1. is visible around 50 m height.

Table 1. Vaisala CL-31 ceilometer and CL-51 ceilometer specifications

Type	CL31	CL51
<u>installation</u>	<u>Decembre 2009</u>	<u>January 2011</u>
<u>firmware</u>	<u>1.72</u>	<u>1.021</u>
range (m)	10 - 7700	10 - 13500
reporting resolution (m)	10	10
reporting cycle (s)	2-120	16-120
measurement interval (s)	2	2
reporting interval (s)	15	15
laser wavelength (nm)	910 \pm 10 at 25 °C	910

snow properties such as particles density, shape or number can not be derived from the ceilometer attenuated backscatter signal at Neumayer III and PE stations.

2.2 The Cloud-Precipitation observatory at Princess Elisabeth station

The Princess Elisabeth (PE) station is located on the Utsteinen ridge in Dronning Maud Land (DML), East Antarctica (~~74~~
5 ~~°57' S and 23 °21' E at 1392 asl and 173 inland~~, Fig. 2 and Table 2). A cloud and precipitation observatory was set up on the roof of the station (approx. 10 m above the ridge) during the summer season of 2009-2010 and is still operational under the Hydrant/Aerocloud project (www.aerocloud.be). The observatory contains an automatic weather station (AWS) and a set of ground-based remote sensing instruments: ~~a Vaisala CL-31 ceilometer, a Heitronix infrared pyrometer and a Metek vertically profiling precipitation radar, with a webcam for weather and instrument status monitoring~~. The observatory was

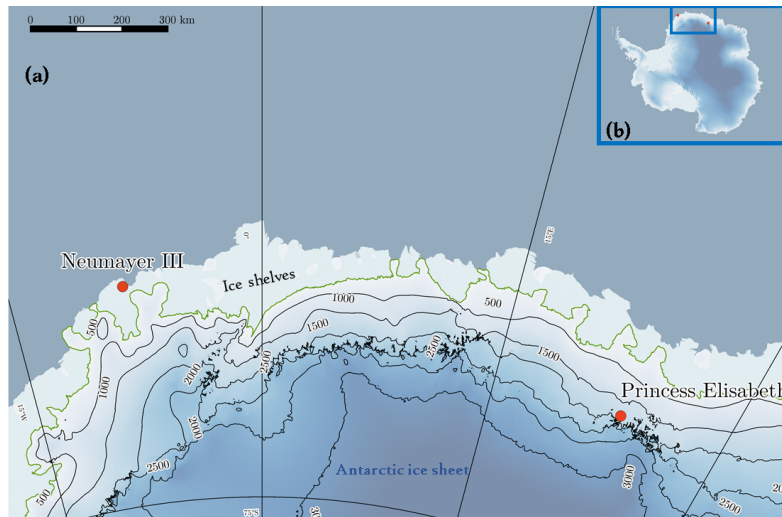


Figure 2. (a) Topographic map of the location of Neumayer and Princess Elisabeth stations in DML. The color intensity represents the Fretwell et al. (2013) surface elevation. We use Bamber et al. (2009) 500 m surface elevation contours and the grounding line from Bind-schadler et al. (2011) (green). (b) Map of the continent with the location of the two stations indicated in red. Source: QuAntarctica.

designed to be operated year-round, including the winter period when PE is unmanned. The station and the set of instruments are controlled remotely via a satellite connection. ~~Specifications of the instruments are given in Table ?? (see also Gorodetskaya et al. (2011, 2015)). Raw data and derived parameters of the instruments set up on the southern roof of Princess Elisabeth station, instrument raw data derived parameters Vaisala CL-31 ceilometer attenuated backscatter vertical profiles~~

5

~~cloud base height and vertical extent, cloud phase, optical depth, blowing snow Metek Micro-Rain radar 2 spectral signal power per range effective reflectivity, spectral width, mean Doppler velocity Infrared radiation pyrometer Heitronics KT15.82~~

~~H atmospheric brightness temperature effective cloud base temperature~~

10

~~(a) the Vaisala CL-31 ceilometer on the roof of PE station, (b) the IMAU Automatic weather station at PE, (c) the Vaisala CL-51~~

~~ceilometer on the roof of Neumayer III station (credits: Hauke Schulz). The Vaisala CL-31 ceilometer (firmware 1.72) was in-~~

15

~~stalled on the roof of the station in December 2009 and is operational at present . It emits laser pulses at central wavelength of~~

~~910 ± 10 at 298 . The measurement resolution is set to 10 and the reporting interval on 15 (see Table 1). Several outages of~~

~~the energy provision system limit the data mainly to Antarctic summer season (December to March is best represented). Only~~

~~one year of continuous measurements was achieved (2015). We collocate information retrieved from the Micro Rain Radar to~~

~~ceilometer blowing snow detection, to attest whether blowing snow happens during a precipitating event during the year 2015~~

~~continuous measurements were obtained.~~

~~The Metek vertically-profiling precipitation radar, set up since 2010, enables to retrieve snowfall rates, using the return from~~

~~the vertically profiling Doppler radar operating at a frequency of 24 GHz. The raw Doppler spectra is post-processed fol-~~

~~lowing Maahn and Kollias (2012) to link radar reflectivity, to calculate radar reflectivity profiles which are then linked to~~

~~snowfall rates using the newly developed Ze-Sr relation for PE by Souverijns et al. (2017). We also use the atmospheric~~

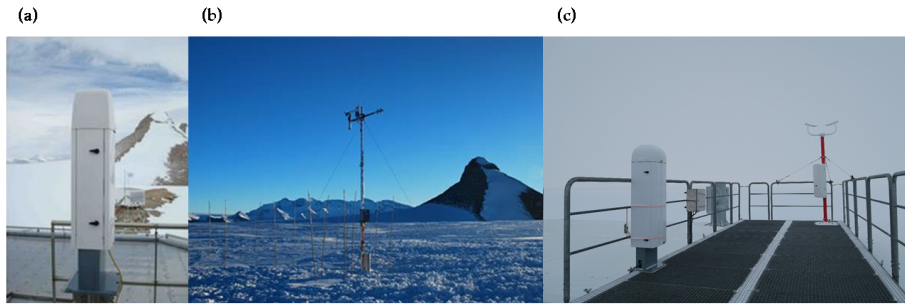


Figure 3. (a) the Vaisala CL-31 ceilometer on the roof of PE station, (b) the IMAU Automatic Weather Station at PE, (c) the Vaisala CL-51 ceilometer on the roof of Neumayer III station (credits:Hauke Schulz).

~~brightness temperature measurement from the infrared radiation pyrometer as cloud base temperature measurement~~ A full description of micro-rain radars can be found in Klugmann et al. (1996) and the radar set up at Princess Elisabeth is described in Gorodetskaya et al. (2015). The monitoring of the instruments set up on the roof of the station is done via a webcam. For a specifications of the instruments, see also Gorodetskaya et al. (2013, 2015).

5 ~~An~~ The Automatic Weather Station ~~has been~~ (AWS) was set up 300 m from the station ($71^{\circ}56'S$; $23^{\circ}20'E$) for recording meteorological parameters, broadband radiative fluxes and snow height changes (Gorodetskaya et al., 2013). It is designed to work continuously in remote locations, enabling studies of mass balance and radiative fluxes. The ~~automatic weather station~~ AWS was established in February 2009, and replaced by a new station in December 2015, both designed by the Institute for Marine and Atmospheric Research, University of Utrecht (Utrecht, The Netherlands). The station provides hourly mean data
 10 of near ground and air temperature, ~~a profile of snow temperature (10 levels)~~, air pressure, wind speed and direction, relative humidity and radiative fluxes (downwards and upwards short- and long wave radiation), ~~and records snow height changes~~ (for details on sensors, see Table S1 in Supplements). Post-processing of the data includes a treatment for relative humidities as described by Anderson (1994) for humidity with respect to ice, and a correction for the relative humidities above 100% following van den Broeke et al. (2004). The temperature gradient is computed as the difference between the 42 m and surface
 15 temperatures over the distance between the sensors (~~(Gorodetskaya et al., 2013)~~).

2.3 Neumayer III research station

Neumayer III research station is located on the Ekström ice shelf, in North East Weddell Sea ($70^{\circ}40'S$; $08^{\circ}16'W$) Fig. 2 and Table 2). Researchers are present year-round at the station and it is equipped with various instruments. Measurements include

Table 2. [Meteorological conditions at Princess Elisabeth, and Neumayer III stations. For extended climatology, see Gorodetskaya et al. \(2013\) for PE station and König-Langlo and Loose \(2007\) for Neumayer station](#)

variable	Princess Elisabeth	Neumayer III
coordinates	71 °57' S; 23 °21' E	71 °56' S; 23 °20' E
distance from the coast	173 km	7km
elevation	1392 m)(Gorodetskaya et al., 2013)-asl	43 m asl
annual mean air temperature	-18 °C	-16 °C
annual mean wind speed	5 m · s⁻¹	9 m · s⁻¹
average wind direction		
<ul style="list-style-type: none"> • synoptic disturbances • katabatic conditions 	90 °to N 180 °to N	100 °to N 170 °to N
relative humidity	56 %	90%
pressure	827 hPa	986 hPa

upper air soundings, ozone soundings, radiation measurements and weather observations. Weather ~~observations~~ [measurements](#) are carried out since 1981 at Neumayer ~~III~~, and the station is the weather forecasting centre for DML. The synoptic observations at Neumayer III include 2m and 10m air temperature, air pressure, wind vector at 2 and 10m height, 2m dew point temperature, presence - type and height of clouds, horizontal visibility, and past and present weather including snowdrift and whiteout (for a description of the sensors, see Table S2 in Supplements). The measurements are carried out ~~routinely daily~~ every 3 hours ~~but visual observations are omitted at except for~~ 03 and 06:00 UTC. In this paper we use the visual observations of blowing snow, classified into 9 categories (S8 code) according to the World Meteorological Organization (WMO) coding system (see Table S3 in Supplements). The visual observations regarding blowing snow are performed as follows (detection procedure from Gert König-Langlo, personal communication, 2016): "if the wind exceeds 5 m · s⁻¹, the observer goes out about 100 m ~~wind-ward~~ [windward](#) from the research station and observes the snow surface. No target is used to detect blowing snow against, and during winter (~~no light at all~~ [in complete darkness](#)), a small flashlight is used. The distinction between blowing and drifting snow is made according to the height of the blowing snow layer in relation to the eye level: drifting snow below the eye level, and blowing snow above. Further, if the blowing snow layer is not too dense, one can distinguish blowing snow with or without ~~precipitation~~ [precipitation](#) by an additional observation from the roof of the station."

15 The set of instruments present at Neumayer III station includes a Vaisala ceilometer CL-51 (~~firmware 1.021~~), set up on the roof of the station and operating continuously since the 15th of January ~~2011. The ceilometer reports attenuated backscatters every 15 from 10 to 13 500 height, with a vertical resolution of 10~~ [2011](#) (see Table 1). The blowing snow record at Neumayer station is analyzed together with the atmospheric measurements available from the synoptic observations. ~~The data (?)~~ [An overview of the climatic conditions is given in Table 2. The data](#) is freely available interactively from <https://www.pangaea.de/>.

3 Data treatment and blowing snow detection algorithm

3.1 Pre-processing

We average every 15s- β_{att} profile over one hour using a running mean, to create mean attenuated backscatter profiles at every time step and ~~get rid of turbulence and~~ avoid the variability due to turbulence and hardware noise. Figure 4 shows the resulting β_{att} at 09:30 UTC, based on the average of 240 profiles (120 preceding and 120 following 09:30 UTC). An additional reason for the integration of the signal over longer time periods, is that it improves the signal to noise ratio (SNR). No additional SNR correction is performed on the raw data, as we found that a temporal SNR higher than 0.3 would remove parts of the blowing snow signal (Gorodetskaya et al., 2015).

There are two sources of noise and artifacts affecting the ceilometer backscatter signal: the hardware of the Vaisala ceilometers, and the internal processing of the data (Kotthaus et al., 2016). Firstly, a heater is incorporated in the device to ~~keep the instrument at a fixed temperature~~ stabilize the laser temperature in cold environments. This heater is placed close to the laser transmitter and the periodic turning on ~~and off~~ (when a minimum temperature is reached by the instrument) and off (when the laser temperature is high enough) of the heater introduces a small periodic variation in the stability of the emitted signal (and therefore of the detected signal). This effect is stronger in the first range bins, closest to the device, and the hourly running mean enables to smooth out most of this signal variation. Secondly, the internal processing of the signal includes a built-in correction for the partial overlap of the laser in the first range bins. This overlap is due to the coaxial configuration of the laser: the same lens is used for the emitted and the received signals, made possible by the use of mirrors (Spirnhirne, 1993; Vande Hey, 2015). The total overlap is only reached at the 7th range bin (65 m) for the CL-31 ~~(Kotthaus et al., 2016; Vande Hey, 2015)~~ (Vande Hey, 2015; Kotthaus et al., 2016). However, the partial overlap in the near-ground range bins does not imply that the minimum detection range is at 65 m only; in case the signal returned by the close range scatterers is large enough (which is mainly the case during blowing snow), it will be recorded even before the overlap onset (Vande Hey, 2015). Lastly, the CL-31 backscatter profile is constrained in the lowest bins by a built-in function to correct for unrealistically high values resulting from window obstruction. Yet, this correction likely introduces artifacts in the signal in the first range bins. As a result of the periodic switching on and off of the heater and the low overlap in the first range gate, the reported value of the combined β_{att} signal in the lowermost range bin is systematically and unrealistically higher than the signal in the next bins (Vaisala, personal communication, 2016). We therefore exclude the signal reported in the lowermost range bin in our analysis, and start investigating the profile from the second range bin, 15 m above the CL-31 and CL-51 ceilometers onwards.

Moreover, artifacts have been observed in the ceilometer profiles at both stations (also visible in Fig. 56). There is a discontinuity in all profiles between the 4th and the 5th range bins (35 and 45 m). This discontinuity is also visible in profiles where the instrument is ~~completely covered~~ hooded, which are supposedly ~~representing full~~ mimicing full atmospheric attenuation, and thus recording the background noise produced by the hardware and electronics. Many authors have reported artifacts in the lowest range bins (below ~~70m~~ 70 m height), that are usually excluded during processing for boundary layer investigation (Wiegner et al., 2014). This local minimum is also reported by Sokol (2014) at the 5th range bin (45 m) during the whole du-

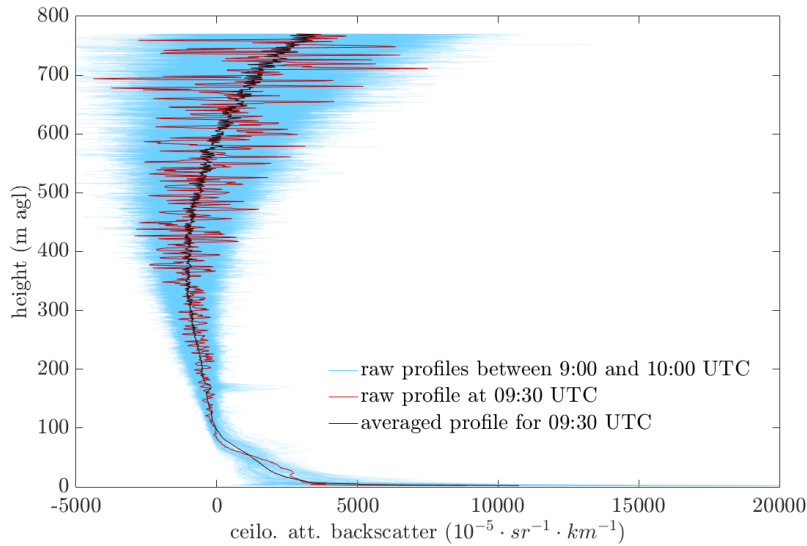


Figure 4. Hourly averaging of the attenuated backscatter profile of the CL-31 at PE. The attenuated backscatter profile at 09:30 UTC (red line) and resulting averaged profile (black) for the same timestep, based on the average of all the 240 profiles in blue.

ration of his campaign, as well as by Martucci et al. (2010) and Tsaknakis et al. (2011). Kotthaus et al. (2016) states that these are likely due to the correction applied by Vaisala to prevent unrealistic values in the lower bins, related to the obstruction of the window and the internal noise. In the case of Vaisala instruments, the output is already corrected with a correction function, unknown to the user, and which cannot be modified (Wiegner et al., 2014). This has to be kept in mind when using the profile information to detect blowing snow.

3.2 The blowing snow detection algorithm

Studies investigating the boundary-layer-boundary-layer properties based on ceilometer attenuated-backscatter- β_{att} make use of both properties of the signal ~~:-its-shape-and-its-intensity~~(shape and intensity), to evaluate ~~of~~ the presence and extent of a particular layer. ~~E~~, e.g. in order to determine the height of the mixing layer (Wiegner et al., 2014). For such analysis, five methods have been developed (Emeis et al., 2008), including a threshold method and a gradient method (Eresmaa et al., 2006). In the first case, the mixing height is attained when the intensity of the signal drops below a fixed threshold value (Münkel and Rasanen, 2004). The second method considers the minimum of the first or second derivative of the backscattering profile as top of the mixing layer (Sicard et al., 2004). To detect the occurrence of blowing snow, Palm et al. (2011) uses a combination of both types of methods on the CALIOP satellite (satellite-borne) backscatter. First, the intensity of the backscatter in the bin closest to the detected ground return must exceeds a certain threshold. Second, the decrease of the profile of the signal with height indicates the presence of blowing snow: the concentration of particles close to the ground is much higher than in the overlying layers (Takeuchi, 1980; Schmidt, 1982; Palm et al., 2011). This is associated with a sharp vertical gradient where the

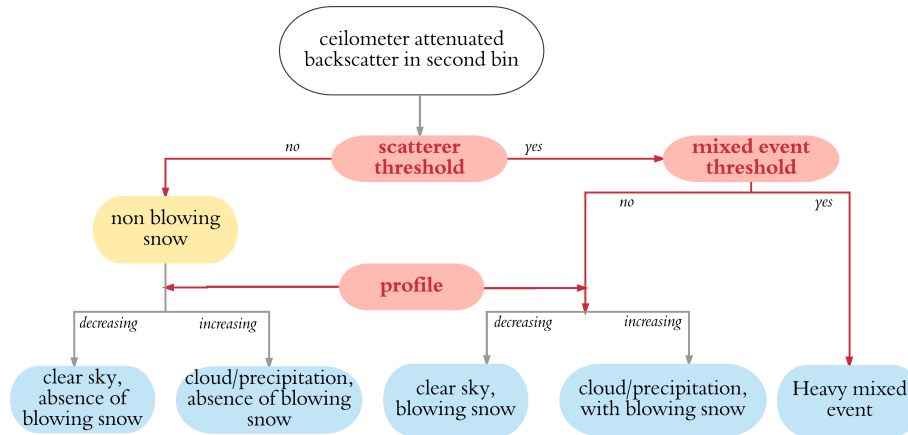


Figure 5. Chart of the blowing snow detection method

β_{att} profile decreases strongly in the very first range bins. In addition, a wind speed threshold is applied ($3 \text{ m} \cdot \text{s}^{-1}$ at 10 m). The approach used [here for the blowing snow detection \(BSD\) algorithm](#) is similar, but there is no wind speed criterion in our analysis. In addition, the ceilometer is ground-based, allowing the detection of blowing snow ~~mixed with snowfall during overcast conditions~~. [The algorithm method is displayed in Fig.5](#). To detect blowing snow, the intensity of the backscatter signal at the lowest usable bin must exceed a certain threshold ([section 3.3](#)), and the intensity of the signal must decrease in the next range bins indicating a particles density greater in the lower levels than at ~~the top of the layer~~ [layers directly above](#). As previously highlighted, clean air molecules cannot be distinguished because the signal associated with it is smaller than the noise generated by the hardware (Wiegner et al., 2014; Kotthaus et al., 2016) and by the background light (Vande Hey, 2015), polluting the signal in the lowest bins. To distinguish the presence of scatterers (aerosols, blowing snow particles, cloud particles...) present in the atmosphere from these artifacts, we need to investigate the signal intensity representative for ~~clear sky cloudless~~ conditions. I.e., the average β_{att} of the ~~second-lowest usable~~ range bin received by the ceilometer during scatterer-free conditions. Clear sky days are ~~selected manually selected for the whole period~~ using the daily quicklooks (Fig. 1) and are days where the quicklook background is uniform and without precipitation or clouds, and where the time series of the signal [in the slowest usable range bin](#) is stable around a low value (corresponding to hardware and background noises), to avoid low-level disrupting signal. Next, we ~~select the compute the 99th percentile of all~~ clear-sky β_{att} signal in ~~the second range bin~~, and ~~compute the 99th percentile this range bin~~ as threshold value (for calculation, see section 3.3). As such, it is representative of the presence of scatterers exceeding the value for clear sky. Since the noise is instrument-dependent, individual pre-processing and thresholds have to be defined for each instrument the BSD algorithm is applied to.

~~If the value of~~ [After comparing](#) the backscatter signal ~~in the second range bin exceeds to~~ the clear-sky threshold, the BSD algorithm investigates the shape of the β_{att} profile. A regular clear sky ceilometer profile (signal intensity versus height) does not show intense vertical variations (Fig. 5): ~~in the infrared, the transmission term is close to one and decreases only slightly~~

with height. This implies that any important variation in the β_{att} signal can be attributed to the particles backscatter. The ~~blowing snow and blowing snow with precipitation lines~~ profiles for blowing snow in Fig. 5 are typical blowing snow profiles: ~~the blue line shows a~~ 6 show a typical sharp decrease until ~~-100-bin 8-10 (75 - 95 m height)~~, above which the signal keeps decreasing steadily (~~blue line~~): this is the signature of clear sky blowing snow. The red profile, on the other hand, shows a re-increase in intensity ~~a bit below 100-around the 15th bin (145 m height-height)~~, overlying the blowing snow signal: this indicates the presence of scatterers ~~interpreted as precipitation (denoted by the arrow on the graph)~~. If there is no blowing snow event, while precipitation is present, the profile does not decrease prior to the increase at higher levels (black line in Fig. 56). The ~~discontinuity, as described in section 3.1., is also detectable in Fig. 1(b) and in all profiles in Fig. 5 between 40 and 50 high.~~ We therefore set a ~~conditional~~ algorithm therefore investigates the shape of the profile in order to detect blowing snow. A ~~condition is set~~, that a blowing snow profile implies that the mean of the overlying bins 3 to 7 (25 to 65 m) must be lower than the signal in the ~~second-range bin (15 m), which is the lowest usable. In this way, the discontinuity, as described in section 3.1. (visible in Figures 1 and 6 between 35 and 45 m), is not affecting our retrievals. In order to detect blowing snow occurring during clouds or precipitation, the profile shape is analyzed to identify a second increases in the signal intensity above the 7th bin (65 m height). A clear differentiation between clouds or precipitation cannot be made on the basis of the ceilometer alone, but the presence of clouds and/or precipitation can be identified. This analysis is carried out for both blowing snow and the absence of blowing snow measurements. The information retrieved from the Micro Rain Radar (hourly precipitation rates) is collocated to ceilometer blowing snow detection, to determine the time (in hours) since the last precipitation event at PE station.~~

Inherent to this profile-based method, the detection of blowing snow during precipitating events is limited to cases when the blowing snow signal is preserved close to the ground. In case of ~~strong~~-precipitation associated with storms, there is always blowing snow due to the high wind ~~gusts-displacing the fresh-displacing the~~ snow, and no distinction between precipitation and blowing snow is possible. ~~The precipitation intensity might cover the blowing snow signal, even close to the ground. Then,~~ as the ceilometer signal is entirely attenuated near the surface (Gorodetskaya et al., 2015) . It is thus not possible to get ~~signal in the overlying bins, and~~ the profile of the backscatter intensity ~~does not decrease with height, and the BSD algorithm does not detect blowing snow. Such events are therefore not considered by the BSD might not decrease upwards. Such intense precipitating events mixed with snowfall are identified as having a second bin signal higher than $1000 \cdot 10^{-5} \cdot \text{km}^{-1} \cdot \text{sr}^{-1}$ (threshold adapted from Gorodetskaya et al. (2015)). In those cases, the events are classified as a intense mixed event, and the profile analysis is eluded by the~~ algorithm.

In addition to the detection of blowing snow, the BSD algorithm quantifies the height of the layer ~~-(see Fig. S3, Supplements)~~ This is done as follows; if the profile decreases steadily (indication of absence of precipitation), the range gate at which the intensity of β_{att} drops under the clear sky threshold value is the top of the layer. Anything above this height is considered clear sky. If there is precipitation or a cloud during the blowing snow event, the shape of the backscatter profile does not decrease monotonously, but shows an increase in higher levels. In that case, the range gate at which the profile increases again is the top of the blowing snow layer, and the base of the cloud and/or precipitation ~~(around the 7th bin in Fig.6, for the black and the red profiles). Layer height definition is illustrated in Fig. S3 (Supplements).~~

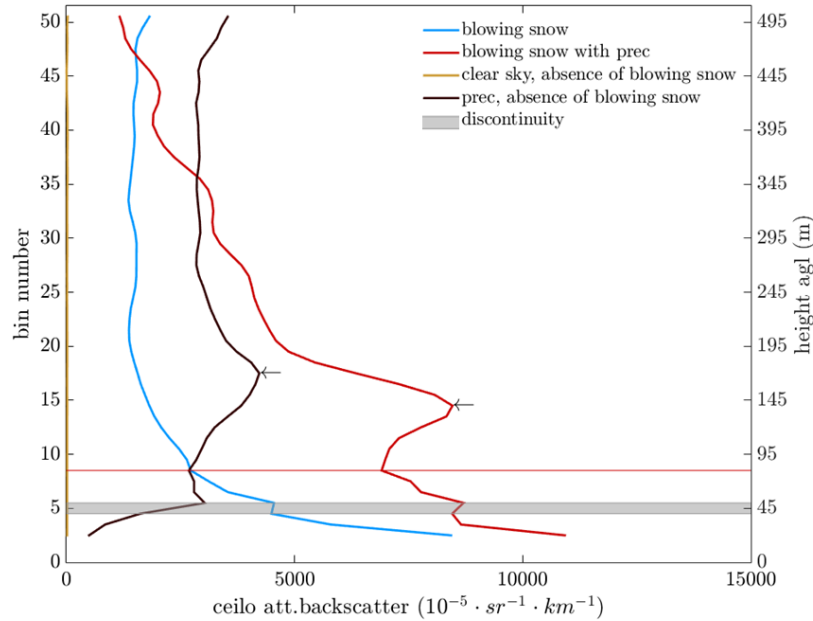


Figure 6. ~~All~~ Different types of hourly-averaged one-event profiles relevant for blowing snow measured by the ceilometer at PE station on 24/04/2016. Typical: blue line - typical blowing snow signal with no precipitation nor clouds in blue, (24-04-2016); red line - blowing snow overlaid by precipitation in red. The (10-02-2016); black line represents - precipitation with no in the absence of blowing snow -, and the (10-02-2014); yellow line shows the - near-zero signal for clear sky conditions (24-04-2016). The height above ground is indicated on the right axis and the corresponding bin number on the left axis. All profiles exclude the lowermost bin, and start at the second bin (15 m agl.). The grey lines represent the discontinuity between bins 4 and 5 (35-45 m). The arrows indicate the presence of precipitation.

3.3 Application of the blowing snow detection algorithm to different stations

The BSD algorithm is designed to detect blowing snow events reaching heights of minimum 15 m and is developed for based on the Vaisala CL-31 located at PE station, for the period 2010-2016. It is applicable to other ceilometers: we applied the BSD algorithm to backscatter data from the Vaisala CL-51 ceilometer at Neumayer station, for the years 2011-2015. The time (15 s) and height resolution (10 m) is are the same for both instruments. We can therefore apply the BSD algorithm in the same fashion to both datasets with the only difference being the attenuated backscatter threshold β_{att} near surface threshold (first step in the BSD algorithm used to identify the presence of blowing snow). We obtain a threshold of $21 \cdot 10^{-5} \cdot \text{km}^{-1} \cdot \text{sr}^{-1}$ for the CL-31 ceilometer at PE, based on 127 clear sky days out of a total of 1064 days. The threshold at Neumayer is of $32.5 \cdot 10^{-5} \cdot \text{km}^{-1} \cdot \text{sr}^{-1}$, based on 125 clear sky days out of 1444 days.

4 Results

4.1 Frequency of blowing snow

Ratio of matches (blue bar) compared to the ratio of mismatches (red and yellow bars) for each of the blowing snow categories. The matches encompass the $N_{BS_{both}}$ and $N_{BS_{none}}$ and the mismatches are $N_{BS_{ceilo}}$ in yellow and $N_{BS_{vis}}$ in red.

5 In order to investigate the type of blowing snow detected by the BSD algorithm, we compare it to visual observations at Neumayer, carried out routinely at 09-12-15-18-21 and 24:00. All ceilometer measurements are considered over one hour, corresponding to the time at which visual observations are carried out. We identify a blowing snow event when blowing snow is present in at least 80 profiles (20 mins). The WMO visual observations are categorized in six classes of blowing and/or drifting snow events, ranging in intensity and whether there is precipitation or not (Table S3 in Supplements). Before we start the comparison, it should be noted that visual observations are difficult to perform, and the error associated with it is not quantified. Therefore, in this part we refer to the number of measurements that match or mismatch between the BSD algorithm and visual observations rather than using the visual observations as "ground truth". The total number of measurements, N , is the total number of visual observations performed during which the ceilometer is also measuring, independently of whether there is blowing snow or not ($N = 10\,854$, 6 measurements per day for the 2011-2015 period). The match ratio is the total agreement between visual and BSD algorithm detections over N ; with $N_{BS_{both}}$ when both the ceilometer and the observer detect blowing snow, and $N_{BS_{none}}$ when neither the ceilometer nor the observer detects blowing snow. Mismatches occur when only one of the methods detects blowing snow, when the other does not : $N_{BS_{ceilo}}$ if blowing snow is only reported by the BSD algorithm (commission error), and $N_{BS_{vis}}$ when only the visual observations record blowing snow.

$$20 \quad \text{match} = \frac{N_{BS_{both}} + N_{BS_{none}}}{N}; \quad \text{mismatch} = \frac{N_{BS_{ceilo}} + N_{BS_{vis}}}{N}$$

The results observer records blowing snow (ommission error).

The results (Table 3 and table S4, in Supplements) show a very good match in the blowing snow detection (Fig-6) and the optimum, 78%, is reached for events classified as heavy all blowing snow with or without precipitation.

$$\frac{N_{BS_{both}} + N_{BS_{none}}}{N} \quad (2)$$

25 The lowest match (65-70%) is found when all blowing and drifting snow is taken into account: the number of visually detected events strongly increases since more categories are included, whereas the number of detections by the BSD algorithm is fixed. For this category covering everything, in 25 In 21% of the cases the time, the visual observer reports something (blowing or drifting snow) that is not detected by the BSD algorithm (Table S4, in Supplements). This is related to the fact that the ceilometer points upwards and is elevated at a height of 17 m above the surface, which prevents it from detecting shallow layers of drifting snow.

Over all visually detected events, the BSD algorithm detects 79% of the A fraction of 84% visually observed heavy blowing

Table 3. Detection numbers and scores of the different categories of observations. The first four columns give the numbers for all four categories: $N_{BS_{both}}$ - stands for blowing snow detected by both the algorithm and the visual observations, $N_{BS_{none}}$ - when both methods agree that there is no blowing snow, $N_{BS_{ceilo}}$ and $N_{BS_{vis}}$ - represent detections by the algorithm and the observer only, respectively (the corresponding percentages are presented in table S4, in Supplements). The four last columns give the scores. B stands for blowing and D for drifting snow. The total number of measurements is 10584.

	$N_{BS_{both}}$	$N_{BS_{none}}$	$N_{BS_{ceilo}}$	$N_{BS_{vis}}$	accuracy	sensitivity	specificity	TSS
B and D snow, with or without prec	2404	5170	972	2308	0.70	0.51	0.84	0.35
B and D snow, without prec	992	6578	2373	897	0.70	0.52	0.73	0.26
heavy B snow, without prec	378	7406	2998	72	0.72	0.84	0.71	0.55
all B snow, without prec	822	6993	2554	485	0.72	0.63	0.73	0.36
all B snow, with or without prec	1856	6665	1520	813	0.78	0.69	0.81	0.51
heavy blowing snow, with or without prec	1114	7249	2262	229	0.77	0.83	0.76	0.59

snow events \neq is detected by the BSD algorithm:

$$\frac{N_{BS_{both}}}{N_{BS_{both}} + N_{BS_{vis}}} \frac{N_{BS_{both}}}{N_{BS_{both}} + N_{BS_{vis}}} \quad (3)$$

In this case, we consider visual observations reported as "heavy blowing snow" only. For 95% of the $N_{BS_{ceilo}}$ events not reported as "heavy blowing snow" by the observer, intensities of the backscatter signal are below $2000-1000 \cdot 10^{-5} \cdot \text{km}^{-1} \cdot \text{sr}^{-1}$; it is therefore likely that those events are classified as 'slight' or 'moderate' "slight" or "moderate" by the visual observer instead of being considered heavy (visible in Fig.S3, in Supplements). For the $N_{BS_{vis}}$, 54% do not attain the threshold indicating the presence of scatterers and in 46% of the cases the ceilometer attenuated backscatter profile does not decrease with height. Details on the division in the match and mismatch categories between $N_{BS_{both}}$, $N_{BS_{none}}$, $N_{BS_{ceilo}}$ and $N_{BS_{vis}}$

We also compare the skills of the BSD algorithm to different evaluation metrics (Allouche et al., 2006) (the equations for each of the metrics are presented in Fig.S3 and Table S4 (Supplements). The accuracy, highest for the category collecting all blowing snow events, is the proportion of correctly detected events. To take into account omission errors, sensitivity is used and the best score is attained by both heavy blowing snow categories (with and without precipitation). Specificity reflects commission errors, and the categories encompassing most events (blowing and drifting snow) perform best. Finally, since the $N_{BS_{none}}$ is larger than the other categories, the matches are likely biased, and we therefore use the true skill statistics (TSS, (Allouche et al., 2006)), which is a method enabling to measure the overall accuracy and correct for the accuracy expecting to occur by chance, which also accounts for commission and omission errors, while being independent of prevalence in the data. TSS statistics range from -1 to +1, where values under zero indicate no better performance than random, and the closest the result to 1, the better the agreement. This metric clearly indicates that heavy blowing snow is the best detected category of events.

The BSD algorithm output is binary at Neumayer: either there is blowing snow or there is no blowing snow, and no distinction can be made as whether there is precipitation or not, since precipitation measurements are not available at the station. The visual observer does however indicate whether there is precipitation or not. To investigate to which extend the BSD algorithm is limited by precipitation, we compare matches and mismatches for ~~the heavy blowing snow category~~ each of the categories with and without precipitation. The value ~~for~~ $N_{BS_{both}}$ doubles and even nearly triples when including events occurring during precipitation while $N_{BS_{ceilo}}$ decreases by nearly ~~a third and~~ $N_{BS_{vis}}$ increases by one third ~~50% and~~ $N_{BS_{vis}}$ increases by the same amount. This indicates that the BSD algorithm is not impeded by the presence of precipitation; the commission errors in the non precipitation category were in majority blowing snow events that are encompassed when taking into account events occurring together with precipitation.

Moreover, we gather that the ceilometer algorithm is not limited to heavy blowing snow, but that it also detects a number of ~~visually detected~~ events referenced under "moderate", or "slight blowing snow events", and even occasionally "drifting snow". This is revealed by the fact that $N_{BS_{ceilo}}$ reduces as we consider less intense and shallower type of events (Table S4, in Supplements).

The frequency is calculated here by reporting the sum of all hours during which blowing snow occurs at Neumayer based on the BSD algorithm over the total number of observation hours. Blowing snow at Neumayer III occurs on average ~~28~~ 36% of the time ~~, as detected by the BSD algorithm (for the 2011-2015)period~~. This is consistent with König-Langlo and Loose (2007), who report ~~drifting and blowing snow frequency of 20% of drifting and 40% , and 20 % for blowing snow only~~ drifting and blowing snow for the 1981 - 2006 period. However, there is ~~a strong inter-annual variability in monthly blowing snow rates (Lenaerts et al., 2010)~~. The frequency is calculated here by reporting the sum of all hours during which blowing snow occurs (n=2 714 164) over the total number of observation hours (n=9 742 717) an inter-annual variability that reaches \pm 5%, also observed by Lenaerts et al. (2010). The pattern visible in Fig. 7 is common for blowing snow over Antarctica: a seasonal cycle peaking during the Antarctic winter (March - November) and displaying lower values for the rest of the year ~~(Mahesh et al., 2003; Lenaerts et al., 2010; Scarchili et al., 2010; Palm et al., 2011)~~ (Mahesh et al., 2003; Lenaerts et al., 2010) (Scarchili et al., 2010; Palm et al., 2011; Amory et al., 2017). The overall blowing snow frequency ~~at PE equals 9%, which is lower than at Neumayer, but is reasonable for~~ is computed at PE for the 2010-2017 period and reaches 13%. This lower blowing snow frequency at PE can be explained by the location of the station: PE the station is shielded from the katabatic winds by the Utsteinen mountain range. ~~The mean annual wind speed at the Princess Elisabeth station (5) is lower compared to Neumayer (9, König-Langlo and Loose (2007)). The frequency retrieved here is coherent with Palm et al. (2011) and analogous to the situation of the Norwegian Troll research station (72°00' 41" S - 2°32' 06" E) as detected by satellite.~~

Annual cycle of blowing snow frequency at Neumayer III station, derived by the BSD algorithm (blue bars), and visual observations (red line) for the period 2010-2015. The error bars represents the inter-annual variability.

4.2 Near-surface atmosphere changes during blowing snow

kernel probability density function of the atmospheric variables at Neumayer. The blue and red curves correspond to non-blowing snow and blowing snow conditions, respectively. The vertical line represents the median, and the shaded area the IQR of the density function, colors according to blowing or non-blowing snow. Bandwidth = 4 for all variables.

5 Analysis of meteorological conditions for blowing snow events compared to the rest of the time shows that the 2wind speed, and mean relative humidity (RH), exhibit statistically significant differences (Figs 8 and 9; Tables S5 and S6, in Supplements). The 2wind direction shows a preferential Easterly orientation at Neumayer and PE during blowing snow events, while non-blowing snow takes place under a wider spectrum of wind directions (Fig. 8 and 10). Part of the non-blowing snow measurements occur during katabatic conditions, when the wind blows from the interior towards the coast. Easterly winds during non-blowing snow conditions are probably related to the synoptic events during which no blowing snow occurs, or during which precipitation is too intense to conserve the blowing snow signal. Positive anomalies in wind speed, RH and incoming long wave radiation at the surface are associated to warm synoptic events, when air masses originating from the easterly winds bring moist air from the ocean precipitating inland. Such events are a common feature at Neumayer (König-Langlo and Loose, 2007) and occur 41-48 % of the time at PE (Gorodetskaya et al., 2013, 2014) . Further, wind speed and RH are both conditions privileging blowing snow, but are also impacted by the blowing snow itself: wind speeds are high enough to be able to lift and bring the snow particles from the surface to drift and saltation. Then, the concentration of particles suspended in the atmosphere brings an extra friction, increasing the roughness length and reducing the wind speed (Bintanja and Reijmer, 2001; King and Turner, 1997) . The increase in RH is both a result of moist air advection during synoptic events, and due to the sublimation of precipitation and blowing snow (Bintanja and Reijmer, 2001) , a self-limiting process (Bintanja, 2001) . This in turn lowers the air temperature close to, making it a quieter zone between the flows diverged to the sides of the station (Parish and Bromwich, 2007) , while Neumayer III station is located on the ice shelf and experiences higher wind speeds (see Table 2) and is more exposed to storms. In addition, the ground (King and Turner, 1997) . At PE, the air temperature varies only slightly during blowing snow events, but the surface temperatures show a bigger increase as synoptic events are often accompanied with clouds and high winds. Those also have an impact on the radiative budget. Finally, the air is less stratified as under katabatic conditions and the vertical temperature gradient is therefore lower as the air mixes during synoptic regimes and blowing snow eventslimited availability of Antarctic winter data (due to power failures at the station) leads to an underestimation of the blowing snow frequency as mostly extended summer period was used, and only one winter is taken into account.

These variables are similar to those found by Gorodetskaya et al. (2013) categorizing the regimes at PE and enable to classify most of the blowing snow events with the warm synoptic regime bringing precipitation and storm, and the transition from this regime to the katabatic conditions. However, a few blowing snow events also occur in clear sky cold conditions, when the wind blows from the interior towards the coast, building up a stable boundary layer.

Kernel probability density function of the atmospheric variables at PE station. The blue and red curves correspond to non-blowing snow and blowing snow conditions, respectively. The vertical line represents the median, and the shaded area the IQR of the density function, colors according to blowing or non-blowing snow. Bandwidths: surface temperature: 5; temperature

inversion: 4; atmospheric brightness temperature: 5; wind speed: 4; wind direction: 35; relative humidity: 10; pressure: 4; incoming long wave radiation: 10.

4.2 Blowing snow and meteorological regimes

In order to differentiate between dry blowing snow, and blowing snow associated with precipitation, we analyze the influence of the wind, air and atmosphere brightness temperature, RH, temperature gradient, time since last precipitation and blowing snow layer height during blowing snow conditions by means of a principle component analysis. At both Neumayer and PE, the dominating parameters are the wind direction, followed by the time since last precipitation and the height of the layer as explanatory factors for the variability. The wind direction is the dominating component, but does not explain the variations within blowing snow in itself. Rather, the wind direction is linked to the type of event and we can distinguish between clear sky blowing snow and The frequencies measured by the BSD algorithm are larger than those retrieved by satellite method: Palm et al. (2011) gives a range of 0-10% blowing snow for both locations. This can be related to the number of blowing snow events occurring together with storm and clouds/or precipitation. A cluster analysis (for details, see Gorodetskaya et al. (2013)) is applied on blowing snow conditions at PE. Blowing snow there occurs mainly during synoptic, or transitional conditions (n = 461; 61 %), often accompanied with precipitation. The attenuated backscatter signal is the highest during this type of events. The added value of the BSD algorithm over satellite detection is that those events are successfully detected by the algorithm, whereas satellite detection is limited to clear sky conditions, implying that a great part of the events during the synoptic regime would be missed, although they represent more than half of the events observed at PE. Less blowing snow is observed during the cold katabatic regime (n = 165; 22 %), as can be seen on the wind rose (Fig. 10). The atmosphere is more stable, with a larger temperature inversion (in agreement with Gorodetskaya et al. (2015)) and the mean blowing snow layer thickness is lower. Blowing snow without precipitation, but with dominant easterly wind direction can be associated with transitional conditions (n = 126; 17 %) precipitation, when the time lag since the last precipitation event is longer.

missed by the satellite, and to the different spatial and temporal dimensions of the different methods. Of all blowing snow detected events, 67% is mixed with intense events at Neumayer III, and 43% at PE station. Cloudless blowing snow is very rare at Neumayer III station (8% of the events), while it reaches 30% at PE station.

4.1.1 Time since last precipitation and blowing snow occurrence

We investigate the time lag between the last precipitation event and the onset of blowing snow events at PE station. The majority of blowing snow occurs during or within a day after a precipitation event (nearly 60 and over 80% of the blowing snow occurrences, respectively). There is a clear drop for larger time lags (Fig. 11(a)). This is, however, not so obvious anymore if we normalize the distribution of blowing snow events taking into account the total number of ceilometer measurements within each time lag after precipitation (Fig. 11(b)). A possible explanation is that the number of observations decrease with there are less measurements as we go in time, and that blowing snow occurred during those observations measurements. This can also be linked to the fact that the blowing snow particles detected by the BSD algorithm might originate from another location where there is precipitation, while no snowfall is detected snowfall is not reported by the precipitation radar at the station itself.

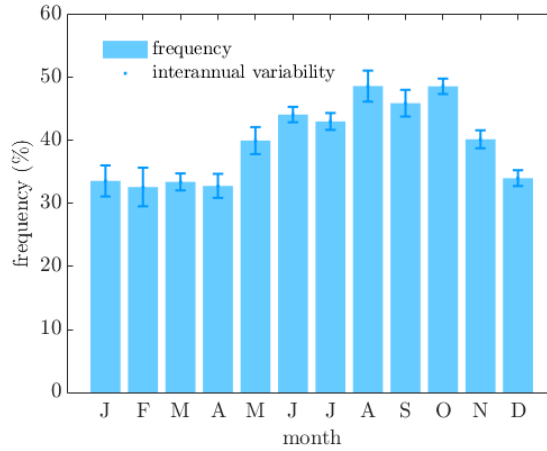


Figure 7. Wind roses presenting the wind direction for all blowing snow, Annual cycle of blowing snow with or without precipitation, and non-blowing snow conditions frequency at Princess Elisabeth-Neumayer III station, derived by the BSD algorithm (blue bars) for the period 2011-2015. The error bars represents the inter annual variability.

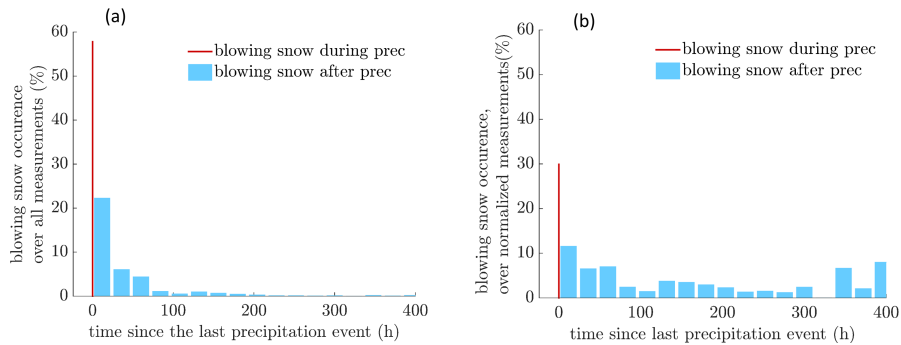


Figure 8. (a) Time between blowing snow and the last precipitation event at PE station. The red bar represents blowing snow occurring during precipitation, and the blue bars represent the fraction of blowing snow occurring each 24h time lag after a precipitation event. (b) Ratio of the number of blowing snow hours happening within the time lag over the total number of measurements for this time lag.

4.2 Blowing snow and meteorological regimes

The near surface atmosphere changes associated with blowing snow events are investigated for both stations, and detailed means and standard deviation are displayed in Tables S5, S6 and S7 in Supplements. We investigate how blowing snow relate to weather regimes, derived from the hierarchical cluster analysis using PE AWS data following Gorodetskaya et al. (2013), which defines the weather regimes at PE station: "cold katabatic", "warm synoptic", and "transitional synoptic". The cold katabatic regime is characterized by slower wind speeds and lower humidity, reduced incoming long wave radiation, a slight surface pressure increase, and a substantial temperature inversion. Warm synoptic conditions involve higher wind speeds and specific humidity, strongly positive anomalies of incoming long wave radiation. The surface pressure is slightly lower, and the temperature inversion is strongly reduced than during average conditions. Finally, average wind speeds, humidity and incoming long wave radiation, as well as slightly lower surface pressure are observed during the transitional regime, when the situation evolves from synoptic to katabatic or the other way around (Gorodetskaya et al., 2013). We therefore investigate the specific meteorological conditions (near-surface temperature inversion, relative humidity, surface temperature, wind speed and direction, in- and outgoing longwave fluxes, and the time since the last precipitation event) during blowing snow events. For all three categories of blowing snow events, the 2m wind direction shows a preferential easterly/north-easterly orientation at both Neumayer and PE, while the absence of blowing snow is characterized by a wider spectrum of wind directions (Figs. 9 and 10). Positive anomalies in wind speed and relative humidity occur during blowing snow events. Cyclonic events are a common feature at Neumayer (König-Langlo and Loose, 2007), bringing easterly winds during which most of the drifting and blowing snow occur. Also at PE, most of the blowing snow events (N = 1643, 92%) are associated with the warm synoptic and transitional regimes, when moist air is brought from the ocean, that precipitate inland (Gorodetskaya et al., 2013). Thiery et al. (2012) also showed that at PE drifting snow sublimation occurs mostly during transitional regimes. These regimes occur 41-48% of the time (Gorodetskaya et al., 2013, 2014). Very few blowing snow events occur in cloudless cold conditions (cold katabatic regime), when the northerly winds blows from the interior towards the coast (N = 139; 8%). Intense mixed events (Fig.5) occur together with north-easterly strong winds : 87° to N, $10 \text{ m} \cdot \text{s}^{-1}$ at PE and 65° to N, $13 \text{ m} \cdot \text{s}^{-1}$ at Neumayer III, warmer surface temperatures and higher relative humidity. These are the signature of storms associated with synoptic events, during which the turbulent mixing reduces the vertical temperature gradient (Gorodetskaya et al., 2013). The majority (60%) of the blowing snow events occur during storms or overcast conditions (with cloud and/or precipitation). These mixed events have generally a short time lag since the last precipitation event and reach high atmospheric levels. Dry blowing snow has a mean wind direction of 120° to N at PE and 77° at Neumayer III, lower wind speeds ($6\text{-}7 \text{ m} \cdot \text{s}^{-1}$) and a greater temperature inversion. The mean time lag since the last precipitation event at PE (23 hours) indicates that these events most likely occur shortly after a storm, and that cloudless blowing snow (8%) is mostly associated to katabatic winds. Apart from these factors, sastrugis might also have an impact on blowing snow (Amory et al., 2017) but are not measured here.

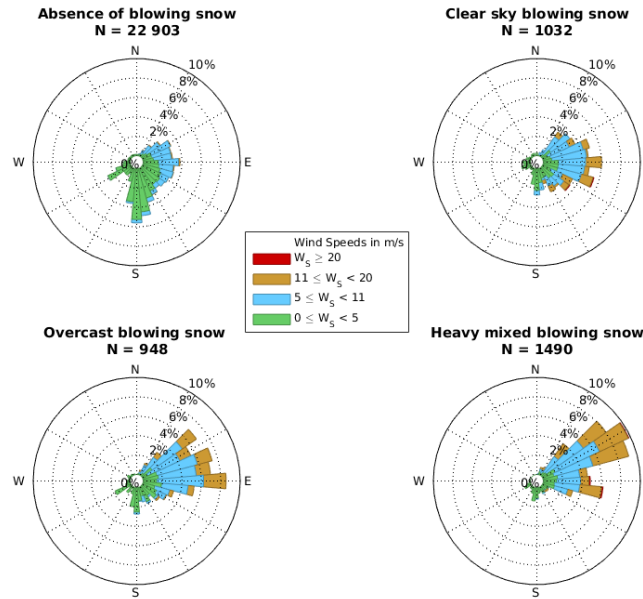


Figure 9. Wind roses presenting the wind direction for the absence of blowing snow (N=20 948), blowing snow with (N = 3834) or without precipitation (N = 1237) , and heavy mixed blowing snow (N = 10351) at Neumayer III station (2011-2015).

4.2.1 Depth of the blowing snow layer

The height of the blowing snow layer (algorithm explained in section 3.2) varies according to different parameters: the wind speed, and the size and density of the snow particles. In addition, the presence of clouds and precipitation also influences the vertical extent of the blowing snow layer. Blowing snow layer depths at Neumayer III and PE show a predominance of shallow layers (over 65-55 and 75% thicknesses below 100 m, respectively, Fig. 12)-11). However, there is little inter-event variability in blowing snow layer height at both stations. Blowing snow during precipitation at PE induces both stations induce in general layers of higher vertical extend: mean layer height during precipitation reaches 234-331 m, while clear sky mean blowing snow layer depth is limited to 74-78 m at PE. The values found for both stations are consistent to-with the mean blowing snow layer height detected by ground-based lidar at South Pole (Mahesh et al., 2003), although somewhat lower. The thickness of the blowing snow layer detected by the BSD algorithm is probably underestimated in case of heavy blowing snow events, due to total attenuation of the signal before reaching the top of the layer.

We further tested the hypothesis that the height of the blowing snow layer is related to wind speed at PE station. While there is no correlation, (also found by Mahesh et al. (2003)), the height of the blowing snow layer is related to the time since last precipitation (Fig. ??12). The height of the blowing snow layer can reach up to 1000 m within 24 to 48 h after precipitation,

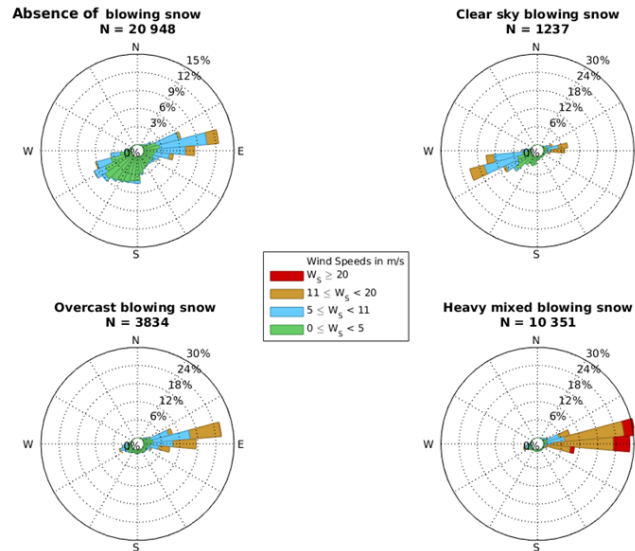


Figure 10. Wind roses presenting the wind direction for the absence blowing snow ($N=22\,903$), blowing snow with ($N = 948$) or without precipitation ($N = 1032$), and heavy mixed blowing snow ($N = 1490$) at Princess Elisabeth station (2010-2017).

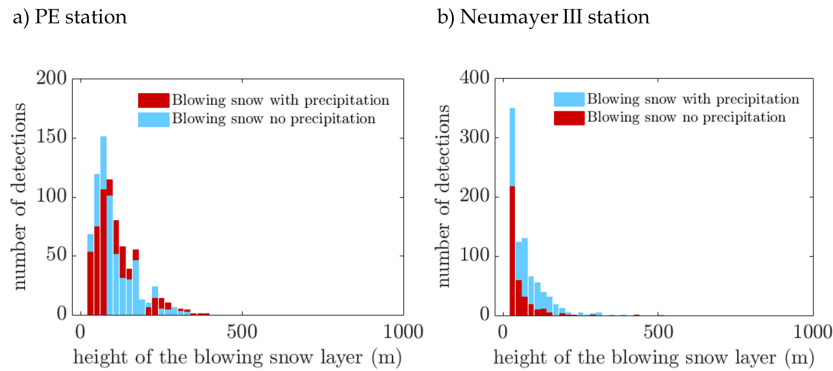


Figure 11. Distribution of the height of the blowing snow layer at (a) Neumayer-PE station (b) at PE-Neumayer station, blowing snow accompanied with precipitation in blue, blowing snow without precipitation in red and the white bar represents periods with missing precipitation data.

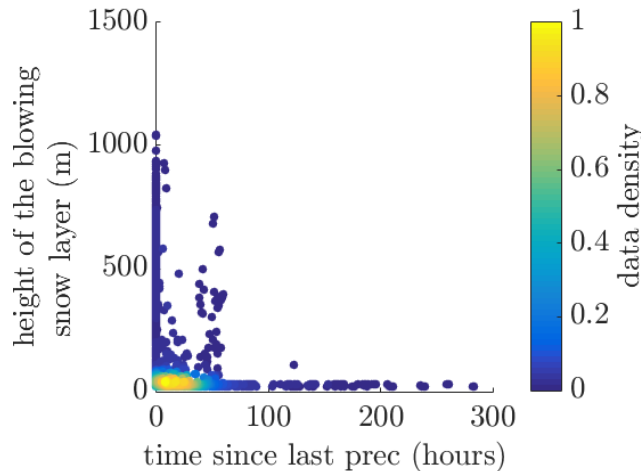


Figure 12. Scatter plot of the time since last precipitation event versus height of the blowing snow layer at PE station. Each point represents a blowing snow event. The colorbar represent the data density (number of observations divided by the entire sample size).

and 95% of the blowing snow layers thicker than 500 m occur shortly after the last precipitation event. Blowing snow events taking place much later after the precipitation event are limited to a vertical extend lower than 100 m thick.

5 Discussion

5.1 Applicability of the algorithm

- 5 The BSD algorithm developed for the Vaisala CL-31 ceilometer at PE was ~~successfully~~ applied to the Vaisala CL-51 ceilometer at Neumayer III station. Comparing the BSD algorithm detections to visual observations at Neumayer ~~proved the applicability~~ showed a good agreement and the ability of the BSD algorithm to detect (heavy) blowing snow events, both under dry and precipitating conditions. ~~The algorithm~~ Satellite detections of blowing snow, although covering the whole continent, are limited to clear sky conditions. The BSD algorithm, however, is able to detect blowing snow during most of the storms, which is an
- 10 improvement ~~compared to satellite detection~~ as the majority of blowing snow occur together with cloud/precipitation. When we limit the analysis to (heavy) blowing snow, the algorithm detects ~~79-78%~~ 79-78% of the events ~~indicated by the observer~~. On the other hand, there are cases where the ceilometer does not detect events classified as heavy events by the observer. However, it has to be kept in mind that ~~snowdrift blowing and drifting snow~~ observations are extremely challenging, with a potential large but unknown error on the observations. Furthermore, the hourly time filtering applied leads to commission errors (events
- 15 detected ~~that were not there) and commission~~ by the algorithm, but not reported by the visual observations) and omission errors (short-lived events are likely removed from the running mean). However, such events induce much smaller blowing snow transport rates than strong events, and we suspect that omitting them will only reduce blowing snow transport rates by a small percentage. A limitation of the BSD algorithm is that both ceilometers are set up on the roof of the station, 17 m at

Neumayer III and 12 m above the ground in the main wind direction at PE. In addition, 15 m have to be added to account for the discard of the first range bin. There, ceilometers will report the most significant blowing snow events (higher than 30 m) and most drifting snow and shallow blowing snow events are not detected. ~~Finally, due to the profile-shape based algorithm, the occurrence of blowing snow during severe storms or very heavy precipitation events can not be reported; then, the signal~~ If setting up a ceilometer in the aim of measuring blowing snow, the device should be placed as close to the ground as possible to also retrieve shallower blowing snow events. Ceilometers can retrieve the presence of blowing snow ~~is mixed with that of precipitating snow, and the steady decrease of the profile until 45 height is no longer valid.~~, but other properties such as optical depth, size and density measurement is only possible if the ceilometer is calibrated, which is very challenging and not done in this paper. The BSD algorithm can be applied to any ceilometer located in Antarctica, but we recommend to use a bin width of 10 m for operating ceilometers to detect blowing snow, which is the case at PE and Neumayer III. Since the Vaisala CT25K at Halley station uses a 30m vertical resolution, it was not used in this study.

5.2 Wind speed versus snow availability

Gallée et al. (2001) stated that snow-pack properties mainly determine snow erosion: dendricity, density, sphericity and particles size regulate the availability of snow for transportation. These parameters change with metamorphism and impact the threshold friction velocity, and ~~therefore the threshold friction velocity and thus the~~ minimum wind speed required for particles movement uplift from the ground. Here, we do not apply any wind speed threshold to the detection of blowing snow, whereas ~~many observations and modelling studies do so. Palm et al. (2011)~~ some modelling studies assume a drifting snow dependency on temperature and wind speed (Giovinetto et al., 1992; Déry and Yau, 1999, 2002; Yang et al., 2010). Palm et al. (2011) for instance, uses a minimum wind speed criterion to detect blowing snow from satellite backscatter, potentially leaving out some events.

We find that the ~~the~~ presence of freshly fallen snow (~~availability and size/density of snow particles~~) has a great impact on blowing snow occurrence and blowing snow layer height. As postulated by Mahesh et al. (2003), the end of a large snow storm with high wind speeds could still hold snow particles suspended in the air, even if the wind speed has already dropped to lower speeds than those required to dislodge the particles from the ground at the onset of the blowing snow event. Conversely, if no particles are available for the wind to pick up, blowing snow might not occur even though the wind speeds are high. ~~Despite the fact that there is no mean to distinguish dry blowing snow from blowing snow occurring during precipitation from ground-based instruments at Neumayer, the~~ The large majority of blowing snow events occur under synoptic disturbances (~~n=867; 96%-92% at PE and Neumayer III~~) rather than katabatic conditions. These disturbances are also associated with higher wind speeds and are often accompanied with precipitation. In those cases, snow is available for transport. At PE, the explanation for the limited occurrence of blowing snow under katabatic conditions might lie in the fact that the station is shielded by the Sør Rondane mountains, but also due to the limited availability of fresh snow and the reduced turbulence during those events compared to synoptic conditions, maintaining particles aloft. This, together with the reduced number of blowing snow events occurring under katabatic winds might indicate that the effect of ~~katabatics~~ katabatic winds on blowing snow occurrence

has been overestimated, and ~~the occurrence of that~~ synoptic events bringing fresh snow is a most possibly determining factor for blowing snow at Neumayer III and PE stations.

6 Conclusions

Various observations, models and satellite studies have been performed to quantify and investigate blowing snow on the Antarctic continent. We present here our novel BSD algorithm, designed to retrieve blowing snow events, but not drifting snow, from ground-based remote-sensing ceilometers.

The algorithm has proven to be reliable in detecting ~~(heavy)~~ blowing snow at Neumayer station in up to 79.78% of the cases when compared to visual observations. The presence of precipitation does not substantially limit the retrieval by the ceilometer. This is an improvement to satellite detection, limited to clear sky conditions and therefore missing a great part of the blowing snow as more than half of the blowing snow happens during a storm at PE and Neumayer III station. Blowing snow detected by the BSD algorithm occurs 36% of the time at Neumayer station, and 13% at PE station, with an interannual variation of $\pm 5\%$ and seasonal cycle that peaks during the Antarctic winter. We further conclude that most of the blowing snow events happen during or shortly after precipitation, brought to the continent by the easterly winds associated to synoptic systems. The availability of fresh snow mainly determines the onset of blowing snow, and the available fresh snow can be lifted to higher heights than during katabatic conditions ~~whose effect is likely to have been overestimated for lifting snow from the surface~~ at PE and Neumayer stations. This highlights again the limitation of wind speed thresholds, when applied to blowing snow retrieval methods, ~~and the need to take into account the~~ The properties of the snow particles, including as well as the availability of fresh snow , need to be taken into account in order to accurately initiate blowing snow in models. Since ceilometers are low-cost robust instruments, and often deployed at stations for the purpose of aircraft operations, our newly developed algorithm opens opportunities for long-term monitoring networks of consistent blowing snow observations. These can further be used to ~~validate~~ evaluate satellite retrieval and combined to produce blowing snow products over the ice sheets.

7 Code availability

The algorithm is freely available upon request to alexandra.gossart@kuleuven.be

8 Data and availability

Data from Neumayer station are freely available on the Pangaea portal and data from the instruments at Princess Elisabeth station are available upon request (www.aerocloud.be).

Acknowledgements. We are grateful to the Research Foundation Flanders (FWO) and the Belgian Federal Science Policy (BELSPO) for the financial support of the AEROCLOUD project (BR/143/A2/AEROCLOUD). We thank the logistic team and the Royal Meteorological

Institute for executing the yearly maintenance of our instruments at the Princess Elisabeth station. We further thank Wim Boot, Carleen Reijmer, and Michiel van den Broeke (Institute for Marine and Atmospheric Research Utrecht) for the development of the Automatic Weather Station, technical support and raw data processing. We warmly thank World Radiation Monitoring Center for providing the Baseline Surface Network Radiation data set at Neumayer station, and Gert König-Langlo for the CL-51 ceilometer data and information about the visual observations. We further thank the Norwegian Polar Institute for the use of the free Quantarctica package, as well as Bindschadler et al. (2011); Bamber et al. (2009) for the datasets.

References

- [Allouche, O., Tsoar, A. and Kadmon, R.: Assessing the accuracy of species distribution models: prevalence, kappa and the true skills statistics \(TSS\), *Journal of applied Ecology*, 43, 1223–1232, 2006.](#)
- Amory, C., Trouvilliez, A., Gallée, H., Favier, V., Naaim-Bouvet, F., Genthon, C., Agosta, C., Piard, L., and Bellot, H.: Comparison between
5 observed and simulated eolian snow mass fluxes in Adélie Land, East Antarctica, *The Cryosphere*, 9, 1373–1383, 2015.
- [Amory, C., Gallée, H., Naaim-Bouvet, F., Favier, V., Vignon, E., Picard, G., Trouvilliez, A., Piard, L., Genthon, C., Bellot, H.: Seasonal Variations in Drag Coefficient over a Sastrugi-Covered Snowfield in Coastal East Antarctica, *Boundary-Layer Meteorol.*, 164, 107–133, 2017.](#)
- Anderson, P. S.: A Method for Rescaling Humidity Sensors at Temperatures Well below Freezing, *J. Atmos. Oceanic Technol.*, 11, 1388–
10 1391, 1994.
- [Bagnold, R. A.: *The Physics of Blown Sand and Desert Dunes*, Mathuen, London, 265 pp., 1954.](#)
- Bamber, J. L., Gomez-Dans, J. L., and Griggs, J. A.: Antarctic 1 km Digital Elevation Model (DEM) from Combined ERS-1 Radar and
ICESat Laser Satellite Altimetry, Boulder, Colorado USA: National Snow and Ice Data Center, Digital media, 2009.
- Barral, H., Genthon, C., Trouvilliez, A., Brun, C., Amory, C.: Blowing snow in coastal Adélie Land, Antarctica: three atmospheric-moisture
15 issues, *The Cryosphere*, 8, 5, 1905–1919, ~~2015~~-2014.
- Bindschadler, R., Choi, H., Wichlacz, A., Bingham, R., Bohlander, J., Brunt, K., Corr, H., Drews, R., Fricker, H., Hall, M., Hindmarsh,
R., Kohler, J., Padman, L., Rack, W., Rotschky, G., Urbini, S., Vornberger, P., and Young, N.: Getting around Antarctica: New High-
Resolution Mappings of the Grounded and Freely-Floating Boundaries of the Antarctic Ice Sheet Created for the International Polar Year,
The Cryosphere, 5, 569-588, doi:10.5194/tc-5-569-2011, 2011.
- 20 Bintanja, R., and van den Broeke, M. R.: The surface energy balance of Antarctic snow and blue ice, *J. Appl. Meteorol.*, 34(4), 902–926,
2005.
- Bintanja, R.: Modelling snowdrift sublimation and its effect on the moisture budget of the atmospheric boundary layer, *Tellus*, 53A, 215-232,
2001.
- Bintanja, R., and Reijmer, C. H.: A simple parametrization for snowdrift sublimation over Antarctic snow surfaces, *J. Geophys. Res.*, 106,
25 D23, 739-748, 2001.
- Bromwich, D. H.: Snowfall in high southern latitudes, *Reviews in Geophysics*, 26(1), 149–168, 1988.
- Budd, W. F., Dingle, W. R. J., and Radok, U.: The Byrd snow drift project: Outline and basic results, *Studies in Antarctic Meteorology*,
Antarct. Res. Ser., 9, M.J.Rubin, 71–134, AGU, Washington, D. C, 1966.
- Dai, X., and Huang, N.: Numerical simulation of drifting snow sublimation in the saltation layer, *Scientific Reports*, 4 (6611), 1–5, doi:
30 10.1038, 2014.
- Déry, S. J., and Tremblay, L. B.: Modeling the Effects of Wind Redistribution on the Snow Mass Budget of Polar Sea Ice, *J. Phys. Oceanogr.*,
34, 258–271, 2004.
- [Déry, S. J., and Yau, M. K.: A climatology of adverse winter-type weather events, *J. Geophys. Res.*, 104, 16,657–16,672, 1999.](#)
- Déry, S. J., and Yau, M. K.: Large-scale mass balance effects of blowing snow and surface sublimation, *J. Geophys. Res.*, 107(D23),
35 doi:10.1029/2001JD001251, 8-1 – 8-17, 2002.
- Emeis, S., Schäfer, K., and Münkler, C.: Surface-based remote sensing of the mixing-layer height - a review, *Meteorol. Z.*, 17, 5, 621–630,
2008.

- Eresmaa, N., Karppinen, A., Joffre, S. M., Räsänen, J., and Talvitie, H.: Mixing height determination by ceilometer, *Atmos. Chem. Phys.*, 6, 1485–1493, 2006.
- [Favier, V., Agosta, C., Parouty, S., Durand, G., Delaygue, G., Gallée, H., Drouet, A. S., Trouvilliez, A., and Krinner, G.: An updated and quality controlled surface mass balance dataset for Antarctica, *The Cryosphere*, 7, 583–597, doi:10.5194/tc-7-583-2013, 2013.](#)
- 5 Fiocco, G., Grams, G.: Observations of the aerosol layer at 20km by optical radar, *J. Atmos. Sci.*, 21, 323–324, 1964.
- [Flynn, C.: Vaisala ceilometer \(model CT25K\) handbook, ARM TR-020, available at: <https://public.wmo.int/en/programmes/global-climate-observing-system> \(last access: 1 September 2017\), 2004.](#)
- Fretwell, P., Pritchard, H. D., Vaughan, D. G., Bamber, J. L., Barrand, N. E., Bell, R., Bianchi, C., Bingham, R. G., Blankenship, D. D.,
- 10 Casassa, G., Catania, D., Callens, D., Conway, H., Cook, A. J., Corr, H. F. J., Damaske, D., Damm, V., Ferraccioli, F., Forsberg, R., Fujita, S., Gim, Y., Gogineni, P., Griggs, J. A., Hindmarsh, C. A., Holmlund, P., Holt, J. W., Jacobel, R. W., Jenkins, A., Jokat, W., Jordan, T., King, E. C., Kohler, J., Krabill, W., Riger-Kusk, M., Langley, K. A., Leitchenkov, G., Leuschen, C., Luyendyk, B. P., Matsuoka, K., Mouginit, J., Nitsche, F. O., Nogi, Y., Nost, O. A., Popov, S. V., Rignot, E., Rippin, D. M., Rivera, A., Roberts, J., Ross, N., Siegert, M. J., Smith, A. M., Steinhage, D., Studinger, M., Sun, B., Tinto, B. K., Welch, B. C., Wilson, D., Young, D. A., Xiangbin, C., and Zirizzotti,
- 15 A.: Bedmap2 : improved ice bed, surface and thickness datasets for Antarctica, *The Cryosphere*, 7, 375 – 393, 2013.
- Frezzotti M., Pourchet, M., Flora, O., Gandolfi, S., Gay, M., Urbini, S., Vincent, C., Becagli, S., Gagnani, R., Proposito, M., Severi, M., Traversi, R., Udisti, R., and Fily, M.: New estimations of precipitation and surface sublimation in East Antarctica from snow accumulation measurements, *Clim. Dyn.*, 23, 803–813, 2004.
- Gallée, H., Guyomarc’h, G., and Brun, E.: Impact of snow drift on the Antarctic ice sheet surface mass balance : possible sensitivity to
- 20 snow-surface properties, *Boundary Layer Meteorol.*, 99, 1–19, 2001.
- [Giovinetto, M.B., Bromwich, D.H., and Wendler, D.: Atmospheric Net Transport of Water Vapor and Latent Heat Across 70°S, *J. Geophys. Res.*, 97, 917–930, 1992.](#)
- Gorodetskaya I. V., Kneifel, S., Maahn, S., Van Tricht, K., , W., Schween, J. H., Mangold, A., Crewell, S., and van Lipzig, N. P. M.: Cloud and precipitation properties from ground-based remote-sensing instruments in East Antarctica, *The Cryosphere*, 9, 286–304, 2015.
- 25 Gorodetskaya, I. V., Tsukernik, M., Claes, K., Ralph, M. F., Neff, W. D., and van Lipzig, N. P. M.: The role of atmospheric rivers in anomalous snow accumulation in East Antarctica, *Geophys. Res. Lett.*, 16, 6199-6206, 2014.
- Gorodetskaya, I. V., van Lipzig, N. P. M., Boot, W., Reijmer, C. H., and van den Broeke, M. R.: AWS measurements at the Belgian Antarctic station Princess Elisabeth, Dronning Maud Land, for precipitation and mass balance studies, *Extended abstracts of the Workshop on Automatic weather stations on glaciers, Pontresina, Switzerland*, 40–44, 2011.
- 30 Gorodetskaya, I. V., van Lipzig, N. P. M., van den Broeke, M. R., Mangold, A., Boot, W., and Reijmer, C. H.: Meteorological regimes and accumulation patterns at Utsteinen, Dronning Maud Land, East Antarctica: Analysis of two contrasting years, *J. Geophys. Res.*, 118, 4, 1700–1715, 2014.
- Groot Zwaartink, C. D., Cagnati, A., Crepaz, A., Fierz, C., Macelloni, G., Valt, M., and Lehning, M.: Event-driven deposition of snow on the Antarctic Plateau: analyzing field measurements with SNOWPACK, *The Cryosphere*, 7(1), 333–347, 2013.
- 35 Haeffelin, M., Angelini, F., Morille, Y., Martucci, G., Frey, S., Gobbi, G. P., Lolli, S., O’Dowd, C. D., Sauvage, L., Xueref-Rémy, I., Wastine, B., and Feist, D. G.: Evaluation of Mixing-Height Retrievals from Automatic profiling Lidars and Ceilometers in View of Future Integrated Networks in Europe, *Boundary Layer meteorol.*, 143, 49–75, 2012.

- Haeffelin, M., Laffineur, Q., Bravo-Aranda, J. A., Drouin, M. A., Casquero-Vera, J. A., Dupont, J. C., and De Backer, H.: Radiation fog formation alerts using attenuated backscatter power from automatic lidars and ceilometers, *Atmos. Meas. Tech.*, 9, 5347–5365, 2016.
- Heese, B., Flentje, D., Ansmann, A., and Frey, S.: Ceilometer lidar comparison: backscatter coefficient retrieval and signal-to-noise ratio determination, *Atmos. Meas. Tech.*, 3, 1763–1770, 2010.
- 5 Illingworth, A., Cimini, D., Gaffard, C., Haeffelin, M., Lehmann, V., Loehnert, U., O'Connor, E., Ruffieux, D.: Exploiting Existing Ground-Based Remote Sensing Networks To Improve High Resolution Weather Forecasts, *Bull. Amer. Meteor. Soc.*, doi: 10.1175/BAMS-D-13-00283.1, 2015.
- King, J. C., and Turner, J., *Antarctic Meteorology and Climatology*, Cambridge University Press, Cambridge, 409 pp, 1997.
- [Klugmann, D., Heinsohn, K., Kirtzel, H.J.: A low cost 24 GHz FM-CW Doppler radar rain profiler, *Contributions to Atm. Phys.*, 69, 247–253, 1996.](#)
- 10 Kobayashi, S.: Snow transport by katabatic winds in Mizuho camp area, East Antarctica, *J. Meteorol. Soc. Jpn.*, 56, 130–139, 1978.
- Kodama, Y., Wendler, G., and Gowink, J.: The effect of blowing snow on katabatic winds in Antarctica, *Ann. Glaciol.*, 6, 59–62, 1985.
- ~~König-Langlo, G.: Ceilometer raw data measured at Neumayer station, links to files. Alfred Wegener Institute, Helmholtz Center for Polar and Marine Research, Bremerhaven.~~
- 15 König-Langlo, G., and Loose, B.: The Meteorological Observatory at Neumayer Stations (GvN and NM-II) Antarctica, *Polarforschung*, 76 (1-2), 25-38, 2007.
- Kotthaus, S., O'Connor, E., Muenkel, C., Charlton-Perez, C., Gabey, M. G., and Grimmond, C. S. B.: Recommendations for processing atmospheric attenuated backscatter profiles from Vaisala CL31 Ceilometers, *Atmos. Meas. Tech. Discuss.*, 9.8, 3769–3791, 2016.
- Lenaerts, J. T. M., Lhermitte, S., Drews, R., Ligtenberg, S. R. M., Berger, S., Helm, V., Smeets, C. J. P. P., van den Broeke, M. R., van de Berg, W. J., van Meijgaard, E., Eijkelboom, M., Eisen, O., and Pattyn, F.: Meltwater produced by wind-albedo interaction stored in an East Antarctic ice shelf, *Nature climate change*, 2016.
- 20 Lenaerts, J. T. M., and van den Broeke, M. R.: Modeling drifting snow in Antarctica with a regional climate model: 2. Results, *J. Geophys. Res.*, 117(D5), D05109, 2012.
- Lenaerts, J. T. M., van den Broeke, M. R., Déry, S. J., König-Langlo, G., Ettema J., and Munneke, P. K.: Modelling snowdrift sublimation on an Antarctic ice shelf, *The Cryosphere*, 4, 179–190, 2010.
- 25 Leonard, K. C., Tremblay, L. B., Thom, J. E., and MacAyeal, D. R.: Drifting snow measurements near McMurdo station, Antarctica: A sensor comparison study, *Cold Regions Science and Technology*, 70, 71–80, 2011.
- Lesins, G., Bourdages, L., Duk, T. J., Drummond, J. R., Eloranta, E. W., and Walden, V. P.: Large surface radiative forcing from topographic blowing snow residuals measured in the High Arctic at Eureka, *Atm. Chem. Phys.*, 9(6), 1847–1862, 2009.
- 30 Li, L., and Pomeroy, J. W.: Estimates of Threshold Wind Speeds for Snow Transport Using Meteorological Data, *Journal of Applied Meteorology*, 36, 205–213, 1997.
- Ligda, M.: Meteorological observations with a pulsed laser radar, *Proceedings 1st Conference on Laser Technology*, U.S. Office of Naval Research, 63–72, 1963.
- Loewe, F.: The transport of snow in the ice sheets by the wind, in: *Studies on drifting snow*, Meteorology Report 13, Melbourne, University of Melbourne, Meteorology department, 21–69, 1970.
- 35 Maahn, M., and Kollias, P.: Improved Micro Rain Radar snow measurements using Doppler spectra post-processing, *Atm. Meas. Tech.*, 5, 2661–2673, 2012.

- Madonna, F., Amato, F., Vande Hey, J., and Pappalardo, G.: Ceilometer aerosol profiling versus Raman lidar in the frame of the INTERACT campaign of Actris, *Atmos.Meas.Tech.*, 8, 2207–2223, 2015.
- Mahesh, A., Spinhire, J. D., Duda, D. P., and Eloranta, E. W.: Atmospheric multiple scattering effects on GLAS altimetry, part II, Analysis of expected errors in Antarctic altitude measurements, *IEEE Trans. Geosci. Remote Sens.*, 40, 2353–2362, 2002.
- 5 Mahesh, A., Eager, R., Campbell, J. R., and Spinhire, J. D.: Observations of blowing snow at South Pole, *Journal of Geophysical Research*, 108 (D22), 4707, 2003.
- Marcowicz, K. M., Flatau, P. J., Kardas, A. E., Remiszewska, J., Stelmasczyk, K., and Woeste, L.: Ceilometer retrieval of the Boundary Layer Vertical Aerosol Extinction Structure, *J. Atmos. Oceanic Technol.*, 25, 928–944, 2007.
- Martucci, G., Milroy, C., and O’Dowd, C.: Detection of Cloud-Base Height Using Jenoptik CHM15K and Vaisala CL31 Ceilometers, *J. Atmos. Oceanic Technol.*, 27, 305–318, 2010.
- [Mellor, M.: Blowing Snow, Cold Regions Science and Engineering: Part II, section A3c., 78pp., 1965.](#)
- Metz, C. E.: Basic Principles of ROC Analysis, *Seminars in Nuclear Medicine*, VIII(4), 283–298, 1978.
- Münkel, C., Eresmaa, N., Räsänen, J., and Karppinen, A.: Retrieval of mixing height and dust concentration with lidar ceilometer, *Bound.-Lay. Meteorol.*, 124, 177–128, doi:10.1007/s10546-006-9103-3, 2006.
- 15 Münkel, C., and Rasanen, J.: New optical concept for commercial lidar ceilometers scanning the boundary layer, *Remote Sensing of Clouds and the Atmosphere IX*, Proc. SPIE 5571, November 30, 2004, doi:10.1117/12.565540, 2004.
- Münkel, C., and Roininen, R.: Investigation of boundary layer structures with ceilometer using a novel robust algorithm. Proc. 90th American Meteorological Society Annual Meeting: 15th Symposium on Meteorological Observation and Instrumentation, 5.3, 2010.
- Nishimura, K., and Nemoto, M.: Blowing snow at Mizuho station, Antarctica, *Phil.Trans. R. Soc. A.*, 363, 1647–1662, 2015.
- 20 [Palermo, C., Kay, J. E., Genthon, C., L’Ecuyer, T., Wood, N. B., and Wood, C.: How much snow falls on the Antarctic ice sheet?. The Cryosphere, 8,1577–1587, doi: 10.5194/tc-8-1577-2014, 2014.](#)
- Palm, S. P., Yang, Y., Spinhire, J. D., and Marshak, A.: Satellite remote sensing of blowing snow properties over Antarctica, *J. Geophys. Res.*, 116, D16123, 2011.
- [Parish, T. R. and Bromwich, D. H.: Reexamination of the Near-Surface Airflow over the Antarctic Continent and Implications on Atmospheric Circulations at High Southern Latitudes, Mon. Wea. Rev., 135, 5, 961–1973, doi:10.1175/MWR3374.1, 2007.](#)
- 25 Rignot, E., and Jacobs, S. S.: Rapid Bottom Melting Widespread Near Antarctic Ice Sheet Grounding Lines, *Science*, 296, 2020–2023, 2002.
- Rignot, E., and Thomas, R.: Mass balance of Polar Ice Sheets, *Polar Sc.*, 297, 1502–1506, 2002.
- Rignot, E., Velicogna, I., van den Broeke, M.R., Monaghan, A., and Lenaerts, J. T. M.: Acceleration of the contribution of the Greenland and Antarctic ice sheets to sea level rise, *Geophys. Res. Lett.*, 38 (L05503), 2011.
- 30 Rowe, P. M., Cox, C. J., and Walden, V. P.: Towards autonomous surface-based infrared remote sensing of polar clouds: Cloud heights retrieval, *Atmos. Meas. Tech. Discuss.*, 49, 3641–3659, 2016.
- Scambos, T. A., Bohandler, J. A., Shurman, C. A., and Scarva, P.: Glacier acceleration and thinning after ice shelf collapse in the Larsen B embayment, Antarctica, *Geophys. Res. Lett.*, 31(18), 2001–2004, 2004.
- Scarchili, C., Frezzotti, M., Grigioni, P., De Silvestri, L., Agnoletto, L., and Dolci, S.: Extraordinary blowing snow transport events in East Antarctica, *Clim. Dyn.*, 34, 1195–1206, 2010.
- 35 Schmidt, R. A.: Threshold wind-speeds and elastic impact in snow transport, *J. Glaciol.*, 26(94), 453–467, 1980.
- Schmidt, R. A.: Properties of blowing snow, *Rev. Geophys.*, 20, 39–44, 1982.

- Shepherd, A., Ivins, E. R., A., G., Barletta, V. R., Bentley, M. J., Bettadpur, S., Briggs, K. H., Bromwich, D. H., Forsberg, R., Galin, N., Horwath, M., Jacobs, S., Joughin, I., King, M. A., Lenaerts, J. T. M., Li, J., Ligtenberg, S. R. M., Luckman, A., Luthcke, S. B., McMillan, M., Maister, E., Milne, G., Mouginot, J., Muir, A., Nicolas, J. P., Paden, J., Payne, A. J., Pritchard, H., Rignot, E., Rott, H., Sørensen, L. S., Scambos, T. A., Scheuchl, B., Scharama, E. J. O., Smith, B., Sundal, A. V., van Angelen, J. H., van de Berg, W. J., van den Broeke, M. R., Vaughan, D. G., Velicogna, I., Wahr, J., Whitehouse, P. L., Wingham, D. J., Yi, D., Young, D., and Zwally, H. J.: A Reconciled Estimate of Ice-Sheet Mass Balance, *Science*, 338, 1183–1189, 2012.
- Sicard, M., Perez, C., Comeran, A., Baldasano, J. M., and Rocadenbosch, F.: Determination of the mixing layer height from regular lidar measurements in the Barcelona area, *Proc. SPIE 5235, Remote Sensing of Clouds and the Atmosphere VIII*, 505 (February 16, 2004); doi:10.1117/12.511481, 2004.
- 10 Sokol, P., Stachlewska, I., Ungureanu, I., and Stefan, S.: Evaluation of the boundary layer morning transition using the CL-31 ceilometer signals, *Acta Geophys.*, 62(2), 367–380, 2014.
- Souverein, N., Gossart, A., Lhermitte, S., Gorodetskaya, I.V., Kneifel, S., Maahn, M., Bilven, F.L., and van Lipzig, N.P.M.: Estimating radar reflectivity - snowfall rate relationships and their uncertainties over Antarctica by combining disdrometer and radar observations, *Atmos. Res.*, accepted.
- 15 Spinhirne, J.: Micro pulse lidar, *IEEE Trans. Geosci. Remote Sens.*, 31 (1), 48–55, 1993.
- Takahashi, S., Naruse, R., Nakawo, M., and Mae, S.: A bare ice fields in east Queen Maud Land, Antarctica, caused by horizontal divergence of drifting snow, *Ann. Glaciol.*, 11, 156-160, 1988.
- Takahashi, S., Endoh, T., Azuma, N., and Meshida, S.: Bare ice fields developed in the inland part of Antarctica, *Proc. NIPR Symp. Polar Meteorol. Glaciol.*, 5, 128–139, 1992.
- 20 Takeuchi, M.: Vertical profile and horizontal increase of drift snow transport, *J. Glaciol.*, 26, 481–492, 1980.
- Thiery, W., Gorodetskaya, I.V., Bintanja, R., van Lipzig, N. M. P., van den Broeke, M.R., Reijmer, C. H., and Kuipers Munneke, P.: Surface and snowdrift sublimation at Princess Elisabeth station, East Antarctica, *The Cryosphere*, 6(4), 841–857, 2012.
- Thomas, W.: Transitioning to Operations: Lidars and Ceilometers, WMO Technical Conference on Meteorological and Environmental Instruments and Methods of Observation, TECO-2012, Belgium, 2012.
- 25 Trouvilliez, A., Naim-Bouvet, F., [Genthon, C., Piard, L., Favier, V.](#), Bellot, H., [Genthon Agosta, C., Palerme, C., Amory, C.](#), and [Gall Gallée, H.](#): [Evaluation of the FlowCapt Acoustic Sensor for the Aeolian Transport of Snow, *J. Atmos. Ocean. Tech.*, 32, 1630–1641, 2015. A novel experimental study of aeolian snow transport in Adelie Land \(Antarctica\), *Cold Regions Science and Technology*, 108, 125–138, 2014.](#)
- Tsaknakis, G., Papayannis, A., Kokkalis, P., Amiridis, V., Kambezidis, H. D., Mamouri, R. E., Georgoussis, G., and Avdikos, G.: Inter-comparison of lidar and ceilometer retrievals for aerosol and Planetary Boundary Layer profiling over Athens, Greece, *Atmos. Meas. Tech.*, 4, 1261-1273, 2011.
- Vaisala, User's Guide, Vaisala Ceilometer CL31. Vaisala Oyj, 2006.
- van de Berg, W., van den Broeke, M. R., Reijmer, C. H., and van Meijgaard, E.: Characteristics of the Antarctic surface mass balance, 1958-2002, using a regional atmospheric climate model, *Ann. Glaciol.*, 41(1), 97–104, 2005.
- 35 van den Broeke, M. R.: Spatial and temporal variation for sublimation on Antarctica: Results of a high-resolution general circulation model, *J. Geophys. Res.*, 102(D25), 29, 765–29, 777, 1997.
- van den Broeke, M., and Bintanja, R.: The interaction of katabatic winds and the formation of blue ice areas in East Antarctica, *J. Glaciol.*, 41, 395–407, 1995.

- van den Broeke, M. R., Reijmer, C. H., and van de Wal, R. S. W.: A study of the surface mass balance in Dronning Maud Land, Antarctica, using automatic weather stations, *J. Glaciol.*, 50 (171), 565–581, 2004.
- van den Broeke M., van den Berg, W. J., and Van Meijgaard, E.: Firm depth correction along the Antarctic grounding line, *Ant. Sc.*, 20 (5), 513–517, 2008.
- 5 Vande Hey , J. D.: A Novel Lidar Ceilometer: Design, Implementation and Characterisation, Springer Theses, ISBN: 978-3-319-12612-8 (Print) 978-3-319-12613-5 (Online), Springer International Publishing, 2015.
- Van Tricht, K., Gorodetskaya, I.V., Lhermitte, S., Turner, D.D., Schween, J.H., and van Lipzig,N.P.M.: An improved algorithm for polar clouds-base detection by ceilometer over the ice sheets, *Atmos.Meas.Tech.*, 7, 1153–1167, 2014.
- Wamser, C., and Lykossov, V. N.: On the friction velocity during blowing snow, *Beitr. Phys. Atmosph.*, 68/01, 85–94, 2005.
- 10 Wiegner, M., Madonna, F., Binietoglou, I., Forkel, R., Gasteiger, J., Geiß, A., Pappalard, G., Schäfer, K., and Thomas, W.: What is the benefit of ceilomteres for aerosol remote sensing? An answer from EARLINET, *Atmos. Meas. Tech.*, 7, 1979–1997, 2014.
- Yamanouchi, T., and Kawaguchi, S.: Effects of drifting snow on surface radiation budget in the katabatic wind zone, Antarctica, *Ann. Glaciol.*, 6, 238–241, 1985.
- [Yang, J., Yau, M.K., Fang, X., and Pomeroy, J.W.: A triple-moment blowing snow-atmospheric model and its application in computing the seasonal wintertime snow mass budget, *Hydrol. Earth Syst. Sci.*, 14, 1063–1079, 2010.](#)
- 15

Supplements to *Blowing snow detection from ground-based ceilometers: application to East Antarctica*

Alexandra Gossart¹, Niels Souverijns¹, Irina V. Gorodetskaya^{2,1}, Stef Lhermitte^{3,1}, Jan T.M. Lenaerts^{4,1,5}, Jan H. Schween⁶, Alexander Mangold⁷, Quentin Laffineur⁷, and Nicole P.M. van Lipzig¹

¹Department of Earth and Environmental Sciences, KU Leuven, Leuven, Belgium

²Centre for Environmental and Marine Sciences, Department of Physics, University of Aveiro, Aveiro, Portugal

³Department of Geosciences and Remote Sensing, Delft University of Technology, Delft, the Netherlands

⁴Institute for Marine and Atmospheric research Utrecht, Utrecht University, Utrecht, The Netherlands

⁵Departement of Atmospheric and Oceanic Sciences, University of Colorado, Boulder CO, USA

⁶Institute of Geophysics and Meteorology, Koeln University, Koeln, Germany

⁷Royal Meteorological Institute of Belgium, Brussels, Belgium

Correspondence to: Alexandra Gossart (alexandra.gossart@kuleuven.be)

1 Equation of the different metrics used in section 4.1.

Equations come from Allouche et al. (2006),

with $a = N_{BS_{both}}$, $b = N_{BS_{ceilo}}$, $c = N_{BS_{vis}}$, $d = N_{BS_{none}}$ and $n = a + b + c + d$.

$$\text{accuracy} = \frac{a + d}{n} \quad (1)$$

5

$$\text{sensitivity} = \frac{a}{a + c} \quad (2)$$

$$\text{specificity} = \frac{d}{b + d} \quad (3)$$

$$10 \quad \text{kappa} = \frac{\left(\frac{a+d}{n}\right) - \frac{(a+b)(a+c) + (c+d)(d+b)}{n^2}}{1 - \frac{(a+b)(a+c) + (c+a)(d+b)}{n^2}} \quad (4)$$

$$\text{TSS} = \text{sensitivity} + \text{specificity} - 1 \quad (5)$$

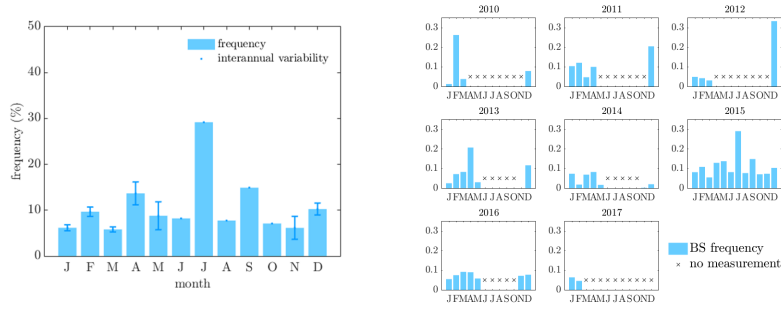


Figure S1. Annual cycle of blowing snow frequency at PE station, for the period 2010-2017. The error bar represents the inter annual variability. Note that ~~there are only measurements for the year 2015~~ measurements between June and October are present in 2015 only.

	2010												2011												2012												2013											
	J	F	M	A	M	J	J	A	S	O	N	D	J	F	M	A	M	J	J	A	S	O	N	D	J	F	M	A	M	J	J	A	S	O	N	D	J	F	M	A	M	J	J	A	S	O	N	D
AWS	Dark												Dark												Dark												Dark											
Ceilometer	Dark												Dark												Dark												Dark											
Micro-rain-radar	Dark												Dark												Dark												Dark											
Webcam	Vertical lines												Vertical lines												Vertical lines												Vertical lines											

	2014												2015												2016											
	J	F	M	A	M	J	J	A	S	O	N	D	J	F	M	A	M	J	J	A	S	O	N	D	J	F	M	A	M	J	J	A	S	O	N	D
AWS	Dark												Dark												Dark											
Ceilometer	Dark												Dark												Dark											
Micro-rain-radar	Dark												Dark												Dark											
Webcam	Vertical lines												Vertical lines												Vertical lines											

Figure S2. Availability of data for each of the PE instruments mentioned in the manuscript. Dark areas represent missing data, light grey areas represent available data and vertical lines represent a period when the instrument was not set up yet.

2 Equation of the different metrics used in section 4.1.

Equations come from (Allouche et al., 2006), with $a = N_{BS_{both}}$, $b = N_{BS_{ceilo}}$, $c = N_{BS_{vis}}$, $d = N_{BS_{none}}$ and $n = a + b + c + d$.

$$accuracy = \frac{a + d}{n}$$

5

$$sensitivity = \frac{a}{a + c}$$

$$specificity = \frac{d}{b + d}$$

$$kappa = \frac{\left(\frac{a+d}{n}\right) - \frac{(a+b)(a+c) + (c+d)(d+b)}{n^2}}{1 - \frac{(a+b)(a+c) + (c+a)(d+b)}{n^2}}$$

Table S1. Detail of the sensors and range used to measure the different meteorological variables by the AWS/IWS at PE station.

Variable measured	sensor	range \pm accuracy
2m temperature	Vaisala HMP35AC	-80 to 56 °C \pm 0,3 °C
2m humidity	Vaisala HMP35AC	0 to 100 % \pm 2%
2m wind direction	Young 05103	0 to 360 ° \pm 3 °
2m wind speed	Young 05103	0 to 60 m \cdot s ⁻¹ \pm 0,3 m \cdot s ⁻¹
2m pressure	Vaisala PTB1011B	600 to 1060 hPa \pm 4 hPa
2m short wave radiation	Kipp CNR1	0 to 2000 W \cdot m ⁻² \pm 2%
2m long wave radiation	Kipp CNR1	-250 to 250 W \cdot m ⁻² \pm 15 W \cdot m ⁻²
height of the instrument	SR50	0,5 to 10 m \pm 0,01 m

Table S2. Details of sensors used to measure the different meteorological variables at Neumayer station

variable measured	sensor
2 and 10 m temperature	Thies 2.1265.10.000 PT-100 platinum resistance sensors
2 m dew point temperature	Vaisala HMP233 hygrometers
relative humidity	dew point temperature and temperature
surface air pressure	Digi quartz 215-AW002
wind vector	Thies 4.3323.21.002 cup anemometer and wind vane combined

$$TSS = sensitivity + specificity - 1$$

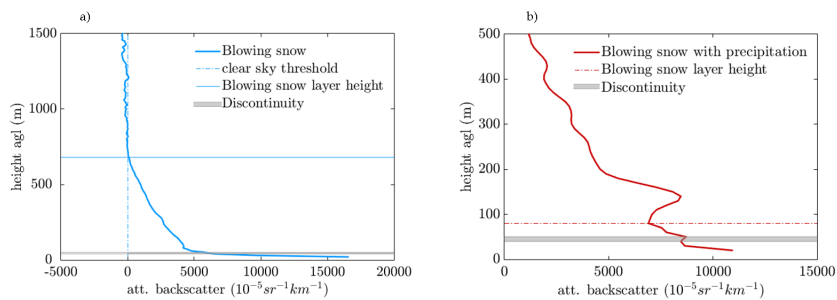


Figure S3. Determination of the height of the layer by the BSD algorithm. (a) in case of a clear-sky-cloudless blowing snow profile, the height of the layer (thin horizontal line) is attained when the backscatter intensity reaches the clear sky threshold (dashed vertical line). (b) in case of precipitation, the height of the blowing snow layer (dashed horizontal line) is reached when the intensity of the backscatter signal re-increases.

Table S3. WMO categorization of blowing snow

WMO code	description
0	snow haze
1	Drifting snow, light or moderate, with or without snow falling
2	Drifting snow, heavy, without snow falling
3	Drifting snow, heavy, with snow falling
4	Blowing snow, slight or moderate, without snow falling
5	Blowing snow, heavy, without snow falling
6	Blowing snow, slight or moderate, with snow falling
7	Blowing snow, heavy, with snow falling
8	Drifting and blowing snow, slight or moderate, impossible to determine whether sno is falling or not
9	Drifting and blowing snow, heavy, impossible to determine whether sno is falling or not

Table S4. Detection numbers rate of the different categories of observations. $N_{BS_{both}}$ stands for the part of blowing snow detected by both the algorithm and the visual observations, $N_{BS_{none}}$ is when both methods agree that there is no blowing snow. $N_{BS_{ceilo}}$ and $N_{BS_{vis}}$ represent detections rates by the algorithm and the observer only, respectively. All columns are expressed in %. B stands for blowing and D for drifting snow. The total number of measurements is 10584.

	$N_{BS_{both}}$	$N_{BS_{none}}$	$N_{BS_{ceilo}}$	$N_{BS_{vis}}$
<u>blowing and drifting</u> <u>B and D</u> snow, with or without <u>pre-precipitation</u> (WMO cat 01 to 09)	2404 <u>22</u>	5170 <u>48</u>	972 <u>9</u>	2308 <u>21</u>
<u>blowing and drifting</u> <u>B and D</u> snow, without <u>pre-precipitation</u> (WMO cat 02, 04 and 05)	992 <u>9</u>	6578 <u>61</u>	2373 <u>22</u>	897 <u>8</u>
heavy <u>blowing</u> <u>B</u> snow, without <u>pre-precipitation</u> (WMO cat 05)	378 <u>3</u>	7406 <u>70</u>	2998 <u>27</u>	72 <u>0</u>
all <u>blowing</u> <u>B</u> snow, without <u>pre-precipitation</u> (WMO cat 04 and 05)	822 <u>7</u>	6993 <u>66</u>	2554 <u>23</u>	485 <u>4</u>
all <u>blowing</u> <u>B</u> snow, with or without <u>pre-precipitation</u> (WMO cat > 03)	1856 <u>17</u>	6665 <u>61</u>	1520 <u>14</u>	813 <u>8</u>
heavy <u>blowing</u> <u>B</u> snow, with or without <u>pre-precipitation</u> (WMO cat 05, 07 and 09)	1114 <u>10</u>	7249 <u>67</u>	2262 <u>21</u>	229 <u>2</u>

References

Allouche, O., Tsoar, A. and Kadmon, R.: Assessing the accuracy of species distribution models: prevalence, kappa and the true skills statistics (TSS), Journal of applied Ecology, 43, 1223–1232, 2006.

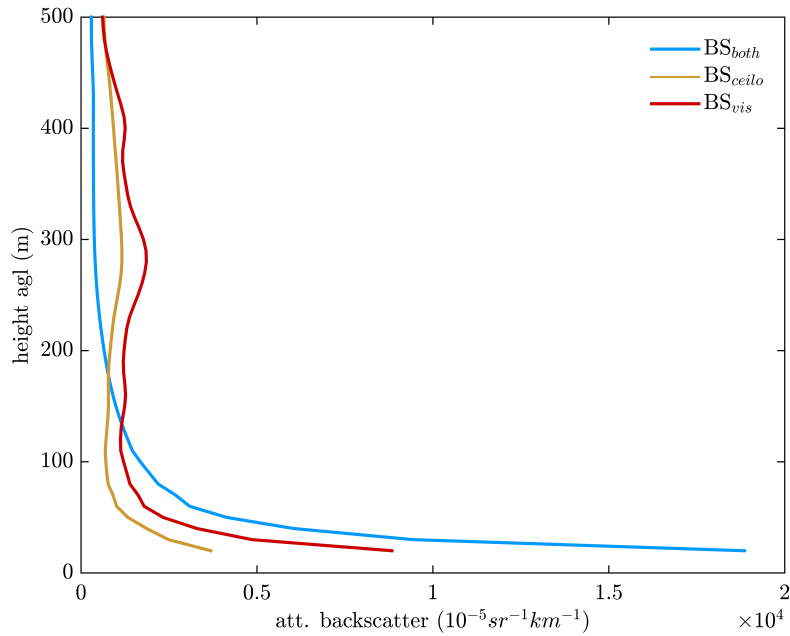


Figure S4. Mean profiles for each of the detection categories at Neumayer: BS_{both} when both methods detect blowing snow, BS_{ceilo} when blowing snow is reported by the BSD algorithm only, and BS_{vis} if blowing snow is detected by the visual observer, but not the BSD algorithm

Table S5. Meteorological conditions at Neumayer during the different events, for years 2011-2015 (mean \pm standard deviation).

variable (units)	BS_{both}	BS_{ceilo}	BS_{vis}	BS_{none}
number of occurrences	3416	23344	1451	1113
temperature 10m ($^{\circ}\text{C}$)	-14.8 ± 06	-15.3 ± 08	-10.5 ± 06	-13.1 ± 08
temperature 2m ($^{\circ}\text{C}$)	-14.8 ± 06	-15.5 ± 08	-10.5 ± 06	-13.2 ± 08
air temperature ($^{\circ}\text{C}$)	-14.8 ± 06	-15.8 ± 09	-10.5 ± 06	-13.4 ± 08
wind speed 10m ($\text{m} \cdot \text{s}^{-1}$)	21.6 ± 04	13.3 ± 04	17.3 ± 03	11.4 ± 03
wind speed 2m ($\text{m} \cdot \text{s}^{-1}$)	18.2 ± 03	11.3 ± 03	14.6 ± 03	9.6 ± 03
wind direction 10m ($^{\circ}$ to N)	93.7 ± 30	118 <u>118.0 ± 68</u>	89.8 ± 27	111 ± 64
wind direction 2m ($^{\circ}$ to N)	93.7 ± 31	118.3 ± 68	89.8 ± 27	111.26 <u>111.3 ± 65</u>
relative humidity (%)	85.4 ± 04	81.0 ± 06	88.3 ± 05	81.9 ± 08
pressure (hPa)	972.3 ± 11	979.3 ± 09	972.6 ± 09	978.8 ± 10
dew/frost point ($^{\circ}\text{C}$)	-16.4 ± 06	-18.0 ± 09	-11.8 ± 09	-15.55 <u>-15.5 ± 09</u>
height (m)	340.0 ± 170	112.0 ± 122	-	-

Table S6. Meteorological conditions at Princess Elisabeth during the different events, for years 2010-2017 (mean \pm standard deviation)

variable (units)	non-absence of blowing snow without no precipitation	non-absence of blowing snow with precipitation	blowing snow without no precipitation	blowing snow with precipitation
number of hours	12 671	10 232	1032	948
wind direction ($^{\circ}$ to N)	147 \pm 66	119 \pm 65	120 \pm 65	107 \pm 60
wind speed ($\text{m} \cdot \text{s}^{-1}$)	3.8 4 \pm 4	4.8 5 \pm 3	7 \pm 2	7 \pm 4
shortwave in ($\text{W} \cdot \text{m}^{-2}$)	194 \pm 206	173 \pm 226	138 \pm 253	142 \pm 206
shortwave out ($\text{W} \cdot \text{m}^{-2}$)	155 \pm 169	141 \pm 182	116 \pm 197	119 \pm 172
longwave in ($\text{W} \cdot \text{m}^{-2}$)	154 \pm 46	197 \pm 37	190 \pm 27	218 \pm 36
longwave out ($\text{W} \cdot \text{m}^{-2}$)	218 \pm 31	236 \pm 33	234 \pm 36	243 \pm 31
air temperature ($^{\circ}\text{C}$)	-16 \pm 6	-15 \pm 6	-16.5 \pm 7	-15 \pm 6
specific humidity ($\text{g} \cdot \text{kg}^{-1}$)	0.65 \pm 0.6	0.9 \pm 0.6	0.96 \pm 0.5	1.2 \pm 0.7
relative humidity (%)	46.5 46 \pm 17	63 \pm 18	73 \pm 16	80 \pm 16
pressure (hPa)	827 \pm 9	828 \pm 7	827 \pm 8	828 \pm 9
surface temperature ($^{\circ}\text{C}$)	-24.5 -24 \pm 8	-19.37 -19 \pm 9	-20 \pm 10	-18 \pm 8
temperature-temp. inversion ($^{\circ}\text{C} \cdot \text{m}^{-1}$)	8 8.0 \pm 3	4.4 \pm 4	3.5 \pm 4	2.5 \pm 3
temperature-temp. gradient ($^{\circ}\text{C} \cdot \text{m}^{-1}$)	2.5 \pm 1	1.4 \pm +1.0	1 \pm 1.4	0.76 0.8 \pm 1
height of blowing snow layer (m)	-	-	78 \pm 272	331 \pm 643

Table S7. Meteorological conditions at Neumayer III during the different events, for years 2011-2015 (mean \pm standard deviation)

variable (units)	non blowing snow without precipitation	non blowing snow with precipitation	blowing snow without precipitation	blowing snow with precipitation	heavy mixed events
number of hours	9599	11 385	1237	3834	10 351
wind direction 2m ($^{\circ}$ to N)	191 \pm 59	135 \pm 68	77 \pm 06	81 \pm 06	65 \pm 06
wind speed 2m ($\text{m} \cdot \text{s}^{-1}$)	4 \pm 3	5 \pm 3	6 \pm 4	7 \pm 5	13 \pm 6
air temperature 2m ($^{\circ}\text{C}$)	-23 \pm 11	-14 \pm 9	-21 \pm 10	-12 \pm 8	-15 \pm 7
relative humidity (%)	73 \pm 7	79 \pm 8	77 \pm 6	81 \pm 6	85 \pm 6
height of blowing snow layer (m)	-	-	139 \pm 180	110 \pm 159	1303 \pm 1581